Quantum diffusion of muons and muonium atoms in solids

Vyacheslav G. Storchak

Rutherford Appleton Laboratory, Chilton, Oxfordshire OX11 OQX, United Kingdom; TRIUMF, 4004 Westbrook Mall, Vancouver, British Columbia, Canada V6T 2A3; and Kurchatov Institute, Kurchatov Sq. 1, Moscow 123182, Russia

Nikolai V. Prokof'ev

Kurchatov Institute, Kurchatov Sq. 1, Moscow 123182, Russia

The diffusion of muons and muonium through solids has been studied over many years using the technique of spin relaxation. At low temperatures, the motion is due to tunneling between lattice sites, and the competition between tunneling rates and decoherence rates is important in determining the dynamics. Coherent propagation is seen in superconductors and insulators at low temperature where dissipation is small. At higher temperatures the motion undergoes a crossover from bandlike propagation to incoherent hopping between neighboring sites. This review covers both theory and experiment, emphasizing the mechanisms for dissipation, the role of barrier fluctuations, and effects of crystal disorder on the transport. The review of experimental data includes an analysis of barrier penetration bandwidths for muon and muonium diffusion in a variety of metals and insulators. [S0034-6861(98)00503-0]

CONTENTS

I. INTRODUCTION

The diffusion of muons (μ^+) and muonium (the bound state of $\mu^+ + e^-$, called Mu) in solids is dominated by quantum tunneling between lattice sites at low temperature. This is a very interesting subject from a theoretical point of view, with the many degrees of freedom of the solid environment playing an essential role in the coherence and barrier penetration rates. Muons are uniquely suited for particle transport tunneling studies because of their intermediate mass, 200 times greater than the electron but several orders of magnitude less than the lattice nuclei. The atoms are too heavy to have perceptible tunneling except in rare cases, and electrons are so light they they are usually delocalized in the lattice.

The dynamics of barrier penetration in a periodic lattice is called quantum diffusion. There are several im-

portant quantities in the theory of quantum diffusion, which will be discussed in detail in the theoretical part of the review. Most fundamental is the bandwidth Δ of the μ^+/Mu states that form a band in a periodic lattice. This is of course proportional to the tunneling rate in the absence of perturbations. The ballistic transport of the pure band picture is changed to diffusion by various perturbations, namely, lattice defects, thermal excitation of phonons, and thermal excitation of electrons. Quantum diffusion is observed over a wide range of temperatures for both μ^+ and Mu, and the review will describe in detail these couplings.

The experiments to observe muon diffusion are based on the spin of the μ^+ and its anisotropic decay to give a positron. The relaxation of the spin polarization of the μ^+ or the Mu, called μSR and MSR, respectively, is measured as a function of time. The experimental techniques have been described in a number of excellent reviews (Schneck, 1985; Cox, 1987; Brewer, 1994), and we shall only concentrate on the general ideas. In a μSR experiment, muons with almost 100% polarization in the direction of the source are imbedded in a sample. The muon comes to rest and experiences the local magnetic environment through its spin. Later it decays asymmetrically with the decay positron emitted preferentially along the μ^+ spin direction.

The decays are typically recorded by two detectors placed in the forward and backward directions. Ignoring efficiencies and backgrounds, they record a time spectrum

$$N_0 e^{-t/\tau_\mu}[1-P(t)], \tag{1}$$

$$N_0 e^{-t/\tau_\mu}[1+P(t)]. \tag{2}$$

Here $\tau_\mu = 2.197$ μs is the muon lifetime, and $P(t)$ is the polarization function that provides information on the μ^+ dynamics in the sample.

The simplest μ^+SR technique for μ^+ diffusion studies is the transverse-field muon spin rotation experiment, in which a large (with respect to internal nuclear magnetic fields) external magnetic field B_0 is applied perpendicular to the muon polarization, causing the muon spin to precess about the external field. This, in turn, will cause $P(t)$ to be oscillatory with the characteristic frequency $\omega_\mu = \gamma_\mu \times B_0$.

Due to random orientation of nuclear moments, muons experience different fields in different unit cells. This results in a decay of the oscillatory signal with characteristic exponential or Gaussian decay times. From this one infers the nature of the diffusion process and the characteristic energy and time scale. Experiments are also done with longitudinal magnetic fields going down to zero (Luke *et al.*, 1991). In this case, $P(t)$ has no oscillatory component.

A number of reviews, monographs, and edited volumes have already been devoted to μSR and its particular aspects. The recent advances in μSR techniques have produced a rapidly growing body of new results, both theoretical and experimental, as evidenced by the proceedings of μSR conferences [see, for example, the conference proceedings edited by Cox *et al.* (1990), Brewer *et al.* (1994), and Nagamine *et al.*, (1997)]. Recent reviews on the theoretical aspects of quantum diffusion are given by Kondo (1986), Kagan and Prokof'ev (1992), and Regelmann, Schimmele, and Seeger (1995). There are some recent experimental reviews, including those of Kadono (1992, 1993; Kadono and Kiefl, 1993), but these tend to be focused on selected materials. There has been considerable progress in the last few years with an abundance of new data, especially in the quantum diffusion of Mu in cryocrystals, and this seems an appropriate moment for a comprehensive review of the experiments.

It is not our intention to discuss *all* the experimental and theoretical results. This task seems to be impossible, taking into account the enormous number of relevant papers published during the past three decades. Instead, we shall try to cover only those topics most pertinent to our current understanding. A number of topics have to be clarified, including inhomogeneous quantum diffusion, long-ranged trapping phenomena, two-phonon interaction at low temperatures, and one-phonon interaction at temperatures comparable to the Debye temperature of the crystal. Of special note are the results on inhomogeneous quantum diffusion in disordered lattices (both metallic and insulating), which have resolved some long-standing puzzles.

For the rest, we refer the reader to the original papers. The most comprehensive bibliography on the subject can be found in the well-documented proceedings of the μSR conferences, edited by Gygax *et al.* (1979), Brewer and Percival (1981), Yamazaki and Nagamine (1984), Hartmann, Karlsson, Lindgren, and Wäppling (1986), Cox *et al.* (1990), Brewer *et al.* (1994), and Nagamine *et al.* (1997).

II. GENERAL REMARKS ON QUANTUM DIFFUSION

In the context of traditional solid-state physics the problem of the tunneling motion of an "impurity" (muon, proton, isotopic defect, etc.) is of special interest. Typically, tunneling occurs between two or more potential wells which would be degenerate in a pure system. In this case the quantum-mechanical coherence between the particle's states in different wells manifests itself (the well-known example is the Bloch-wave propagation of electrons in crystalline solids). The basic concept introduced to describe this effect is that of a band motion (coherent tunneling) of a particle with a bandwidth Δ determined by the amplitude of the particle's resonance transitions between the potential minima (Andreev and Lifshitz, 1969; Guyer and Zane, 1969).

At $T \neq 0$, however, tunneling occurs on the background of strong coupling to the excitations of the environment, which results in a fluctuating (dynamic) energy bias between the potential wells and destroys coherence. Since Δ is exponentially small, the tunneling kinetics in a solid is a problem of motion in a system with weak quantum correlations and strong dynamic interactions with the excitations of the medium. One may character-

ize the strength of the dephasing interaction by the damping rate (or level broadening) Ω. Even at low temperatures Ω may be as large as Δ; a temperature rise results in an exponential suppression of coherent tunneling transition amplitude and a crossover from coherent band motion to incoherent tunneling (Kagan and Maksimov, 1973; Kagan and Klinger, 1974).

Here we encounter differing behavior of the diffusing particle in a metal and in an insulator due to essentially different infrared properties of the environmental spectrum. In a metal the crossover to incoherent tunneling takes place at temperatures as low as $T\sim\Delta$, with a peculiar temperature dependence of the diffusion coefficient originating from the electron-polaronic effect (Kondo, 1984; Yamada, 1984). In insulators, incoherent tunneling takes over at temperatures $T\gg\Delta$, which can still be much lower than the Debye temperature Θ. The interaction responsible for the suppression of coherence was found to be two-phonon in character (Andreev and Lifshitz, 1969; Kagan and Maksimov, 1973). The one-phonon interaction is not important in this temperature range (except for the renormalization of Δ), taking over only at temperatures comparable to Θ. Although coherent motion and incoherent tunneling are fundamentally different regimes, they have the same temperature dependences for the diffusion coefficient (Kagan and Maksimov, 1973). The value of Ω, being determined by the relative fluctuations of the particle interaction with the medium at neighboring sites, is independent of Δ. An increase of the particle mass results in the exponential reduction of Δ, which in turn leads to an exponential decrease of the transition temperature from band motion to incoherent tunneling. In order to keep this transition temperature reasonably high, one is bound to consider the tunneling dynamics of a reasonably light particle.

Since Δ is so small, quantum diffusion is extremely sensitive to crystal imperfections. Therefore particle localization often takes place at a relatively low defect concentration. Until very recently theoretical studies of μ^+ and Mu diffusion have focused on nearly perfect crystals, in which bandlike motion persists at low temperatures. Crystalline defects have been treated mainly as local traps with trapping radii of the order of the lattice constant a. The justification for such an approach was that the characteristic energy of the muon coupling to the crystalline distortion, $U(a)$, is usually much less than Θ. However, this comparison is irrelevant to the problem of particle dynamics, for which the crucial consideration is that Δ is usually several orders of magnitude less than $U(a)$. For example, a typical Mu bandwidth in insulators is of order of $\Delta\sim 0.01$–0.1 K, whereas in insulators $U(a)$ could be as large as 10 K. In metals the mismatch is even more drastic: $U(a)\sim 10^3$ K and $\Delta\sim 10^{-1}-10^{-4}$ K may differ by seven orders in magnitude. Under these circumstances, the influence of crystalline defects extends over distances much larger than a. If the ''disturbed'' regions around defects overlap, a complete particle localization can result. In this case the interaction with the thermal bath makes quantum diffusion possible, and its study provides information on crystal disorder. This phenomenon is common for both ''dirty'' insulators and ''dirty'' metals.

III. SOME THEORETICAL ASPECTS OF QUANTUM DIFFUSION

During the last ten years our understanding of tunneling phenomena in interacting systems has evolved significantly. Not only do we now understand better the role played by different interaction Hamiltonians, like the two-phonon or conduction-electron couplings, but we also have a general framework in which to discuss the effects of dissipation on tunneling, which originates from the oscillator bath model of Caldeira and Leggett (Caldeira and Leggett, 1983; Leggett *et al.*, 1987). It is simply impossible, however, to fit a thorough discussion of the tunneling problem with all the derivations into this review, and in fact we believe it is not necessary, because the theory has been recently reviewed (see, e.g., Kagan and Prokof'ev, 1992; Weiss, 1993; Regelmann, Schimmele and Seeger, 1995). In this section, we shall instead discuss the basic concepts of the theory and skip formal derivations. Also, we shall discuss quantum diffusion, always bearing in mind μSR experiments and possible relevance of quantum diffusion effects for the muon relaxation.

A. Hamiltonian and coherent band motion in a perfect crystal

We start by writing the Hamiltonian of the light particle in a crystal as

$$\mathcal{H}=\mathcal{H}_o+V_{inh}(\vec{r})+\mathcal{V}_{int}+\mathcal{H}_{mag}, \tag{3}$$

$$\mathcal{H}_o=-\frac{1}{2m_\mu}\nabla^2+U(\vec{r}), \tag{4}$$

where $U(\vec{r})$ is the crystal potential when all the host atoms are in their equilibrium sites and form a perfect lattice, $V_{inh}(\vec{r})$ is the contribution to the potential coming from crystal imperfections and impurities, $\mathcal{V}_{int}$ describes the coupling between the particle and crystal excitations (phonons, electrons, magnons, etc.), and H_{mag} couples the spin of the particle to the external magnetic field $\vec{B}_o$ and to the local magnetic fields $\vec{B}(\vec{r})$ (see below).

We assume that for the particle with the mass $m_\mu \gg m_e$, where m_e is the electron mass, zero-point vibrations around local minima of the crystal potential are small as compared with the interwell separation a (or lattice constant, if there is only one minimum in the unit cell). This condition implies that tunneling splitting of the lowest levels in each well is much less than the zero-point vibration frequency $\omega_o=2\pi\nu_o$, and the lowest states are well separated from the rest of the particle spectrum. The standard expression for the tunneling amplitude between the two nearest wells is given in the semiclassical approximation (Landau and Lifshitz, 1974) as ($\hbar=1$)

$$\Delta_o = \nu_o e^{-S_o}. \tag{5}$$

Here the tunneling action $S_o = \int_{\vec{r}_1}^{\vec{r}_2} p\,dx$ is given by the integral along the optimal path connecting turning points $\vec{r}_1$ and $\vec{r}_2$ on different sides of the barrier. It follows immediately from the Bohr-Sommerfeld quantization rule that $S_o \approx \pi n$, where n is the number of levels in the potential well $-U(x)$ obtained by inverting the barrier between the turning points. In what follows we consider the case $S_o \gg 1$, which in fact is already satisfied when the barrier height (or activation energy) U_B is only a few times larger than the zero-point vibration energy, because $n \approx U_B/\omega_o$ (for qualitative estimations we make no distinction between the zero-point vibration energy *in the well* and in the inverted barrier potential).

In this review we restrict ourselves to the discussion of quantum diffusion only and consider the low-temperature particle dynamics, for which classical over-barrier transitions are irrelevant. To define the crossover temperature T_*, one has to find the maximum value of the transition probability between the wells (Lifshitz and Kagan, 1972),

$$W_{12}(T) = \sum_{E_i} e^{-E_i/T} W^Q(E = E_i), \tag{6}$$

where $W^Q(E)$ is the probability of a quantum tunneling transition at energy E, and the sum is over energy levels in the well. Since $W^Q(E) \sim e^{-2S_o(E)}$, one may rather accurately estimate the crossover temperature from the minimum of the semiclassical exponent, $[2S_o(E) + E/\mathrm{T}_*]'_E = 0$, or, equivalently, $-\nu_o + 1/T_* = 0$. At temperatures

$$\mathrm{T} \ll \mathrm{T}_* = \nu_o, \tag{7}$$

the maximum of Eq. (6) is obtained for the lowest level in the well. At higher temperatures classical over-barrier transitions take over. A more detailed discussion of different barrier shapes and the corresponding crossover temperatures is given by Lifshitz and Kagan (1972).

The above two restrictions allow us to simplify the problem considerably by truncating the original Hamiltonian (3) to the low-energy effective Hamiltonian dealing only with the lowest particle levels in each potential well. The first three terms in the Hamiltonian (3) then become

$$\mathcal{H}_o = \sum_{\vec{n},\vec{g}} \Delta_o^{(g)} d^\dagger_{\vec{n}+\vec{g}} d_{\vec{n}} + \sum_{\vec{n}} \epsilon_{\vec{n}} d^\dagger_{\vec{n}} d_{\vec{n}}, \tag{8}$$

where the index $\vec{n}$ is over all possible particle sites, the index $\vec{g}$ denotes nearest-neighbor sites, $\epsilon_{\vec{n}}$ is the particle on-site energy, and $d^\dagger_{\vec{n}}$ creates particles on site $\vec{n}$. For simplicity (and definiteness) we shall consider below the case in which allowed particle sites form a simple cubic lattice, as, for example, in alkali-halides. Then all $\Delta_o^{(g)} = \Delta_o$, $|\vec{g}| = a$, and nonzero energies $\epsilon_{\vec{n}}$ are due to crystal defects only. Generalizations to other crystal symmetries are obvious, and there are cases with many interstitial positions for the muon inside the unit cell, e.g., μ^+ in Bi, which requires the consideration of several different parameters $\Delta_o^{(g)}$ and even nonzero $\epsilon_{\vec{n}}$ in a perfect crystal (if different interstitial sites have different energies). In a perfect crystal the particle eigenstates are delocalized and

$$E_{\vec{k}} = 2\Delta_o(\cos ak_x + \cos ak_y + \cos ak_z), \tag{9}$$

with the bandwidth equal to $\Delta = 2Z\Delta_o$, where Z is the coordination number.

Assuming that muons are ballistically propagating in a crystal, what are the consequences for the observed μSR spin dynamics? The dominant mechanism for muon spin relaxation in most nonmagnetic solids is due to randomly oriented local magnetic fields produced by nuclear moments. It is widely accepted that nuclear fields in different unit cells are uncorrelated,

$$\gamma_\mu^2 \langle \vec{B}(\vec{n}) \vec{B}(\vec{n}') \rangle = \delta^2 \delta_{\vec{n},\vec{n}'}, \tag{10}$$

where $\gamma_\mu/2\pi = 0.01355342$ MHz/Oe is the μ^+ gyromagnetic ratio. [This assumption is valid provided that a large number of nuclear moments contribute to $\vec{B}(\vec{n})$, and different nuclei are responsible for nuclear fields in different unit cells.] Each time the particle changes its position in the lattice it experiences a fluctuation in the magnetic field acting on the particle spin. Since nuclear field correlations are short ranged, μSR is most sensitive to the particle dynamics on the atomic scale. For the band spectrum (9) we may easily calculate the autocorrelation function describing time fluctuations in the particle occupation numbers at some site $\vec{n}$:

$$C_{\vec{n}}(t) = \mathrm{Tr}\ \rho^{(0)} \vec{n} e^{i\mathcal{H}t} \vec{n} e^{-i\mathcal{H}t} \equiv \langle \vec{n}(t) \vec{n}(o) \rangle. \tag{11}$$

Here $\rho^{(0)} = e^{-\mathcal{H}/T}/\mathcal{Z}(T)$ is the equilibrium density matrix with the free-particle partition function $\mathcal{Z}(T) = \Sigma_{\vec{k}} \exp\{-E_{\vec{k}}/T\} = NI_o^3(2\Delta_o/T)$, where N is the number of unit cells and I_o is the Bessel function. In the Fourier representation Eq. (11) reduces to

$$C(t) = \sum_{\vec{k},\vec{p}} \rho_k^{(0)} e^{i(E_{\vec{k}} - E_{\vec{p}})t} \equiv \frac{J_o^3(2\Delta_o t) J_o^3(2\Delta_o t + i2\Delta_o/T)}{I_o^3(2\Delta_o/T)} \tag{12}$$

[in the homogeneous case $C_{\vec{n}}(t)$ is independent of $\vec{n}$].

In the high-temperature limit $C(t)$ gives the probability of return to the same site after time t for the simple cubic lattice:

$$C(t) = J_o^6(2\Delta_o t), \quad (T > \Delta). \tag{13}$$

Substituting this result into the definition of the on-site correlation time, or the average time spent at a unit cell (McMullen and Zaremba, 1978),

$$\tau = \int_0^\infty dt C(t) \approx (2\sqrt{2}\Delta_o)^{-1}, \tag{14}$$

we find it to be temperature independent in the coherent high-T limit (Petzinger, 1982). These results will be used

in our analysis of the low-temperature quantum diffusion in pure crystals of KCl, NaCl, and GaAs.

Consider now the longitudinal relaxation of the particle spin assuming its coherent dynamics. Since in all cases studied so far magnetic interactions with the nuclear (dipole or contact in origin) fields were much less than the particle bandwidth, we can use the perturbation theory and thus write

$$T_1^{-1}=2\pi\sum_{\vec{k}\vec{p},ss'}\rho_{k,s}^{(0)}\left|\langle\vec{p},s'|\sum_{\vec{n}}\ \gamma_\mu\hat{\vec{S}}\vec{B}(\vec{n})|\vec{k},s\rangle\right|^2 \times\delta(E_{\vec{k}}-E_{\vec{p}}+\omega_{ss'}), \tag{15}$$

where $\hat{\vec{S}}$ is the particle spin operator. As discussed in the next section, typically only one magnetic transition $s\to s'$ with the frequency $\omega_{ss'}$ contributes to the relaxation. Denoting the spin-matrix element squared as $M_{mag}^2(\vec{B}_o)$ (some particular examples are given in the next section), we write Eq. (15) as (Kondo, 1992)

$$T_1^{-1}=M^2\int_{-\infty}^{\infty}dte^{i\omega t}Tr\rho^{(0)}\vec{n}(t)\vec{n}(0)\equiv M^2C(\omega). \tag{16}$$

Obviously, $T_1^{-1}=0$ when $\omega\geqslant\Delta$ because of the energy conservation law, i.e., when the Zeeman energy is larger than the bandwidth; near the threshold T_1^{-1} goes to zero as $(27/2\pi^3)M^2(\Delta-\omega)^2/\Delta^3$.

In the high-T limit the answer is remarkably simple:

$$T_1^{-1}=2M^2\tau\quad(T>\Delta\gg\omega), \tag{17}$$

with τ from Eq. (14). In the low-temperature region, where one can use the long-wavelength expansion for the energy spectrum $E_{\vec{k}}\approx-\Delta/2+\vec{k}^2/2m_*=-\Delta/2+\Delta_o\vec{k}^2a^2$, we find

$$T_1^{-1}=\frac{M^2|\omega|e^{\omega/2T}}{2(\pi\Delta_o)^{3/2}\sqrt{T}}K_{-1}\left(\frac{|\omega|}{2T}\right)\quad(T,\omega\ll\Delta), \tag{18}$$

where K_{-1} is the Bessel function. Now $T_1^{-1}\sim\omega^{1/2}$ or $T_1^{-1}\sim T^{1/2}$ depending, on the ratio ω/T. This result has a clear physical interpretation. At low temperatures the relevant length scale in the problem is the particle wavelength $\lambda\gg a$. The effective hyperfine interaction must be averaged over the volume λ^3 with the result $\delta_{eff}^2\sim\delta^2(a/\lambda)^3$. On the other hand, it takes time $\tau_{eff}\sim\lambda/v\sim1/T$ to move over a distance of order λ. Using standard motional narrowing arguments (Abragam, 1961) we then write the depolarization rate as $\delta_{eff}^2\tau_{eff}\sim T^{1/2}$ and recover the result by Kondo (1986).

We note also that the above results are independent of the diffusion rate provided the mean free path is much larger than the particle wavelength. The fundamental reason for this is the short-ranged character of the nuclear field correlations in Eqs. (10) and (16), and thus only the smallest length scale is relevant to the problem. The physics of quantum diffusion with a large mean free path is rather standard and is usually described within the semiclassical Boltzmann equation (see, for example, Kagan and Prokof'ev, 1992). Since it has no effect whatsoever on the muon/Mu relaxation, we do not consider it here.

B. Coherent (dissipationless) motion in a disordered crystal

Let us now add crystal disorder to the coherent picture just described. The crucial point for the rest of the discussion in this review is that disorder *cannot* be treated as an uncorrelated random potential (Kondo, 1986; Sugimoto, 1986) and/or local traps. As we shall see, both approaches are misleading in the general case and quite often give incorrect results because (i) at low defect content, $x_{im}=n_{im}a^3\ll1$ the disorder potential is spatially correlated at least up to the distance between the defects, $\overline{R}\approx a(4\pi x_{im}/3)^{-1}\gg a$; (ii) in the motional narrowing regime the depolarization rate is proportional to the inverse hopping rate, and the procedure of averaging the hopping rate is meaningless; (iii) in the case of particle motion over large distances the effective diffusion coefficient cannot be obtained by averaging the local hop rate; (iv) trapping is out of the scope of the random potential treatment.

In this subsection we ignore all inelastic interactions and consider the problem of particle spin depolarization assuming the dissipationless dynamics described by the Hamiltonian (8). Imagine a particle in an extremely narrow tunneling band, and let us study its elastic scattering cross section off the impurity potential

$$V_{inh}(\vec{r})=U_0(\hat{\vec{r}})(a/r)^m, \tag{19}$$

($m=3$ corresponds to the strain-induced field), with the amplitude $U_0\equiv U(a)\gg\Delta$. An obvious answer for the cross section is $\sigma\approx\pi R_\Delta^2\gg\pi a^2$ where

$$V_{inh}(R_\Delta)\approx\Delta. \tag{20}$$

The particle cannot penetrate elastically into the region where potential energy exceeds the bandwidth, and these regions around each impurity are rather long ranged. For the same reason, if we put the particle *inside* the impurity region it will never escape. Furthermore, inside the radius R_{loc} defined by

$$a\frac{\partial V_{inh}(R_{loc})}{\partial r}\approx\Delta, \tag{21}$$

the particle displacement even to the nearest neighboring lattice site is forbidden by energy considerations. Thus, in the absence of inelastic scattering on phonons and electrons, the particle will be moving fast in the band or be static depending on the initial conditions, i.e., how far from the defect center it stopped after the thermalization process.

With increasing impurity concentration, less and less space is left for coherent band propagation. Above some critical concentration the impurity regions of radius R_{loc} overlap, resulting in complete particle localization in a crystal volume, and this concentration is very small:

$$x_{loc} \approx \frac{3}{4\pi}\left(\frac{a}{R_{loc}}\right)^3. \tag{22}$$

The above picture (Andreev, 1976; Kagan and Maksimov, 1983, 1984) was observed experimentally for quantum diffusion of ^{3}He atoms in solid ^{4}He (Mikheev *et al.*, 1983). We note that the strain potential between the ^{3}He atoms is very weak, $U_0 \sim 10^{-2}$ K, while in the case of μ^+ or Mu one can expect it to be as strong as $U_0 \geqslant 10$ K in insulators and $U_0 \sim 10^3$ K in metals. In all experiments on μ^+ or Mu quantum diffusion carried out so far, the tunneling band was found to be much less than the typical amplitude of the impurity potential, e.g., $\Delta \leqslant 1$ K in KCl, NaCl, GaAs, N_2, Ne, and Xe, while $\Delta \sim 10^{-1}$, 10^{-2}, 10^{-4} K in Al, V, and Cu, respectively.

Consider now how this physics will reveal itself in a μSR experiment. To be specific, we consider μ^+ depolarization in the transverse-field geometry when external magnetic field $B_0 \gg B(\vec{n})$. By definition, the polarization function in this case is given as an ensemble average,

$$P(t) = \left\langle \exp\left[i \int_0^t dt' \, \omega(\vec{n}(t')) \right] \right\rangle, \tag{23}$$

where $\omega(\vec{n}(t)) = \gamma_\mu [B_0 + B(\vec{n}(t))]$ is the time-dependent precession frequency, which changes each time the particle goes from one site to another. Here $\langle \ldots \rangle$ stands for the average over nuclear fields [see Eq. (10)] and particle dynamics, both of which result from the statistical nature of the muon experiment. One may further write Eq. (23) in the form

$$P(t) \approx \int \frac{d\vec{r}}{V} \exp\left[-\frac{\delta^2}{2} \int_0^t dt' \int_0^{t'} dt'' C(\vec{n}, t'-t'') \right], \tag{24}$$

where we made use of the correlation function $C(t)$ [see Eq. (11)], which now depends on the crystal site and is defined as a local property. The approximation used in Eq. (24) implies that there is no relaxation toward thermal equilibrium during the time t, which is consistent with the dissipationless dynamics.

In a long-ranged potential we have to distinguish between three possibilities: Those particles which stop after thermalization inside the regions of radius R_{loc} around impurities are static, and their contribution to the polarization function is given by $P_{loc} = f_{loc} \exp\{-1/2 \delta^2 t^2\}$ where $f_{loc} \approx (4\pi/3) n_{im} R_{loc}^3$ is the fraction of the static component. Assuming the motional narrowing effect to operate for fast-moving particles in the band, we write the second contribution as $P_b = f_b \exp\{-\delta^2 \pi t\}$, where $f_b \approx (4\pi/3) n_{im} R_\Delta^3$ is the fraction of particles delocalized in the band. In general there will be particles that are delocalized over a few unit cells. Their fraction, f_d, is given by the volume between the radii R_{loc} and R_Δ and thus depends on the structure of the impurity potential; it is comparable with the $1 - f_b$ if the defect regions do not overlap and the potential is due to the strain field (19), because in this case $a dV_{inh}/dr \ll V_{inh}$. If the potential is mainly due to the electron-density oscillations around the impurity

$$V_{inh}(r) = U_0 \cos(2k_F r + \varphi)(a/r)^3, \tag{25}$$

then for $k_F a \sim 1$ we find that $a dV_{inh}/dr \sim V_{inh}$ (because of the cosine term), and $R_{loc} \approx R_\Delta$. In this case we conclude that the third fraction plays essentially no role. An exception may be the case of a semimetal with $k_F a \ll 1$, where electron density oscillations are smooth on the atomic scale—then we are back to $f_d \sim 1 - f_b$. There is no simple way to write down the third contribution to the polarization function, because it is essentially inhomogeneous. Indeed, for the particle state delocalized over $N_d \gg 1$ unit cells Eq. (24) gives (Stoneham, 1983) $P(t) \approx \exp\{-1/2(\delta^2/N_d)t^2\}$ [the probability of finding the particle in the same well at a long time is just $C(t) \sim 1/N_d$], which is Gaussian relaxation with the state-dependent $\delta_{eff}^2 \sim \delta^2/N_d$. Since delocalized states range from $N_d \sim 1$ to $N_d \sim R_\Delta^3 \gg 1$ one has to sum all the contributions with the proper weighting $W(N_d)$,

$$P_d = f_d \sum_{N_d} W(N_d) \exp\{-1/2(\delta^2/N_d)t^2\}. \tag{26}$$

The result will depend on the potential. In the most simple-minded approach, N_d is obtained from the relation that the energy change over a distance $N_d^{1/3} a$ is of the order of the bandwidth, $N_d^{1/3} a [\partial U(r)]/\partial r \sim \Delta$. One then finds $W(N_d) \sim (N_d R_\Delta^3/a^3)^{-3/4}$, but we do not believe that the result is accurate enough to be compared with the experiments except, perhaps, the characteristic time scale $\sim \delta^{-1}(R_\Delta/a)^{3/2}$. Thus in a disordered crystal the polarization function will be split into three independent contributions,

$$P = P_b + P_d + P_{loc}, \tag{27}$$

with the relative weights depending on the potential, the impurity concentration, and the value of Δ.

The relevance of the above description for μSR experiments depends on the nature of the inelastic processes and the temperature range (Kagan and Prokof'ev, 1987). Of course, the formation of two (or three) quasi-independent ensembles of particles in real systems holds only at very low temperatures when inelastic interactions with the thermal excitations are weak enough. At higher T, particles will easily gain sufficient energy from the crystal to overcome the defect potential and to move even if the tunneling states are out of resonance. Then particles can penetrate inside and outside the disturbed spheres on the time scale of the muon lifetime, and the decomposition into independent fractions is no longer valid. How to proceed in this case and what are the consequences for muon/Mu spin relaxation are discussed in the coming subsections. Furthermore, coupling to phonons and conduction electrons broadens energy levels, and this broadening, $\Omega(T)$, in many cases exceeds the particle bandwidth and the crystal disorder. Most muon experiments in the past were carried out in normal metals where damping $\Omega \sim T$ was very strong and masked the effects of long-ranged defect potentials, at least at high temperatures. However, in the superconducting state, where electron scattering is suppressed, and in insulators, low-temperature quantum diffusion is

often dominated by crystal disorder, the long-ranged character of which can no longer be ignored.

C. Coupling to the environment. Interaction Hamiltonians

Consider now what happens to the interaction term V_{int} describing the coupling between the particle and crystal excitations when we truncate the Hamiltonian. The two examples that we shall discuss here, i.e., phonons and conduction electrons, are fundamentally different because, for a light particle like a muon, strong inequalities in the mass ratios are valid, $M_h \gg m_\mu \gg m_e$, where M_h is the mass of the host atoms. Consequently quite opposite adiabatic limits seemingly apply to these two cases.

We start with the phonons and simply note that light muon mass allows us to consider coupling to the host atoms as motion in a slightly deformed crystal potential due to atom displacements from the equilibrium positions $\{\vec{R}_j^{(0)}\}$. That is, the interaction potential is obtained by expanding $U(\vec{r},\{\vec{R}_j\})$ in a series in $\vec{u}_j=\vec{R}_j-\vec{R}_j^{(0)}$. All corrections to the above procedure are expected to be small, at least in the parameter $(m_\mu/M_h)^{1/2}$. However, even with these corrections included (see Kagan and Klinger, 1974, 1976) the structure of the coupling Hamiltonian hardly changes at all, except for the small renormalization of the effective coupling constants. Thus we write the coupling to the lattice vibrations as

$$\mathcal{H}_o+\mathcal{V}_{int}\to\sum_{\vec{n}}\ \mathcal{V}(\vec{n})d_{\vec{n}}^\dagger d_{\vec{n}}+\Delta_o\sum_{\vec{n},\vec{g}}\ e^{\mathcal{B}(\vec{n},\vec{g})}d_{\vec{n}+\vec{g}}^\dagger d_{\vec{n}}, \tag{28}$$

where the on-site interaction can be written as the sum of one-, two-, and higher-order phonon processes by using the standard normal oscillator representation for the atomic displacements $\mathcal{V}(\vec{n})=\mathcal{V}^{(1)}(\vec{n})+\mathcal{V}^{(2)}(\vec{n})+\cdots$

$$\mathcal{V}^{(1)}(\vec{n})=\sum_j\ \frac{\partial\mathcal{V}_{int}}{\partial R_j^{(0)}}u_j=\sum_\alpha\ C_\alpha(\vec{n})(b_\alpha+b_{-\alpha}^\dagger), \tag{29}$$

$$\mathcal{V}^{(2)}(\vec{n})=\frac{1}{2}\sum_{jj'}\ \frac{\partial^2\mathcal{V}_{int}}{\partial R_j^{(0)}\partial R_{j'}^{(0)}}u_ju_{j'}$$

$$=\sum_{\alpha,\beta}\ C_{\alpha,\beta}(\vec{n})(b_\alpha+b_{-\alpha}^\dagger)(b_\beta+b_{-\beta}^\dagger). \tag{30}$$

Here α and β denote different phonon modes, e.g., $\alpha=(\vec{q},\lambda)$, where $\vec{q}$ is the phonon momentum and λ is its polarization state; $b_\alpha^\dagger$ is the Bose creation operator. We are considering only one- and two-phonon terms, because the higher-order terms are small in the parameter $u_j/a\ll 1$, and, according to our present understanding, no new physics is introduced by these extra terms. One may consider $\mathcal{V}_{\vec{n}}$ as the variation of the particle zero-point vibrational energy in the deformed lattice.

The site dependence of the coupling constants is governed by translational invariance. If there is only one particle state in the unit cell, then

$$C_\alpha(\vec{n})=C_\alpha e^{i\vec{q}\vec{n}},\quad C_{\alpha,\beta}(\vec{n})=C_{\alpha,\beta}e^{i(\vec{q}+\vec{q}')\vec{n}}. \tag{31}$$

In some cases, however, there are several interstitial sites in the unit cell that have the same energy but couple to phonons differently (Fujii, 1979). In this case one has to describe each site in the unit cell with its own set of coupling constants. As we shall see shortly, the relevant quantity is the difference $C_\alpha(\vec{n})-C_\alpha(\vec{n}+\vec{g})$, which has differing dependence on the phonon momentum for small qa in the two cases just mentioned (the same consideration applies to the two-phonon coupling constants).

We now turn to the second coupling term in Eq. (28), which may be viewed as the variation in the tunneling action S_o caused by the lattice distortion (Kagan and Klinger, 1976) [we truncate the particle Hamiltonian in an instantaneous potential $U(\vec{r},\{\vec{R}_j\})$]. Assuming that the variation in the barrier height is small $|\delta U|\ll U_B$, where $\delta U=U(\vec{r},\{\vec{R}_j\})-U(\vec{r},\{\vec{R}_j^{(0)}\})$, we write

$$S=\int_{\vec{r}_1'}^{\vec{r}_2'}dx\sqrt{2m_\mu[U(x,\{\vec{R}_j^{(0)}\})+\delta U-\omega_o/2]}$$

$$\approx S_o+\int_{\vec{r}_1}^{\vec{r}_2}\frac{dx}{v(x)}\delta U(x)-\frac{\pi}{2}\frac{\delta U(\vec{r}_1)+\delta U(\vec{r}_2)}{\omega_o},$$

where $v(x)$ is the particle velocity in the inverted potential (one has to account for the change in the position of the turning points to get the correct result). This correction to the "bare" action S_o is written in Eq. (28) as an operator $\mathcal{B}$. The linear expansion in the atom displacements then gives

$$\mathcal{B}(\vec{n},\vec{g})=\sum_\alpha\ \frac{B_\alpha(\vec{n},\vec{g})}{\omega_o}(b_\alpha+b_{-\alpha}^\dagger). \tag{32}$$

The two interaction terms in the Hamiltonian have opposite effects on the tunneling amplitude. Since Δ_o is small, in particular $\Delta_o\ll\Theta$, the particle will cause a lattice deformation around its site to minimize the interaction energy and will then find itself in an even deeper potential well (or "self-trapped" state). Any attempt to tunnel to the neighboring well without adjusting the lattice deformation will be out of resonance. But the lattice is not static and may fluctuate to a deformed state (not energetically favored and thus very rare) in which the two nearest wells come into resonance. At this moment the particle may tunnel to another well, and the lattice will then complete the transition by forming a self-trapped state around the new particle site. Since now not only the particle but also the surrounding host atoms are involved in tunneling, we get an exponential suppression of the effective tunneling amplitude known as the polaron effect (Holstein, 1959; Flynn and Stoneham, 1970),

$$\Delta_o\to\Delta_o e^{-\Phi}. \tag{33}$$

This mechanism is quite general in nature and even caused the misconception in the past that interaction effects must *always* suppress tunneling.

On the other hand the "barrier fluctuation" effect (Kagan and Klinger, 1976) suggests that the potential

barrier between the two wells may fluctuate to a lower value, e.g., when the coupling between the particle and the host atoms is repulsive and the atoms move away from the tunneling path. Clearly, among different possibilities, the particle will choose to tunnel when the barrier height is the lowest. The effect will be to increase the tunneling amplitude,

$$\Delta_o \to \Delta_o e^G. \tag{34}$$

In fact, the polaron effect and the effect of the barrier fluctuation interfere, and the net effect depends on the system, i.e., the interaction potential, host atom mass, tunneling configuration, etc. Although the barrier fluctuation term contains an extra factor $\Theta/\omega_o \ll 1$ (which is small according to our adiabatic approximation), one has to admit that Φ and G are defined by the coupling to the lattice in absolutely different regions—the first one in the potential well and the second mostly in the middle of the barrier. Thus no definite conclusion on whether the interaction suppresses or promotes tunneling is possible in the general case.

We now turn to the problem of coupling to the conduction electrons, which apparently corresponds to the opposite adiabatic limit $m_e \ll m_\mu$. It turns out, however, that the mass ratio is not at all the relevant parameter to determine which system is following the other. Instead, one has to compare the frequencies of the two (Kagan and Prokof'ev, 1986). In a metal, elementary excitations range from zero energy up to the Fermi energy $\epsilon_F \gg \omega_o$ (or the conduction bandwidth), and one has to treat electron-hole pairs near the Fermi surface as slow $|\epsilon_k - \epsilon_{k'}| < \omega_o$ and the rest of them as fast. The role of fast excitations is easy to understand. In the adiabatic approximation they adjust themselves to the instantaneous position of the particle, and their only effect is to renormalize the effective crystal potential $U(\vec{r}) \to \tilde{U}(\vec{r})$, which thus has to be understood as corrected, e.g., for screening effects (the change of the particle mass is small because of the large mass ratio).

Slow excitations in the Fermi liquid behave in exactly the same way as lattice vibrations, i.e., they further contribute to the self-trapped state in the well and to the barrier fluctuations (Kondo, 1976; Vladar and Zawadowski, 1983). The effective Hamiltonian is given by the same expression (28) with

$$\mathcal{V}_{el}(\vec{n}) = \sum_{\vec{k}\vec{k}',\sigma} V_{\vec{k}\vec{k}'} e^{i(\vec{k}-\vec{k}')\vec{n}} a^\dagger_{\vec{k}\sigma} a_{\vec{k}'\sigma}, \tag{35}$$

$$\mathcal{B}_{el}(\vec{n},\vec{g}) = \sum_{\vec{k}\vec{k}',\sigma} \frac{V^{(b)}_{\vec{k}\vec{k}'}(\vec{n},\vec{g})}{\omega_o} a^\dagger_{\vec{k}\sigma} a_{\vec{k}'\sigma}, \tag{36}$$

where $a^\dagger_{\vec{k}\sigma}$ is creating an electron in a state with momentum $\vec{k}$ and spin σ. We do not expect any essential difference in the coupling constants $V_{\vec{k}\vec{k}'}$ and $V^{(b)}_{\vec{k}\vec{k}'}$ because the electronic state is essentially delocalized over the unit cell, and the scattering off the particle may not change drastically from one point to another. The electron-polaronic effect is logarithmically enhanced at low temperature $\Phi_{el}(T) \approx K \ln(\omega_o/T)$ (see below), and since the barrier fluctuation term G_{el} is roughly proportional to $K \sim 1$ (Kagan and Prokof'ev, 1989a) and is thus indistinguishable from the unknown numerical coefficient in the ln function in Φ_{el}, we shall ignore it in the rest of the paper.

D. Incoherent tunneling

We are now ready to derive the interaction effects on the particle dynamics. Detailed calculations are well represented in the literature (Grabert, 1987; Leggett *et al.*, 1987; Kagan and Prokof'ev, 1992; Weiss, 1993). Here we shall only establish the framework for such calculations and discuss the physics around it.

Even in the truncated Hamiltonian (28) most of the environmental degrees of freedom have frequencies much larger than Δ. It seems natural then to begin by solving the on-site problem exactly (if possible), that is, by assuming zero Δ, and then proceed with the perturbation theory in Δ. This approach should work well in the incoherent (or hopping) regime of quantum diffusion, and its breakdown signals the onset of coherent delocalization. Suppose that the solution of the on-site problem is described by the unitary transformation connecting free and interacting environmental states, $\Psi^{(0)}_\alpha = \Lambda_{\alpha\beta}(\vec{n})\Psi^{(int)}_\beta$, for the particle sitting at $\vec{n}$. In this site-dependent representation of the environmental states the effective Hamiltonian will take the form

$$\mathcal{H} = \Delta_o \sum_{\vec{n},\vec{g}} \Lambda^\dagger(\vec{n}+\vec{g}) e^{\mathcal{B}(\vec{n},\vec{g})} \Lambda(\vec{n}) d^\dagger_{\vec{n}+\vec{g}} d_{\vec{n}} + \sum_{\vec{n}} \epsilon_{\vec{n}} d^\dagger_{\vec{n}} d_{\vec{n}}, \tag{37}$$

that is, all the interaction effects are now contained in the hopping term. For the one-phonon coupling the unitary transformation is nothing but the famous normal-oscillators displacement operator (see Flynn and Stoneham, 1970); an exact form of Λ was given by Kagan and Prokof'ev for the two-phonon interaction in (1989b) and for the coupling to conduction electrons in (1989a).

We start with the high-temperature limit, where the coherent correlations between successive tunneling events are suppressed, and the dynamics is described by the hopping probabilities calculated in the second order in Δ,

$$W_{\vec{n}_1 \to \vec{n}_2} = \Delta_o^2 \int_{-\infty}^{\infty} e^{i\xi t} \langle R^\dagger_{(\vec{n}_1,\vec{n}_2)}(t) R_{(\vec{n}_1,\vec{n}_2)}(0) \rangle, \tag{38}$$

where $R_{(\vec{n}_1,\vec{n}_2)} = \Lambda^\dagger(\vec{n}_1) e^{\mathcal{B}(\vec{n}_1,\vec{n}_2)} \Lambda(\vec{n}_2)$. Calculating the thermal average is a straightforward, but lengthy procedure. One finds the probability in the most general form as (Kagan and Prokof'ev, 1992)

$$W_{\vec{n}_1 \to \vec{n}_2} = \Delta_o^2 e^{-\xi/2T} \int_{-\infty}^{\infty} e^{i\xi t} e^{2B_o + 4G(T) - \Psi(t)} dt, \tag{39}$$

where $\xi=\epsilon_{\vec{n}_1}-\epsilon_{\vec{n}_2}$ is the energy bias between the wells, and

$$\Psi(t)=\int_0^{\omega_o} d\omega \times\frac{f(\omega)[\cosh(\omega/2T)-\cos(\omega t)]+ih(\omega)\sin(\omega t)}{\omega\,\sinh(\omega/2T)}. \tag{40}$$

We absorb all interaction effects into the definition of spectral functions $f(\omega)\equiv f_{1ph}(\omega)+f_{2ph}(\omega)+f_{el}(\omega)$ and $h(\omega)\approx h_{1ph}(\omega)$. To simplify future notations we introduce effective coupling constants $\overline{C}_\alpha\equiv C_\alpha(\vec{n}_1)-C_\alpha(\vec{n}_2)$ and the same definitions for $\overline{C}_{\alpha\beta}$ and $\overline{V}_{\vec{k}\vec{k}'}$. Now,

$$B_o=\sum_\alpha \frac{\overline{C}_\alpha B_{-\alpha}}{\omega_o\omega_\alpha},\quad G=\frac{1}{2}\sum_\alpha \frac{|B_\alpha|^2}{\omega_o^2}\coth(\omega_\alpha/2T), \tag{41}$$

$$f_{1ph}=\sum_\alpha\left[\frac{|\overline{C}_\alpha|^2}{\omega_\alpha}+\frac{|B_\alpha|^2}{\omega_o^2}\omega_\alpha\right]\delta(\omega_\alpha-\omega), \tag{42}$$

$$h_{1ph}=2\sum_\alpha \frac{\overline{C}_\alpha B_{-\alpha}}{\omega_o}\delta(\omega_\alpha-\omega), \tag{43}$$

$$f_{2ph}=\sum_{\alpha\beta}|\overline{C}_{\alpha\beta}|^2\left[\frac{N_\beta-N_\alpha}{\omega_\alpha-\omega_\beta}\delta(\omega_\alpha-\omega_\beta-\omega) +\frac{N_\beta+N_\alpha+1}{2(\omega_\alpha+\omega_\beta)}\delta(\omega_\alpha+\omega_\beta-\omega)\right], \tag{44}$$

$$f_{el}=2K, \tag{45}$$

where K is the dimensionless electron coupling (the most general expression for K was given by Yamada *et al.*, 1986); in the perturbation theory, K is given by the Fermi-surface average $K\approx 2\rho_F^2\langle|\overline{V}_{\mathbf{kk}'}|^2\rangle_F$. A straightforward generalization to the case of a superconducting metal within the BCS theory gives (Black and Fulde, 1979)

$$f_{el}=\frac{4K}{\omega}\left[\int_{\Delta_c} dE g_E g_{E+\omega}[E(E+\omega)-\Delta_c^2](n_E-n_{E+\omega}) +\theta(\omega-2\Delta_c)\int_{\Delta_c}^{\omega-\Delta_c} dE g_E g_{\omega-E}[E(\omega-E)+\Delta_c^2] \times\left(\frac{1}{2}-n_E\right)\right]. \tag{46}$$

Here $g(E)=(E^2-\Delta_c^2)^{-1/2}$, and Δ_c is the superconducting energy gap. We note that this expression was derived by assuming a weak-scattering potential $V_{\vec{k}\vec{k}'}$. In the strong-coupling case one has also to take into account the change of the scattering matrix in the superconducting state. To our knowledge this effect has never been calculated (see, however, Prokof'ev, 1995).

This set of equations can be used for computing the tunneling rate over a wide temperature range both above and well below Θ down to the temperature where coherent band propagation (if any) sets in. All existing results concerning incoherent quantum diffusion in insulators, metals, and superconductors can be obtained directly from Eqs. (39) and (40). We shall analyze the high- and low-T limits for these equations in more detail in the corresponding sections devoted to metals and insulators to make it easier to connect them with the experiments. Here we shall only describe the crossover between the coherent and incoherent regimes in a perfect crystal to define the coherent tunneling amplitude and the crossover temperature.

By "coherent" we usually mean a motion that preserves phase correlations over a very long time scale. In our case it would require tunneling without exciting the environment, so that subsequent tunneling events could interfere. To find the coherent tunneling amplitude we consider the diagonal matrix element for the "dressed" amplitude in Eq. (37), i.e., $\Delta_{coh}=\Delta_o\langle R_{(\vec{n}+\vec{g},\vec{n})}\rangle$, with the final result

$$\Delta_{coh}=\Delta_o e^{B_o+2G(T)}\exp\left\{-\int_0^{\omega_o} d\omega\frac{f(\omega)}{2\omega}\coth\left(\frac{\omega}{2T}\right)\right\}. \tag{47}$$

Clearly, the answer crucially depends on the low-frequency limit of the spectral function f. The one-phonon interaction is not dangerous in this respect, because $f_{1ph}\sim\lambda_1\omega^{2+(2)}$ at low frequencies [the factor two in the parentheses corresponds to the "transport effect" in Eq. (31)]. On the other hand, both the two-phonon and the normal-electron couplings give $f(\omega)\to$const at low frequencies, and the integral in the exponent of Eq. (47) diverges. Since we expect (and prove below) that the crossover temperature is much less than ω_o and Θ, we use these inequalities to write the answer as

$$\Delta_{coh}=\Delta_o(T)\exp\{-\tau_{max}(\Omega_{2ph}+\Omega_{el})/2 +K[\Psi(1+1/(2\pi\tau_{max}T))-\Psi(1)]\}, \tag{48}$$

$$\Delta_o(T)=\Delta_o e^{B_o-\Phi(T)+G(T)}\left(\frac{2\pi T}{\gamma\omega_o}\right)^K, \tag{49}$$

$$\Omega_{el}=2\pi KT, \tag{50}$$

$$\Omega_{2ph}=\pi\sum_{\alpha\beta}|\overline{C}_{\alpha\beta}|^2(N_\alpha+1)N_\beta\delta(\omega_\alpha-\omega_\beta), \tag{51}$$

where $\Psi(1)=-\ln\gamma$ is Euler's constant, τ_{max}^{-1} is the formal low-energy cutoff and the damping rate is defined as the zero-frequency limit, $\Omega=\pi Tf(\omega\to 0)$. No matter how strong, the one-phonon polaron exponent

$$\Phi=\frac{1}{2}\sum_\alpha\frac{|\overline{C}_\alpha|^2}{\omega_\alpha^2}\coth(\omega_\alpha/2T) \tag{52}$$

and the barrier preparation effect G are saturated at low temperature and always preserve coherence. Indeed, as can be clearly seen from Eq. (39), when only one-phonon interaction is present, the integral over time diverges and is ill defined. In the past this difficulty was avoided by subtracting the coherent channel from Eq. (39) and treating the coherent tunneling separately (Flynn and Stoneham, 1970).

With the two-phonon or electron coupling added, the situation changes drastically. Let us analyze first whether coherence may exist even at $T=0$. Calculating Eq. (48), we made use of the unitary transformation relating the free and interacting environmental states assuming a *static* particle. If it is moving, and its lifetime in the well is given by τ, then the low-frequency divergence has to be cut at the energy scale $\tau_{max}=\tau$. If τ is defined by coherent delocalization, then $\tau^{-1}\approx 2\sqrt{2}\Delta_{coh}$ [see Eq. (14)]. Thus we arrive at a self-consistent equation for Δ_{coh}. At $T=0$ it reads (Schmid, 1983)

$$\Delta_{coh}=\Delta_o e^{B_o-\Phi+G}\left(\frac{2\sqrt{2}\Delta_{coh}}{\omega_o}\right)^K. \tag{53}$$

For $K<1$ the solution has the form

$$\Delta_{coh}=\Delta_o e^{(B_o-\Phi+G)/(1-K)}\left(\frac{2\sqrt{2}\Delta_o}{\omega_o}\right)^{K/(1-K)}, \tag{54}$$

(we remind the reader that the bandwidth is defined as $\Delta=2Z\Delta_{coh}$). In the superconducting state there is a natural low-energy cutoff at the superconducting energy gap Δ_c. If in the normal state we find $\Delta_{coh}\ll\Delta_c$, then no self-consistent solution is necessary, and one finds from Eq. (47) that at zero temperature

$$\Delta_{coh}=\Delta_o e^{B_o-\Phi+G}\left(\frac{e\Delta_c}{2\omega_o}\right)^K. \tag{55}$$

If $K\geqslant 1$ the only solution in the normal state is $\Delta_{coh}=0$, that is, coherence is suppressed even in the ground state and despite the translational symmetry of the crystal potential (disregarding longer-range hopping terms as those are of only academic interest in our case). The physical picture behind this phenomenon may be viewed as follows: In a very short time $t\ll\Delta_o^{-1}$ an electronic cloud is formed around the particle. Any attempt to tunnel should now involve a reconstruction of this cloud around another unit cell, which due to Anderson's "orthogonality catastrophe" (Anderson, 1967) severely suppresses the tunneling amplitude. Hence the "waiting" time becomes longer, which in turn allows the electronic cloud to extend in size, and its reshaping becomes even more difficult. For $K>1$ the process never stops, and the particle localizes at $T=0$. The important question of whether in a real muon problem, K can be larger than the critical value seems to have been answered in the negative. The general expression for K was given by Yamada (1984) and Yamada *et al.* (1986) as $K=1/8\pi^2\mathrm{Tr}\ \ln^2 S_{(\vec{n})}S^{-1}_{(\vec{n}+\vec{g})}$, where $S_{(\vec{n})}$ is the scattering matrix centered at point $\vec{n}$. All eigenvalues of the matrix $S_{(\vec{n})}S^{-1}_{(\vec{n}+\vec{g})}$ are equal to $e^{2i\delta_j}$ with $|\delta_j|\leqslant\pi/2$ (Kagan and Prokof'ev, 1989a); thus more than eight strong scattering channels (including spin degeneracy) are necessary to have $K>1$. The maximum value of K for the s-scattering case (which results in four scattering channels in this nonlocal scattering problem) is only 1/2 (Yamada *et al.*, 1986). It seems that the screened potential in most metals (Al, Cu, Nb) is simply not long ranged enough to generate many strong scattering channels.

Consider now nonzero temperature and $K<1$. At temperatures $2\pi T>\Delta_{coh}$ Eq. (48) simplifies to $\Delta_{coh}=\Delta_o(T)e^{-1/2\Omega\tau}$, again with $\tau^{-1}\approx 2\sqrt{2}\Delta_{coh}$. This equation has only a trivial solution $\Delta_{coh}=0$ for

$$\Omega>2e\sqrt{2}\Delta_o(T). \tag{56}$$

In metals the crossover happens at a temperature comparable with $\Delta_{coh}(0)$ itself. In insulators it is shifted to a higher temperature, $T\gg\Delta_{coh}$, but still $T\ll\Theta$. Thus we find that when the phase-correlation damping rate Ω becomes of the order of the particle bandwidth, the coherent delocalization stops. To be more precise it is suppressed exponentially, because incoherent transitions start contributing to τ^{-1}, but Δ_{coh} is exponentially small for $\Omega\gg\Omega_c$ and can be neglected. The same crossover point can be derived by analyzing the transition probability integral (39). One can easily verify that the time integral is convergent and well defined when two-phonon or electron couplings are present; thus no artificial procedure of subtracting the coherent channel is necessary. However, the very notion of the transition probability makes sense only if the time integral is convergent on a time scale $t\ll W^{-1}$. Since the convergence is governed by Ω and $W\sim\Delta_o(T)^2/\Omega$, we arrive at the same criterion for the onset of coherent motion.

E. Kinetic equation for spin depolarization in the hopping regime

In this subsection we establish a mathematical framework for the study of muon spin depolarization in the incoherent regime, when its dynamics is described as uncorrelated jumps, i.e.,

$$\frac{\partial F_{\vec{n}}(t)}{\partial t}=L(F)\equiv\sum_{\vec{g}}\left[F_{\vec{n}+\vec{g}}(t)W_{\vec{n}+\vec{g}\to\vec{n}}-F_{\vec{n}}(t)W_{\vec{n}\to\vec{n}+\vec{g}}\right], \tag{57}$$

where $F_{\vec{n}}(t)$ is the probability of finding the particle at site $\vec{n}$. Between jumps the particle spin is precessing in the local magnetic field $\dot{\vec{s}}(t)=-\gamma_\mu[(\vec{B}_o+\vec{B}(\vec{n}))\times\vec{s}(t)]$. One may then proceed in two ways. In computer simulations we first prepare a "sample," which is a 3D lattice of possible muon sites with the defect potential and random nuclear fields corresponding to a real crystal. Then we put a particle at random at some initial site and organize its random walk through the lattice according to the quantum diffusion theory and Eq. (57). For each trajectory thus generated, $\vec{n}(t)$, one may solve the equation for spin evolution to obtain $\vec{s}_{(traj)}(t)$. The statistical sum of the results for spin evolution gives for polarization function $\vec{P}_{theor}(t)=\langle\vec{s}_{(traj)}(t)\rangle_{traj}$. In this way we can directly compare the theory and experiment, thus avoiding artificial model fitting. This approach, however useful, nevertheless masks our understanding of why the final results have the particular time decay of $\vec{P}(t)$ or why we get an unusual temperature dependence of the depolarization rate. We thus consider below an alterna-

tive approach, which allows us to gain a much deeper insight into the physics involved.

Since the μSR experiment is statistical in nature, we have to average the results of spin evolution over all possible starting points and particle trajectories. The first average is equivalent to considering an ensemble of noninteracting muons forming a "spin liquid" with constant density, $\vec{s}(\vec{n},t=0)=\vec{s}_o=\text{const}$. Statistically, we now have to think not about the trajectories of a single particle, but rather about the diffusion flows in this liquid. The muon polarization function is the sum over the lattice sites,

$$\vec{P}(t)=N^{-1}\sum_{\vec{n}}\vec{s}(\vec{n},t), \tag{58}$$

with the spin-distribution function obeying an equation of motion

$$\dot{\vec{s}}(\vec{n},t)-L(\vec{s})=-\gamma_\mu[(\vec{B}_o+\vec{B}(\vec{n}))\times\vec{s}(\vec{n},t)], \tag{59}$$

i.e., the change of the spin density at point $\vec{n}$ is due to particle transitions between the lattice sites and spin rotation in the total magnetic field [the operator $L(\vec{s})$ is identical to the operator $L(F)$ in Eq. (57)]. The statistical average also means that we have to average over the realizations of the nuclear fields. After this procedure the effect of the local nuclear fields is to "evaporate" (depolarize) the spin liquid, with the depolarization rate $\Lambda(\vec{n},t)$ depending on the local muon motion (Kagan and Prokof'ev, 1987, 1991),

$$\dot{\vec{s}}-L(\vec{s})=-\gamma_\mu[\vec{B}_o\times\vec{s}(\vec{n},t)]-\Lambda(\vec{n},t)\vec{s}(\vec{n},t). \tag{60}$$

Thus we arrive at a picture in which the initially homogeneous distribution has to evolve toward its equilibrium distribution in the presence of the defect potential, $\vec{s}_{eq}(\vec{n})\propto e^{-V_{inh}(\vec{n})/T}$ (for simplicity we assume that in a perfect crystal all relevant muon sites have the same energy) while being "evaporated" with a spatially inhomogeneous depolarization rate $\Lambda(\vec{n},t)$.

For $t\gg\tau$ the depolarization rate takes the form (motional narrowing)

$$\Lambda(\vec{n},t)=\delta_{eff}^2\tau(\vec{n}), \tag{61}$$

where δ_{eff}^2 depends on the experimental geometry (see Sec. IV), and the local correlation time is given by the integral (14) with the site-dependent probability of return $C(\vec{n},t)$ [formally $C(\vec{n},t)=G(\vec{n},\vec{n}'=\vec{n},t)$, where G is the lattice Green's function: $\dot{G}-L(G)=\delta(t)\,\delta(\vec{n}-\vec{n}')$].

1. Long-range trapping

At low temperatures even rather weak defect potentials introduce traps for muons with binding energies $E_t\sim U_o\gg T$. Assuming the long-ranged character of the potential we can calculate the trapping rate Λ_{tr} from Eq. (57) in the continuum limit assuming smooth variation of $\epsilon_{\vec{n}}\equiv V_{inh}(\vec{n})$ and $F(\vec{n},t)$ on $\vec{n}$:

$$\frac{\partial F}{\partial t}+\text{div}\,\vec{J}=0,\quad \vec{J}_\alpha=-D_{\alpha\beta}\frac{\partial F}{\partial\vec{r}_\beta}+\vec{v}_\alpha F, \tag{62}$$

where the diffusion tensor and the "hydrodynamic" velocity

$$D_{\alpha\beta}(\vec{r})=\frac{1}{2}\sum_{\vec{g}}\vec{g}_\alpha\vec{g}_\beta W_{\vec{r},\vec{r}+\vec{g}}, \tag{63}$$

$$\vec{v}_\alpha=-\frac{D_{\alpha\beta}(\vec{r})}{T}\frac{\partial V_{inh}(\vec{r})}{\partial\vec{r}_\beta} \tag{64}$$

are defined via the local transition probabilities. At low impurity concentration, trapping proceeds independently at each defect center, and the total trapping rate Λ_{tr} is proportional to n_{im}. To calculate the trapping rate at a given defect center we adopt for simplicity the spherical symmetry of the problem and make use of the standard quasistationary solution of Eq. (62) in the form $\Lambda_{tr}=n_{im}4\pi r^2J(r)$, with $r^2J(r)=\text{const}$, and the boundary conditions $F(0)=0$ and $F(\infty)=n_{im}$ (Waite, 1957). One finds then

$$\Lambda_{tr}=\frac{4\pi n_{im}}{\left\{\int dr\,\dfrac{\exp\{V_{inh}(r)/T\}}{r^2D(r)}\right\}}=4\pi c_t n_{im}R_TD(T,R_T), \tag{65}$$

where $c_t\sim1$ is a numerical coefficient, and the trapping radius is defined by the condition $|V_{inh}(R_T)|=T$, or

$$R_T=a(U_o/T)^{1/3}. \tag{66}$$

First, we note that the trapping radius depends on temperature and $R_T\gg a$ at low T. Second, the temperature dependence of the diffusion coefficient at the trapping radius can differ drastically from $D(T)$ in a perfect crystal, because it is defined in the region where the impurity potential is relatively strong. We shall see below how the theory works for particular examples, such as superconducting Al and insulating crystals.

2. Inhomogeneous T_2 relaxation

In this section we consider a peculiar depolarization mechanism, which is due to the diffusion's slowing down near the impurity. It applies to the case of transverse relaxation, which is the fastest for static particles. In many cases (see theory sections devoted to metals and insulators) impurity-induced bias between the neighboring lattice sites, $\xi(\vec{n},\vec{g})=\epsilon_{\vec{n}+\vec{g}}-\epsilon_{\vec{n}}$, suppresses incoherent tunneling, and

$$D(T,r)\sim\xi(r)^{-2}\propto r^s, \tag{67}$$

where the exponent s is defined by the impurity potential derivative. For the strain field $s=8$. For the oscillating potential (25) we find $\xi(r)\sim r^{-3}$ ($s=6$). The mechanism we shall consider here is of importance only if the particle depolarizes *before* it is trapped; thus we shall ignore the velocity term in the mass current Eq. (62).

To find the depolarization rate we have to solve Eqs. (60) and (61) with $\tau(r)$ related to the diffusion coefficient $\tau \approx a^2/4D$. When the particle motion becomes very slow its spin density "evaporates." This induces the diffusion flow toward the impurity center due to the gradient in the spin distribution function. To solve the problem we follow the same procedure as in the case of trapping and consider the stationary equation (spherically symmetric)

$$\frac{1}{r^2}\frac{\partial}{\partial r} r^2 D(r) \frac{\partial}{\partial r} s(r) = \Lambda(r) s(r), \tag{68}$$

with the boundary conditions $s(0)=0$ and $s(\infty)=1$. The depolarization rate is defined by the integral $\Lambda_* = 4\pi n_{im} \int_0^\infty \Lambda(r) s(r) r^2 dr$. For arbitrary power dependence of $D(r)$, Eq. (68) can be solved analytically with the result

$$\Lambda_* = (4\pi c_* n_{im} R_*^2 a)\,\delta. \tag{69}$$

Here c_* is a numerical coefficient of order 1, and the depolarization radius R_* is defined explicitly from

$$\delta\tau(R_*) = \frac{s+1}{2}\left(\frac{a}{R_*}\right). \tag{70}$$

In fact, the radius R_* is nothing but the distance from the defect where the muon completely depolarizes before diffusing at a distance of order R_*.

The most remarkable feature of Eq. (69) is that it depends on quantum diffusion implicitly through the radius R_* only. This happens because the depolarization rate in the motional narrowing regime is inversely proportional to the diffusion rate D, while the rate at which particles may get to the slow-motion region is proportional to D; as a result, the diffusion rate drops from the final answer. What is left is the volume of strong depolarization regions defined by R_*. It follows from Eq. (70) that the temperature dependence of the effective depolarization rate is much weaker than expected from the $D(T)$ dependence in a perfect crystal (Kagan and Prokof'ev, 1987, 1990a),

$$\Lambda_* \propto R_*^2 \propto \Omega^{-2/(s-1)}. \tag{71}$$

Thus in a transverse field we may approximately divide the crystal volume into two parts: one part consisting of all those regions of radius R_* around the defects, where the hop rate is small and particles are static, the other consisting of the rest of the crystal volume where particles move fast with the hop rate $\overline{\tau}$ and depolarize only when they happen to approach the defect center too closely [we assume here that $R_* < \overline{R} = (4\pi n_{im}/3)^{-1/3}$; otherwise $R_* = \overline{R}$]. We then write the polarization function as

$$P_{TF} \approx (1-f_*) e^{-\Lambda_* t - \delta^2 \overline{\tau} t} + f_* g(t), \tag{72}$$

where $f_* = V(R_*) n_{im} = (4\pi/3) R_*^3 n_{im}$ and $g(t)$ is the static relaxation function (see next section).

3. Inhomogeneous T_1 relaxation

The physics of inhomogeneous longitudinal relaxation at low temperatures is completely different, because in a strong enough magnetic field the local depolarization rate is proportional to the inverse τ (see Sec. IV.B below). More precisely, $\Lambda(\vec{r}) = 2\delta^2/[\omega^2 \tau(\vec{r})]$ where ω is the Zeeman energy and we assume that $\omega\tau(\vec{r}) \gg 1$. Now particles that are far from impurities and diffuse rapidly determine the longitudinal relaxation rate T_1^{-1}, and the low-n_{im} approximation as for T_2^{-1} is not valid. In this case the only characteristic distance is $\overline{R}$. Suppose that diffusion is so slow that muons depolarize locally, and there is no particle exchange between different parts of the crystal during the measurement time. It is then possible simply to average the polarization function over the sample and write (Storchak *et al.*, 1995)

$$P_{LF}(t) = \int \frac{dV}{V} e^{-\Lambda(\vec{r}) t}. \tag{73}$$

One may further substitute the power-law dependence $\tau(r)^{-1} = \overline{\tau}^{-1} (r/\overline{R})^{-s}$ in Eq. (73) in order to express the answer in terms of a single dynamic parameter $\overline{\tau}^{-1}$—the typical hopping rate far from impurities.

The validity of Eq. (73) depends on the impurity concentration. During the local depolarization time $\Lambda^{-1}(\vec{r})$, the particle moves over a distance $\Delta r \sim a/\sqrt{\Lambda\tau} \sim a\omega/(2^{1/2}\delta)$, which is independent of τ. The assumption of local depolarization holds as long as $\Lambda(r+\Delta r)/\Lambda(r) \sim s\Delta r/r < 1$. Since the dominant contribution to the relaxation comes from distances $r \sim \overline{R}$ we conclude that Eq. (73) is valid only for $n_{im} < n_c$ where

$$n_c = \frac{3}{\sqrt{2}\pi a^3}\left(\frac{\delta}{s\omega}\right)^3. \tag{74}$$

When $n_{im} > n_c$, the majority of particles experience all relevant diffusion rates during their longitudinal relaxation time. In this case the relaxation is exponential with T_1^{-1} obtained by a simple average over the volume,

$$P_{LF} = e^{-\langle T_1^{-1}\rangle t}, \quad \langle T_1^{-1}\rangle = \int \frac{dV}{V} \Lambda(\vec{r}). \tag{75}$$

It should be noted, however, that in the case of slow diffusion one can expand the exponent in (73) up to the second term and get the same result for $\langle T_1^{-1}\rangle$ at short times, thus the regions of validity of Eqs. (73) and (75) overlap.

IV. EXPERIMENTAL TECHNIQUES

The techniques of muon spin relaxation have been described in detail in a number of excellent reviews (Schneck, 1985; Cox, 1987; Brewer, 1994). As mentioned in the Introduction, the quantity that is directly measured is the polarization as a function of time, $P(t)$. This has a different functional form depending on the experimental conditions.

A. Transverse-, zero-, and longitudinal-field muon spin relaxation

The simplest μ^+SR technique for μ^+ diffusion studies is the transverse-field muon spin rotation experiment, in

which a large (with respect to internal nuclear magnetic fields) external magnetic field B_o is applied perpendicular to the muon polarization, causing the muon spin to precess about the external field. Due to the random orientation of the nuclear moments, muons experience different local field at different unit cells. As a result, there is a continuum of frequencies which can be parametrized with a Gaussian envelope,

$$P_x(t)=\exp\left(-\frac{1}{2}\delta^2t^2\right)\cos\,\omega_\mu t. \tag{76}$$

This applies if the muons are fixed in the lattice sites. In the fast-diffusion regime ($\delta\tau_c\ll 1$) the time evolution of $P(t)$ is determined by the phenomenon well known from NMR as motional narrowing (Abragam, 1961). In this regime the polarization decay is given by

$$P_x(t)=\exp(-T_2^{-1}t)\cos\,\omega_\mu t, \quad T_2^{-1}=\delta^2\tau_c. \tag{77}$$

This phenomenon forms the basis for the muon diffusion studies first carried out by Gurevich *et al.* (1972).

The smallest relaxation rate accessible by μ^+SR is basically limited by the muon lifetime. In a real experiment special arrangements should be made to reliably measure a μ^+ relaxation rate lower than about 10^4 s^{-1}. The local field from nuclear magnetic moments for the interstitial position in a metallic lattice is about 1 G, which corresponds to a typical value of δ of about 10^5 s^{-1}. Therefore, the highest muon hop rate in metals measured by transverse-field μ^+SR does not exceed 10^7 s^{-1}. The fastest relaxation rate of the μ^+SR signal that can be measured is limited by the dead time of the electronics which registers the incoming muons and outgoing positrons. This time typically does not exceed 10 ns. Therefore, the lower limit on the μ^+ hop rate that can be measured by the transverse-field technique is set by δ (Slichter, 1980).

In zero-field and longitudinal-field techniques some of these limitations are absent, which allows one to get more information on μ^+ dynamics. The time evolution of the muon polarization function in zero field and in a longitudinal field is formulated in the classical treatment of Kubo and Toyabe (1967; see also Hayano *et al.*, 1979). In the approximation of isotropic static local fields with a Gaussian distribution

$$P(\vec{B})\sim\exp\{-\gamma_\mu^2B^2/(2\delta^2)\} \tag{78}$$

the μ^+ relaxation function in zero field for a static muon is given by the Kubo-Toyabe formula

$$P_z^{KT}(t)=\frac{1}{3}+\frac{2}{3}(1-\delta^2t^2)\exp\left(-\frac{1}{2}\delta^2t^2\right). \tag{79}$$

It should be noted that the initial ($t\ll\delta^{-1}$) relaxation is faster than in a transverse field because $P_z^{\mathrm{KT}}(t)\approx 1-\delta^2t^2$. This circumstance reflects the fact that in zero field the muon interaction with the nuclei is determined by the full dipole Hamiltonian, while in a transverse field by the so-called *secular* part of it only (Slichter, 1980). The difference in relaxation rates may be not just $\sqrt{2}$, but as large as $\sqrt{5}$ (Hayano *et al.*, 1979). This fact can be taken as an unquestionable advantage of the zero-field technique over the transverse-field one, as it effectively extends the time scale limited by the muon lifetime. Moreover, at short times one has more muons and, therefore, the zero-field technique also has an advantage over the transverse-field technique in collecting necessary statistics. The 1/3 asymptotic component in Eq. (79) comes from muons' having spin polarization initially aligned with the local magnetic field. The remaining 2/3 of the muon polarization undergoes relaxation in transverse local fields.

The muon polarization function in longitudinal fields, where an external field is applied along the initial muon polarization, can be derived the same way as in zero field (Hayano *et al.*, 1979). The asymptotic value of the μ^+ polarization in longitudinal fields is always higher than 1/3, approaching 1 at high longitudinal fields. Usually this relatively simple Kubo-Toyabe model gives results precise enough to evaluate the muon polarization in both zero and longitudinal fields in the static case. However, direct theoretical calculation of μ^+ polarization function by solving the spin Hamiltonian for the muon plus its nearest neighboring nuclei in the lattice (Celio, 1986a) allows for a more accurate comparison with experiment (Luke *et al.*, 1991).

To move to the dynamic case, one has to solve the spin Hamiltonian of the system "muon plus magnetic environment" in the presence of μ^+ diffusion. In general, this is a very complicated problem, as for low magnetic field several terms in the Hamiltonian (like the dipole and quadrupole terms) cannot be treated as perturbations. However, the muon polarization function for a diffusing particle can be described precisely enough by "dynamicizing" (under certain assumptions) the static polarization function for both zero and longitudinal fields (Hayano *et al.*, 1979). The muon diffusion is often approximated in the framework of a stochastic model for the time evolution of a local field, experienced by the moving μ^+, assuming a Markovian process (the so-called *strong-collision model*),

$$\langle B_i(t+\tau_c)B_i(\tau_c)\rangle=\delta^2/\gamma_\mu^2e^{-t/\tau_c} \quad i=x,y,z. \tag{80}$$

Equation (80) assumes that there are no correlations between the local field experienced by μ^+ before and after the hop, and one identifies τ_c^{-1} with the hopping rate τ^{-1}. This model is just an approximation of Eqs. (59) and (60) for the homogeneous case, simple enough to derive an analytic solution suitable for the experimental fittings of dynamic effects. The probability that μ^+ is still at its initial site is approximated here by an exponential law. This assumption neglects the effect of "back diffusion," which brings the particle to already visited sites (Celio, 1986b); for the same reason $a^2\tau^{-1}$ and D are related by a factor 1/4 instead of 1/6 (see Sec. III). Figure 1 shows polarization functions for zero field and longitudinal field for different muon hop rates obtained numerically in the framework of the strong-collision model (Luke *et al.*, 1991).

In the slow-hopping limit ($\tau_c^{-1}\ll\delta$) for long times ($t\gg\delta^{-1}$), the μ^+ polarization function is expressed by a

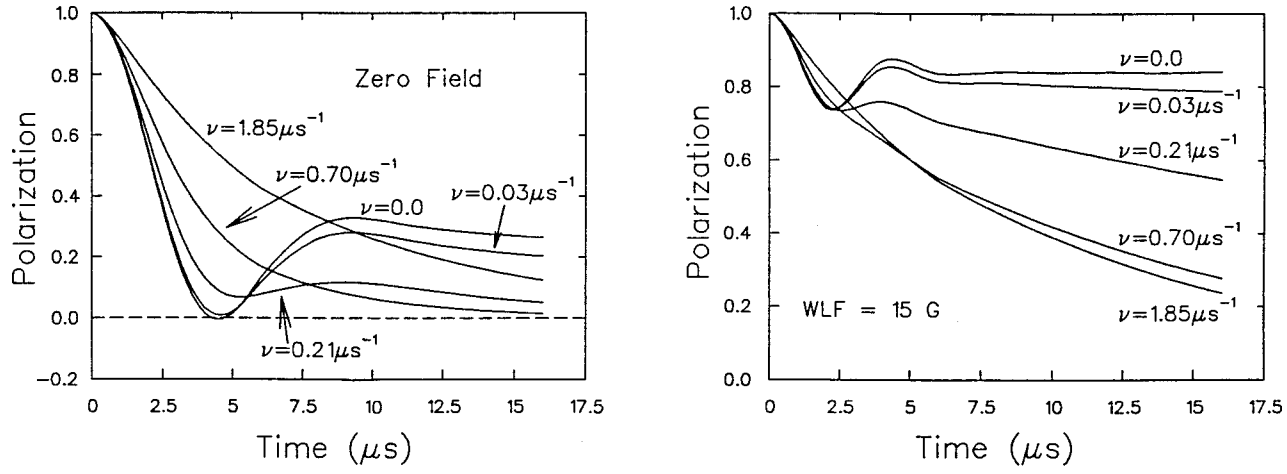

FIG. 1. Muon polarization functions for zero field and weak longitudinal field for several muon hop rates, calculated using the strong-collision model (Luke *et al.*, 1991).

simple exponential decay of the "$\frac{1}{3}$ tail" in the zero-field static Kubo-Toyabe expression

$$P_z(t)\simeq\frac{1}{3}\exp\left(-\frac{2}{3}\tau_c^{-1}t\right), \tag{81}$$

which is independent of δ. The value of δ can be extracted from $P(t)$ at short times where it is independent of τ_c^{-1}. Thus, in a zero-field experiment the form of the μ^+ polarization function allows one to extract independently τ_c^{-1} and δ even in the low-τ_c limit, in contrast to a transverse-field experiment. In the fast-hopping limit ($\delta\ll\tau_c^{-1}$), the polarization function is exponential,

$$P_z(t)\simeq\exp(-2\delta^2\tau_c t). \tag{82}$$

The minimum in $P(t)$ then disappears, as can be seen in Fig. 1.

In real zero-field μ^+SR measurements the experimental time range limited by the muon lifetime is sometimes not long enough for the asymptotic "tail" to be observed with the required precision in order to determine the μ^+ hop rate. In this case the weak-longitudinal-field technique, which has several essential advantages over both zero-field and transverse-field methods, can be applied. First, the amplitude of the μ^+ polarization "tail" in a weak longitudinal field is higher than 1/3. Second, this "tail" is shifted to earlier times, where there are statistically more muons (an effective stretch of the μ^+SR time window). Moreover, the change in shape of $P(t)$ versus τ is more pronounced in a weak longitudinal field. In addition, it is sometimes impossible to distinguish the almost static case with different muon site occupation (and, subsequently, different δ) from the fast-dynamics regime in zero field (Petzinger, 1980, 1981), while in a weak longitudinal-field the static case is easily distinguished from the dynamic one. Therefore, the weak-longitudinal field technique developed by Brewer *et al.* (1986, 1987) often seems to be the most adequate one for μ^+ diffusion measurements (at least in the slow-diffusion regime).

B. Transverse-, zero-, and longitudinal-field muonium spin relaxation

Since μ^+ is much heavier than an electron, the electronic structure of the Mu atom is almost the same as that of the H atom, and Mu can be considered as a light hydrogen isotope. This establishes a close analogy between the muonium spin resonance MSR and electron-spin resonance (ESR) techniques. Although the instrumental arrangements of these techniques are quite different, the physical concepts of the spin-relaxation mechanisms could be directly transferred from ESR and NMR (Abragam, 1961; Poole, 1967; Slichter, 1980).

The effective spin Hamiltonian of muonium in the crystals in the case of isotropic hyperfine and nuclear hyperfine interactions has the form

$$\mathcal{H}=A\vec{\mathbf{S}}_e\cdot\vec{\mathbf{S}}_\mu-g_e\mu_B\vec{\mathbf{S}}_e\cdot\vec{\mathbf{B}}-g_\mu\mu_\mu\vec{\mathbf{S}}_\mu\cdot\vec{\mathbf{B}}$$
$$+\sum_n\delta_{Mu}\vec{\mathbf{S}}_e\cdot\vec{\mathbf{S}}_n-\sum_n g_n\mu_n\vec{\mathbf{S}}_n\cdot\vec{\mathbf{B}}, \tag{83}$$

where A is the muonium hyperfine frequency (about 2.8×10^{10} s^{-1} rad for the ground state in vacuum), and the $\vec{\mathbf{S}}$, g, and μ are, respectively, the spins, g factors, and magnetic moments of the various particles. The summations are over all nearby nuclei. The nuclear hyperfine interaction between the muonium electron and neighboring nuclear dipoles is characterized by the parameter δ_{Mu} (we have neglected a possible nuclear quadrupole interaction).

Qualitatively, modulation of the nuclear hyperfine interactions results in relaxation of the muonium electron spin, which in turn leads to depolarization of the muon spin via the muonium hyperfine interaction. As the muonium hyperfine frequency usually turns out to be several orders of magnitude higher than the nuclear hyperfine frequency, it is the nuclear hyperfine interaction which sets the time scale for muonium spin relaxation.

The first three terms in Eq. (83) are known as the Breit-Rabi Hamiltonian. Its four eigenvalues are given by

$$E_{1,3}=+\frac{1}{4}A\pm A\frac{\Gamma_-}{2\Gamma_+}x,\quad E_{2,4}=-\frac{1}{4}A\mp\frac{1}{2}A\sqrt{1+x^2},$$

where $\Gamma_\pm=\frac{1}{2}(g_e\mu_B\pm g_\mu\mu_\mu)$ and $x=2\Gamma_+B/A$. The dependence of the energy eigenvalues on the applied magnetic field is presented by the so-called Breit-Rabi diagram (see, for example, Schenck, 1985).

For simplicity the nuclear hyperfine interaction term is represented as isotropic in Eq. (83). The inclusion of this term and the nuclear Zeeman interactions causes energy-level splittings, which result in a very complicated MSR spectrum (Patterson, 1988). However, there are several limiting cases in which one can form an opinion on the time evolution of the muon polarization function.

Let us forget for a moment about the last two terms in Eq. (83). When the Zeeman interaction is small compared with the hyperfine interaction, one usually observes four (out of six) allowed transitions between the Breit-Rabi levels: ω_{12}, ω_{23}, ω_{34}, and ω_{14} (here $\omega_{\alpha\beta}=E_\alpha-E_\beta$). All transitions that constitute a flip of the muon spin lead to reduction of the muon polarization. Precession frequencies of the order of A (typically about 10^{10} s^{-1}) are too high to be observed by the conventional μ^+SR spectrometers (this restriction comes from the limited time resolution). In a low transverse field one may also neglect the x^2 terms and write approximately

$$\omega_{12}=\omega_{23}=\omega_{\rm Mu}=\Gamma_-B. \tag{84}$$

This is the well-known phenomenon of the *triplet muonium precession*. It is standard practice to reveal Mu formation in the sample by observation of this precession signal with the characteristic frequency 1.39 MHz/Oe in magnetic fields below about 10 Oe. At higher fields $\omega_{\rm Mu}$ splits into two triplet Mu frequencies, ω_{12} and ω_{23}, from which one can obtain the hyperfine frequency A using

$$A=\frac{1}{2}\left[\frac{(\omega_{12}+\omega_{23}+2\omega_\mu)^2}{\omega_{23}-\omega_{12}}+\omega_{12}-\omega_{23}\right]. \tag{85}$$

In a transverse magnetic field low enough to observe only one line ω_{12}, which is, however, higher than the nuclear hyperfine frequency ($\omega_{\rm Mu}\gg\delta_{\rm Mu}$), we have the familiar situation from the transverse-field technique for μ^+ diffusion measurements. Expressions (76) and (77), as well as the corresponding discussion of the relaxation process, apply equally well to Mu. It should be noted, however, that the Mu precession frequency exceeds that of μ^+ by a factor of about 103 in the same transverse field. Therefore the effect of dephasing (or frequency "spread") for Mu atoms precessing in different local fields is enhanced greatly over that for μ^+. Now, for a static Mu atom one finds $T_2^{-1}\geqslant 10^7$ s^{-1}. Such a high relaxation rate is close to the upper limit of the standard spectrometers. In fact, in many solids the Mu relaxation rate is further enhanced by contact interaction, which may be much stronger than the dipole one. Also, in transverse fields higher than about 10 Oe the intratriplet frequencies are split, which introduces unnecessary complication into the analysis. Thus muonium T_2^{-1} measurements are restricted to being carried out in rather low transverse fields, which are sometimes comparable with the local magnetic fields (this makes the MSR signal linewidth comparable to its frequency). Finally, precession amplitude of Mu drops by a factor of 2 due to the distribution of the Mu polarization between singlet and triplet states. All of the above reasons make T_2^{-1} measurements of static Mu relaxation in crystals very complicated if not impossible. However, if the Mu atom diffuses rapidly in the lattice its relaxation rate is measurable in low transverse fields. Figure 2 shows a perfect example of MSR time spectra taken in solid nitrogen (s-N_2) at different temperatures in order to measure Mu dynamics in a low transverse field (Storchak *et al.*, 1993). Solid nitrogen presents one of those rare cases when T_2^{-1} for muonium remains in the "MSR window" in the entire measured temperature range.

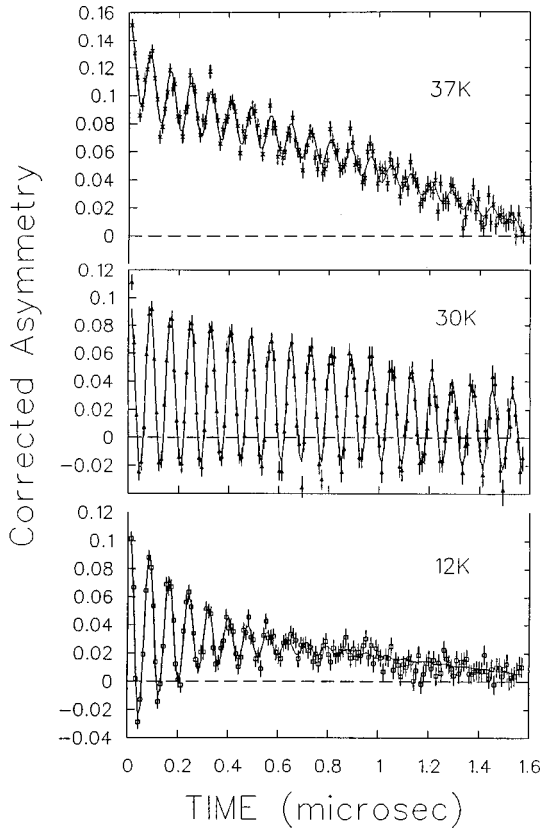

FIG. 2. Muonium precession signals in s-N_2 in a transverse magnetic field of 8.9 Oe at several temperatures (Storchak *et al.*, 1993).

It is, however, possible to extend muonium diffusion measurements by several orders of magnitude in the hop rate by applying the longitudinal-field technique. If the Mu atom is static, the polarization function is known to be (Beck *et al.*, 1975)

$$P_z(t)=1-\frac{1-\cos(A\sqrt{1+x^2}t)}{2(1+x^2)}\to\frac{1+2x^2}{2(1+x^2)}, \tag{86}$$

in a relatively high longitudinal field ($\Gamma_\pm B\gg\delta_{\rm Mu}$). The oscillating component is unresolvable in the standard MSR experiments and averages to zero. The Mu longi-

tudinal spin relaxation can then be evaluated using Redfield's theory (see, for example, Slichter, 1980) by treating the nuclear hyperfine interaction as an effective time-dependent (due to Mu diffusion) magnetic field acting on the Mu electron, which causes transitions between the coupled spin states of the electron and muon. A general expression involves various transitions, but a reasonable approximation is obtained by considering the lowest-frequency transition (within the muonium triplet spin states), leading to an exponential T_1^{-1}-relaxation of the residual non-oscillating component (86):

$$P_z(t)=\frac{1+2x^2}{2(1+x^2)}e^{-t/T_1},$$

$$T_1^{-1}\approx\left(1-\frac{x}{\sqrt{1+x^2}}\right)\frac{2\delta_{\rm Mu}^2\tau_c}{1+\omega_{12}^2\tau_c^2}. \tag{87}$$

For $x\ll 1$, i.e., in a weak field, Eq. (87) reduces to

$$T_1^{-1}=\frac{2\delta_{\rm Mu}^2\tau_c}{1+\omega_{\rm Mu}^2\tau_c^2},\quad (T_1^{-1})_{max}=\frac{\delta_{\rm Mu}^2}{\omega_{\rm Mu}}, \tag{88}$$

where $\omega_{\rm Mu}=\gamma_{\rm Mu}B$, $\gamma_{\rm Mu}$ is the muonium gyromagnetic ratio.

The main feature of Eq. (88) is the well-known T_1^{-1}-maximum (better known from NMR as a T_1-minimum effect; Slichter, 1980) at $\omega_{\rm Mu}\tau_c=1$. The observation of the T_1-minimum effect allows an independent determination of the nuclear hyperfine frequency $\delta_{\rm Mu}$ and an absolute calibration of the muonium hop rate (Celio, 1987; Yen, 1988). Figure 3 shows an example of T_1^{-1} measurements in which longitudinal muonium spin relaxation was proved to be due to Mu diffusion in the lattice of a solid nitrogen crystal (Storchak *et al.*, 1994a). The temperature dependence of the T_1^{-1} is shown in Fig. 4. The T_1^{-1} maxima are clearly seen at all longitudinal fields used in the experiment. At temperatures above about 12 K, T_1^{-1} becomes independent of magnetic field, as is expected in the fast-hopping regime ($\omega_{\rm Mu}\tau_c\ll 1$) according to Eq. (88). The undoubted advantage of the longitudinal-field technique is the fact that one can choose the magnitude of the applied field to put T_1^{-1} values into the MSR window (the most convenient range of the T_1^{-1} is between 10^5 s^{-1} and 10^7 s^{-1}). This approach is restricted to the limit of relatively high longitudinal fields, however, since the effective magnetic-field approximation is valid only if $\gamma_e B \gg \delta_{\rm Mu}$.

Measurements in zero field and weak longitudinal fields turn out to be much more sensitive to slow muonium dynamics (as they are to slow μ^+ diffusion), at least when relaxation is due to dipole interactions with neighboring nuclei. This is due primarily to the fact that these techniques involve the full dipole Hamiltonian rather than its secular part (as is adequate for the transverse-field technique; see, for example, Slichter, 1980). The approach of Kubo and Toyabe (1967) is equally applicable for the triplet state of muonium, which can be treated in low magnetic field as one particle with spin $S=1$. However, the observation of Kubo-Toyabe-type relaxation for Mu is impossible in most solids, because its characteristic minimum is shifted to the dead time of a μSR spectrometer (because of the huge value of $\delta_{\rm Mu}$). The "1/3 tail" forms a time-independent baseline that cannot be distinguished from any other instrumental baseline. To observe Kubo-Toyabe relaxation for Mu one has to choose a solid with a low abundance of magnetic nuclear isotopes in order to reduce the value of $\delta_{\rm Mu}$ and to shift the minimum of $P^{KT}(t)$ to the experimentally observable time range. The basic idea is to use the next-nearest neighbors as a source of Mu relaxation; the ideal situation for the hcp lattice is to have about 10% of nonzero magnetic moments. Also, the compensation of any kind of external magnetic field should be made to the level of about 10 mOe; this pro-

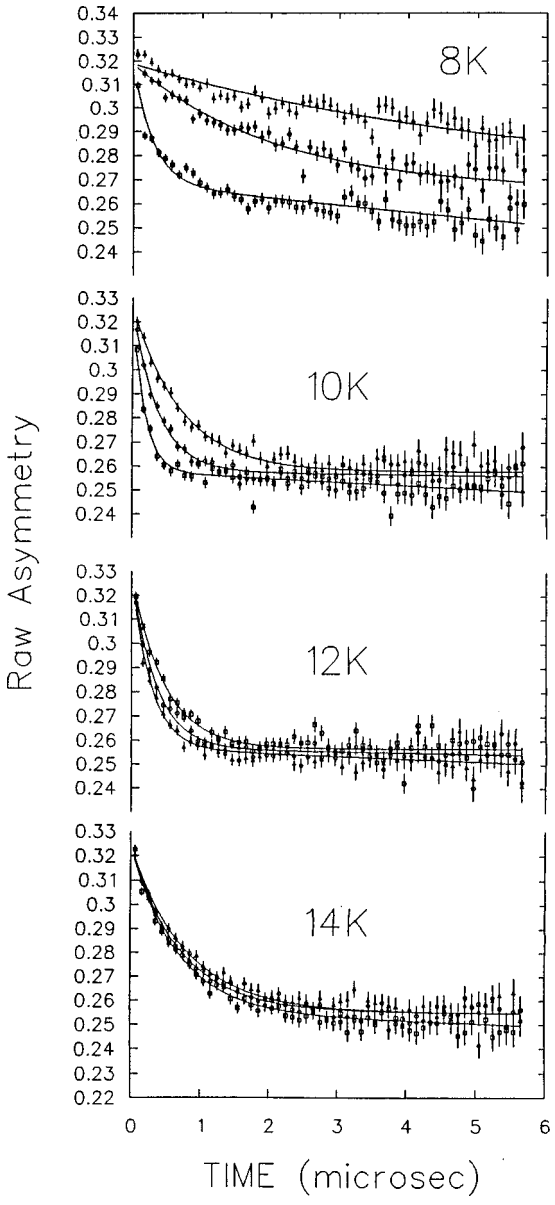

FIG. 3. μSR spectra in a longitudinal field in solid nitrogen at different temperatures: ▲, for $B_\parallel=4$ G; ●, 8 G; □, 12 G (Storchak *et al.*, 1994a).

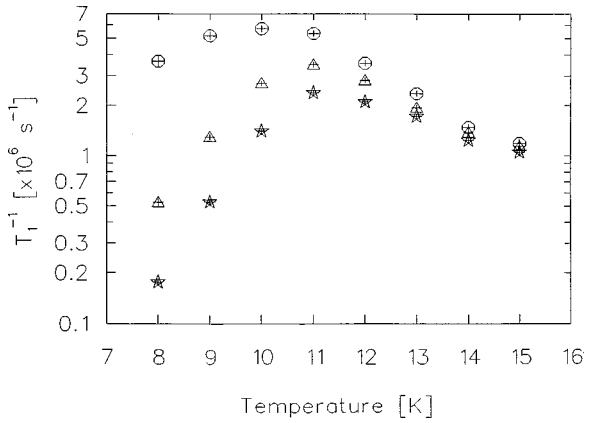

FIG. 4. Temperature dependences of Mu relaxation rates in solid N_2 in several longitudinal fields: stars, 12 G; △, 8 G; ⊕, 4 G (Storchak *et al.*, 1994a).

cedure can be done using the Mu atom as a magnetometer (the technique invented and adopted by J. H. Brewer).

This idea was successfully implemented in a recent experiment in solid krypton (s-Kr), which possesses only 11.55% of the isotope ^{83}Kr with a nonzero nuclear magnetic moment (Storchak *et al.*, 1996). Figure 5 presents the time spectrum of the Mu polarization in s-Kr at low temperature, where it is believed to be static. The line drawn through the experimental points represents a best fit to a "dynamicized" version (Brewer *et al.*, 1987; Luke *et al.*, 1991) of Eq. (79), taking into account sites both with and without nearest-neighbor ^{83}Kr nuclear spins. The former contribute a Kubo-Toyabe function with its characteristic minimum shifted to very early times. The "1/3 tail" of this component constitutes a baseline to the Kubo-Toyabe relaxation due to more distant nuclear spins at the latter type of sites. For comparison, Fig. 5 also shows the muonium polarization function (stars) in solid Kr for a weak longitudinal field of 5 G. This experiment allowed direct [see Eq. (81)] measurement of Mu hop rates two orders of magnitude slower than the inverse μ^+ lifetime by using both zero field and weak longitudinal field, in a regime of such slow dynamics that it was previously inaccessible. The ideas, advantages, and limitations of the weak-longitudinal-field technique for Mu diffusion measurements are analogous to those for μ^+. Figure 6 shows an example of the application of the weak-longitudinal-field technique for measurements of very slow Mu diffusion in a solid.

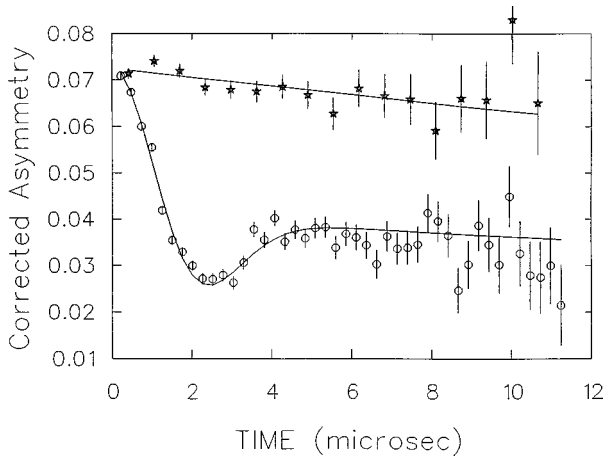

FIG. 5. Time dependence of the muonium polarization in solid Kr at $T=20.3$ K: ○, in zero magnetic field; stars, in a weak longitudinal magnetic field $B=5$ G. Note the Kubo-Toyabe form of the muon polarization function in zero magnetic field (Storchak *et al.*, 1996).

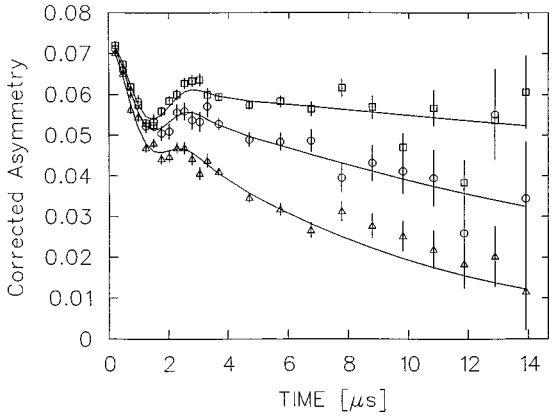

FIG. 6. Muonium polarization time spectra in solid Kr in a very weak longitudinal magnetic field $B=0.22$ G at different temperatures: □, 25 K; ○, 28 K; △, and 30 K (Storchak *et al.*, 1996).

V. QUANTUM DIFFUSION OF μ^+ IN METALS

A. Transition probabilities and diffusion rates in metals and superconductors

In this section we present more specific expressions derived from Eq. (39) for the case of particle diffusion in metals. We begin with the transition probability in the low-temperature limit. In metals, phonons do not influence quantum diffusion in any significant way at $T \ll \Theta$, and their only effect is the renormalization of the tunneling amplitude (49). We find then from Eq. (39) (Fisher and Dorsey, 1985; Grabert and Weiss, 1985; Kagan and Prokof'ev, 1986)

$$W(\xi,T)=2\frac{\Delta_o^2(T)\Omega}{\xi^2+\Omega^2}e^{\xi/2T}\frac{|\Gamma(1+K+i\xi/2\pi T)|^2}{\Gamma(1+2K)}, \quad (89)$$

where Ω was defined in Eq. (50). In the zero-bias case (perfect crystal) this gives the diffusion rate as [see Eq. (63)]

$$D(T)=\frac{Za^2}{3}\frac{\Delta_o^2(T)}{\Omega}\frac{\Gamma^2(1+K)}{\Gamma(1+2K)}\sim T^{-(1-2K)}. \quad (90)$$

This result was first established by Kondo (1984) and Yamada (1984). Usually $K<1/2$, and the diffusion rate increases towards low temperatures.

The other interesting limit is that of large bias $\Omega, T \ll \xi$, when

$$W(\xi)=\frac{2\pi\Delta_o^2(\xi)}{\Gamma(2K)\xi}\frac{1}{1-e^{-\xi/T}}\sim\left(\frac{1}{|\xi|}\right)^{1-2K}, \tag{91}$$

with the bias-dependent tunneling amplitude $\Delta_o(\xi)=\Delta_o e^{B_o-\Phi(T)+G(T)}(|\xi|/\gamma\omega_o)^K$ [compare Eq. (49)]. If, for some reason, the coupling constant is very small, $K\ll 1$ (e.g., in semimetals), then there is a temperature range $T>\xi>\Omega$ where

$$W(\xi,T)=2\frac{\Delta_o^2(T)\Omega}{\xi^2}\sim\frac{T^{1+2K}}{\xi^2}, \tag{92}$$

i.e., the temperature dependence is opposite to that in Eq. (90).

It is also worth mentioning here that the large damping rate in a metal ($\Omega_{el}\sim T$ even for $K\sim 0.1$) almost eliminates the possibility of observing crystal disorder effects through particle diffusion in the bulk. The disorder is of importance (excluding the special case of extremely small K) only when $\xi>T$, but at this point the muon is already trapped. Thus most of the μSR data in the normal state *can* be interpreted in terms of the diffusion rate in a perfect crystal, Eq. (90). The only point, then, where the long-range character of the defect potential enters the problem is the temperature dependence of the trapping radius.

In the superconducting state the appearance of the gap Δ_c in the electron spectrum and an exponential decrease in the number of normal excitations has a twofold effect on quantum diffusion. On the one hand, the temperature dependence of the tunneling amplitude stops at a level determined by Eq. (55). On the other, the rate at which phase correlations are lost now decreases exponentially when the temperature is lowered. From Eq. (46) we find

$$\Omega_S=\frac{4\pi KT}{1+\exp\{\Delta_c/T\}}. \tag{93}$$

Thus in a perfect crystal we expect an exponential increase in the diffusion rate in the superconducting state right from the transition point (with infinite derivative at T_c) (Black and Fulde, 1979; Morosov, 1979),

$$D(T)\approx\frac{Za^2}{3}\frac{(\Delta_{coh}^{(s)})^2}{\Omega_S}. \tag{94}$$

The crucial difference from the normal-metal case at $T\ll T_c$ is that now even small bias (but still, $\xi>\Delta$) will localize particles, because at $\xi\gg\Omega_S$ the transition probability goes to zero as [compare with Eq. (92)]

$$W(\xi,T)=2\frac{(\Delta_{coh}^{(s)})^2\Omega_S}{\xi^2}. \tag{95}$$

This law is slightly modified near the threshold $T\ll\xi<2\Delta_s$ (Kagan and Prokof'ev, 1991):

$$W(\xi>0)=2\frac{(\Delta_{coh}^{(s)})^2\Omega_S}{\xi^2}\left(\frac{\pi T}{16\xi(1+\xi/2\Delta_s)}\right)^{1/2}. \tag{96}$$

(An obvious Boltzmann factor is not mentioned here.) To summarize, the effect of the superconducting transition is to "liberate" particles in the unperturbed lattice regions ($\xi<\Delta$) and "freeze" them otherwise. The best confirmation of these predictions has been recently found in experiments performed on doped superconducting Al samples.

As was mentioned above, these equations hold true up to rather high temperatures, comparable with Θ, where the temperature dependence of $\Phi(T)$ and $G(T)$ in the exponent is important. Now the T dependence of the transition probability is dominated by one-phonon processes, while the role of conduction electrons is reduced to almost constant renormalization of the bare tunneling amplitude, $\Delta_o\to\tilde{\Delta}_o\approx\Delta_o e^{B_o}(\Theta/\gamma\omega_o)^K$. Thus in the high-temperature limit (in fact, already at $T<\Theta$) we find

$$W(T)=\frac{\sqrt{\pi}}{2}\frac{\tilde{\Delta}_o^2}{\sqrt{(E+E_1)T}}e^{-E/T+T/E_B-T\nu_B^2/[16(E+E_1)]}, \tag{97}$$

where different parameters are given by spectral sums: $E=\Sigma_\alpha|\bar{C}_\alpha|^2/(4\omega_\alpha)$, $E_1=\Sigma_\alpha|B_\alpha|^2\omega_\alpha/(4\omega_o^2)$, $E_B^{-1}=4\Sigma_\alpha|B_\alpha|^2/(\omega_o^2\omega_\alpha)$, $\nu_B=4\Sigma_\alpha\bar{C}_\alpha B_{-\alpha}/(\omega_o\omega_\alpha)$ (Kagan and Klinger, 1976). Using the Schwartz inequality one can prove that the sum of the two terms linear in T has a positive sign. If we neglect barrier fluctuations ($B_\alpha=0$), then Eq. (97) reduces to the small-polaron expression (Flynn and Stoneham, 1970)

$$W(T)=\tilde{\Delta}_o^2\sqrt{\frac{\pi}{4ET}}e^{-E/T}, \tag{98}$$

which has been widely used to fit the experimental data at high temperature. The crossover temperature T_{min}, from Eqs. (90) to (97), may be obtained by comparing these two expressions. If the two-phonon processes are of any importance in a metal, then their role may be seen near the crossover point only, provided $\Omega_{2ph}(T_{min})>\Omega_{el}(T_{min})$ [see Eq. (51)], in which case one has to understand Ω in Eq. (90) as the total dephasing rate, $\Omega_{2ph}+\Omega_{el}$ (Kondo, 1986).

We observe that at high temperatures the relative role of the on-site interaction (polaronic effect) and barrier fluctuations may change and the latter always dominate at high T. The reason seems to be rather obvious: at high T it is much easier for the lattice to fluctuate to the state where the two nearest sites are in resonance, while the increase of lattice vibrations with temperature creates more opportunities for the particle to tunnel when the barrier height is the lowest.

B. Experimental results on μ^+ quantum diffusion in metals

Starting from the first experiment of Gurevich *et al.* (1972), μ^+ diffusion has been studied in a large number of different metals: Cu and Al, Nb and V, Bi and Au, etc. Quantum tunneling was suggested as a cause of μ^+ dynamics in metallic matrices from the very beginning of these studies more than two decades ago. However, it

was not until the breakthrough results of Kondo (1984) and Yamada (1984), which recognized the crucial role of the conduction electrons, that we obtained a consistent understanding of muon quantum diffusion in metals [scattering on electrons was in fact discussed already by Andreev and Lifshitz (1969) and later by Jäckle and Kehr (1983), but these theories were perturbative band-type (large-mean-free-path) calculations, which simply do not apply to the problem of μ^+ relaxation]. It turns out that, in all metals, the tunneling band is so large that coherently moving muons do not depolarize because of the motional narrowing effect. Spin relaxation takes place only in regions where coherent motion is not possible, i.e., when ξ or Ω exceed Δ. When $\xi > \Omega, \Delta$, the problem is essentially inhomogeneous, requiring a solution of the kinetic equation taking into account both μ^+ local diffusion and local relaxation with space-dependent $\tau_c^{-1}(\vec{n}, T)$ (Kagan and Prokof'ev, 1992). In the case $\Omega > \xi, \Delta$ one may introduce a space-independent parameter $\tau_c^{-1}(T)$. In this section we shall give a detailed description of both homogeneous and inhomogeneous processes in metals, employing the cases of μ^+ diffusion in Cu and Al. We shall also briefly review some other metals in which μ^+ dynamics is believed to be quantum in character.

1. Copper

A perfect example of a system that can be treated as homogeneous is copper. The first measurements of muon diffusion in copper (Gurevich *et al.*, 1972; Grebinnik *et al.*, 1975) were carried out in a transverse field $B = 62$ Oe. The μ^+ hop rate was determined using the motional narrowing effect and was found to depend strongly on temperature in the range of 80–330 K. The μ^+ hop rate was extracted using an approximate interpolation formula by Abragam (1961),

$$P(t) = \exp(-2\delta^2 \tau_c^2 [e^{-t/\tau_c} - 1 + t/\tau_c]). \tag{99}$$

Below about 80 K the relaxation rate was temperature independent. This was considered to be evidence of static relaxation, and the value of δ was readily found to equal $\delta = 0.252 \times 10^6$ s^{-1} in the polycrystalline Cu. In the single crystal of copper this parameter was slightly (albeit, noticeably) higher (Hartmann *et al.*, 1980). Good agreement between δ and the Van Vleck (1948) value for the second moment of the field distribution due to dipole coupling to unlike spins in a strong transverse field has supported the assumption that μ^+ localizes at interstitial sites, later identified as octahedral (Camani *et al.*, 1977).

The temperature dependence of the μ^+ hop rate extracted from Eq. (99) using a fixed value of δ is presented in Fig. 7. Grebinnik *et al.* (1975) fitted this temperature dependence to the Arrhenius law

$$\tau_c^{-1} = \nu_\mu \exp(-E/T) \tag{100}$$

with the parameters $\nu_\mu \approx 10^{7.5}$ s^{-1} and $E \approx 550$ K. These parameters indicate unambiguously the quantum nature of μ^+ diffusion in Cu in the temperature range 100–250 K. First, the preexponential factor is about six orders of magnitude less than the particle vibration frequency in the well (which is as high as 10^{13} s^{-1}). Second, the activation energy E is about an order of magnitude less than that for proton diffusion in copper (Katz *et al.*, 1971). At temperatures above 250 K the deviation of the experimental results from the Arrhenius law with the above parameters was attributed to over-the-barrier transitions. The analysis of the experimental data by Teichler (1977) showed, however, that one can get a better fit by using the small-polaron expression with the temperature-dependent preexponential factor, Eq. (98). Subsequent experiment (Schilling *et al.*, 1982) in a single crystal confirmed that this is indeed the case. The results for the polaron energy and the tunneling matrix element were found to be $E = 920 \pm 35$ K and $\tilde{\Delta}_0 = 0.21 \pm 0.01$ K.

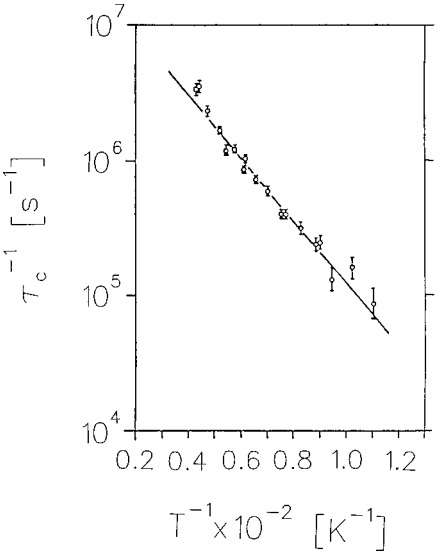

FIG. 7. Temperature dependence of the μ^+ hop rate in Cu (Grebinnik *et al.*, 1975).

It was not until Hartmann *et al.* (1980) carried out the transverse-field experiment in a Cu in a magnetic field of 520 Oe, down to about 60 mK, that the μ^+ transverse relaxation rate was found to decrease below about 2 K. The sample used in this experiment was a high-purity polycrystalline copper with less than 20 at. ppm of residual impurities. Some decrease in the muon relaxation rate was also found in a single crystal, but the data were available only down to 2 K. All experimental spectra were corrected for background arising from muons stopping in the sample holder and the cryostat walls, and all agreed with Grebinnik *et al.* (1975) and Camani *et al.* (1977) in the temperature range between 10 K and 75 K. Subsequent transverse-field experiments (Welter *et al.*, 1983, 1984) confirmed that the muon spin-relaxation rate decreases below about 20 K with decreasing temperature. Below about 0.5 K it seemed to have reached a temperature-independent value of about 0.15×10^6 s^{-1}, while the muon site was determined to be still octahedral (Chappert *et al.*, 1982). Some experimental attempts were made to see the influence of weak crystalline disorder on the muon spin-relaxation rate through

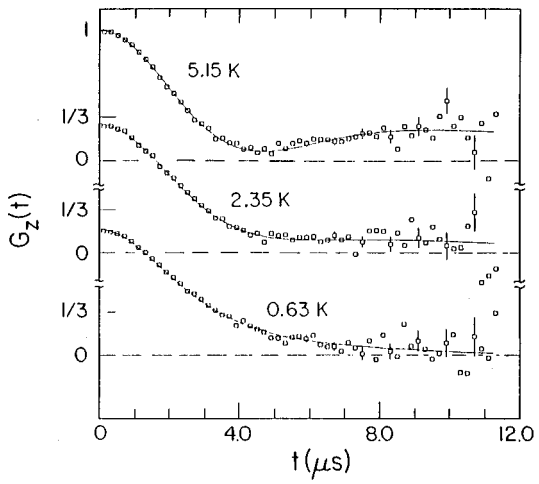

FIG. 8. Time dependences of the muon polarization in copper at different temperatures in zero magnetic field (Clawson *et al.*, 1983).

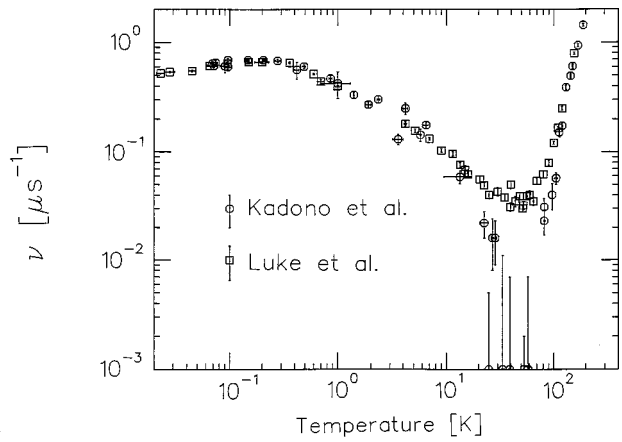

FIG. 9. Temperature dependences of the μ^+ hop rate in high-purity copper; data by two groups: circles, Kadono *et al.* (1989); squares, Luke *et al.* (1991).

trapping-detrapping effects. Radiation damage in thin (50μ) foils of Cu, resulting in a defect concentration of approximately 80 ppm, was shown to have no effect (Echt *et al.*, 1978). Experiments on isotopically enriched samples containing over 99% of either ^{63}Cu or ^{65}Cu also revealed almost no deviation from the natural composition samples (Welter *et al.*, 1984). To summarize, attributing the decrease in μ^+ relaxation rate below 20 K to the motional narrowing effect, one was bound to consider quantum diffusion, because $\tau^{-1}(T)$ was increasing with decreasing temperature [the failure of the trapping model (Petzinger, 1980, 1981) in explaining the data was later verified by zero-field experiments (see below)]. However, the precision of the transverse-field experiments was not sufficient to measure reliably the temperature dependence of the muon hop rate.

The first zero-field μ^+SR measurements in copper (Clawson *et al.*, 1982; Clawson *et al.*, 1983) confirmed an increase in the μ^+ hop rate at low T. Two high-purity samples—a slice of the same polycrystal used by Hartmann *et al.* (1980) and an oxygen-annealed single crystal with a residual resistivity ratio (RRR) of 4000—both showed a dynamically narrowed Kubo-Toyabe relaxation function below 5 K. Although experimental spectra appeared to be almost identical up to about 4 μs, the tails of the relaxation function were qualitatively different at $T=5.15$ K and $T=0.63$ K (Fig. 8), indicating dynamic behavior at the lowest temperature. Identical shot-time behavior further proved that $\delta=$ const, and the difference in the relaxation function at long times was then attributed entirely to the increase of the μ^+ hop rate from about 10^5 s^{-1} at 5 K to about 4×10^5 s^{-1} at 0.5 K. This was made possible due to the intrinsic power of the zero-field technique, in which it is possible to determine independently the static linewidth and the particle's hop rate. The octahedral position for μ^+ and temperature independence of δ at all relevant T were also confirmed later by the level-crossing resonance technique (Luke *et al.*, 1991).

The extension of zero-field measurements in Cu down to 70 mK (Kadono *et al.*, 1984, 1985, 1986, 1989) confirmed these results. All of these experiments revealed a minimum in the muon hop rate in the temperature interval 30–70 K (although there is a large variation in the fitted values of τ_c^{-1} at this minimum), and leveling off below 0.5 K even in ultrapure samples (RRR 18 000 and 7350). Thorough analysis (Kadono *et al.*, 1989) showed that the experimental spectra are better approximated using the Celio model (Celio, 1986a) which goes beyond the Kubo-Toyabe Gaussian approximation for the local-field distribution and accounts exactly for the μ^+ interaction with nearest nuclei in the lattice (see also Celio and Meier, 1983; Holzschuh and Meier, 1984). The difference is most pronounced in the quasistatic region, where the difference in the tails of relaxation functions in the two models is the largest. The resultant temperature dependence $\tau_c^{-1}(T)$ is shown in Fig. 9 (circles).

Below the minimum the increasing hop rate was found to obey a power law,

$$\tau_c^{-1}\sim T^{-\alpha}, \tag{101}$$

where the value of α is expected to determine the scale of the muon interaction with the conduction electrons $K=(1-\alpha)/2$, [see Eq. (90)]. The parameter α depends on the temperature range used to extract it. The data between 0.5 and 10 K follow Eq. (101) with $\alpha=0.67\pm0.03$, which agrees with the value $\alpha=0.7$ obtained from transverse-field measurements (Welter *et al.*, 1983). Similar analysis in the extended temperature region (up to $\sim$80 K) gave $\alpha=0.8\pm0.02$. This ambiguity leads to a scattering of the muon-electron constant between $K=0.16$ and $K=0.1$. The uncertainty mostly originates from rather large error bars in the temperature range 10–80 K, where the μ^+ hop rate is too small ($\tau_c^{-1}\sim10^3-10^4$ μs^{-1}) to be accurately extracted from zero-field data (see Sec. IV), and the results extracted in this region are extremely sensitive to the choice of theoretical model.

Experiments using the weak-longitudinal-field technique (Brewer *et al.*, 1986, 1987; Luke *et al.*, 1990, 1991) were much more precise in the determination of slow

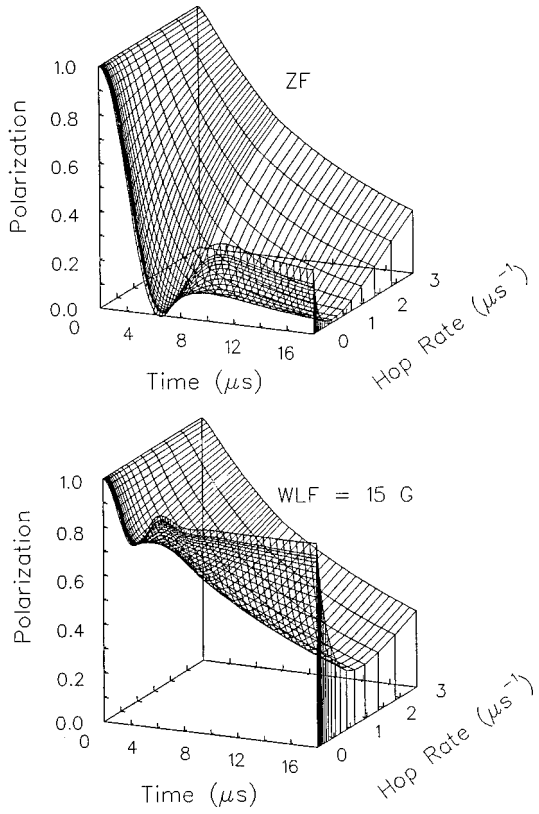

FIG. 10. Dynamic muon relaxation functions in zero field and weak longitudinal field, as a function of the muon hop rate (Luke *et al.*, 1991).

muon hop rates (see Sec. IV). At each temperature a series of spectra were taken at several values of longitudinal field. In addition to the inherent advantages of this technique, discussed in Sec. IV, there are further advantages in taking a series of runs at several fields, since one may then compare the results of fittings and estimate their uncertainty. The choice of the longitudinal field allows one to apply a field that is most sensitive to small changes of τ_c^{-1}, which is very important around the "T_1^{-1} minimum," as illustrated in Fig. 10. Furthermore, the analysis of the experimental data using an exactly solved, quantum-mechanical, microscopic Hamiltonian, which determines the time evolution of the static μ^+ polarization function (Luke *et al.*, 1990, 1991), made it possible to avoid theoretical modeling. The temperature range of the weak-longitudinal-field measurements was extended down to 12 mK.

Weak-longitudinal-field results for the hop rate are presented as a function of temperature in Fig. 9, along with the results of Kadono *et al.* (1989). The greatest difference appears in the temperature range near the minimum of the hop rate. [Apart from the less sensitive technique of the τ_c^{-1} measurements in zero field, the source of the discrepancy around the minimum may be explained by the difference in muon beams. The pulsed structure of the muon beam at KEK along with the rather higher energy of the incoming muon (backward decay muons) with respect to that of the dc surface muon beam at TRIUMF may also cause an underestimate of μ^+ hop rates in the quasistatic limit (Luke *et al.*, 1991).]

Some misinterpretations of the results in cited papers should be noted. The high-temperature region was correctly described using Eq. (98). The values of the polaron energy $E=697\pm15$ K and $\tilde{\Delta}_o=(36.1\pm3.2)\times10^{-6}$ eV were extracted from the $\tau_c^{-1}(T)$ in the temperature range 100–190 K by Kadono *et al.* (1989). However, it should be pointed out that at temperatures above about 150 K the muon hop rate exceeds the frequency of the electric quadrupole splitting of the Cu nuclei (~1 MHz), which effectively increases the static dipole width. The absolute values of the muon τ_c^{-1} in Cu at temperatures above 150 K extracted from the "dynamicized" static relaxation function in a weak longitudinal field or zero field can no longer be considered as reliable due to the fact that the strong-collision model no longer gives accurate results (Luke *et al.*, 1991). When the μ^+ hop rate exceeds the characteristic quadrupole splitting frequency one should rather use the transverse-field technique as the most accurate in this region. Therefore we are inclined to believe that the results of Schilling *et al.* (1982) are the most reliable for μ^+ dynamics in copper at high temperatures.

In the temperature range between 1 K and 10 K, the data of Luke *et al.* (1991) are best fit with $\alpha=0.553(7)$. In terms of the Kondo-Yamada theory this implies a muon-electron coupling parameter in copper of $K=0.224(4)$. We consider this value of K as the most reliable so far. It should be compared with the theoretical estimate of $K_{theor}=0.33$ obtained by Hartmann *et al.* (1988) from the results of the Fermi-level phase shifts for atoms in a homogeneous electron gas (Puska and Nieminen, 1983).

It is easy to estimate the value of the coherent tunneling amplitude for the muon in copper by taking, say, the experimental values for K and τ_c^{-1} at $T=1$ K and employing Eqs. (90), (53), and (49). The estimate thus obtained gives

$$\Delta_{coh}\sim10^{-4}\ \text{K}. \tag{102}$$

Clearly, at all temperatures studied, the muon dynamics is incoherent and thus described by the theory of Kondo and Yamada. To check the consistency of the high- and low-temperature data, we may separate the electronic polaron effect by assuming $\omega_o=0.1$ eV, and extract the one-phonon renormalization of the tunneling amplitude. We have found that the value of $\Phi(0)-G(0)\approx4$–5 is necessary to account for the renormalization $\Delta_{coh}\to\tilde{\Delta}_o$ [$\tilde{\Delta}_o$ defines the preexponential factor in Eq. (98)]. Within the Debye model for the phonon spectrum and the simplest assumption for the muon-phonon coupling constants $f_1\sim\omega^2$, one finds $E=(1/3)\Theta\Phi(0)$, which is not in contradiction with the experimental value, keeping all the reservations for the uncertainty of such a calculation. Thus we conclude that all the data are consistent with the tunneling model.

Some ambiguity exists concerning the shallow maximum in the hop rate at about 0.2 K. Most experiments

claim that the data are not sensitive to the crystal disorder, at least in the purest samples (see above). However, one has to accept that at temperatures as low as 0.1 K the trapping radii in metals are as large as $R_T \sim 20a$ [see Eq. (66)], and muons that move faster at low temperatures will undergo trapping to these long-ranged traps. On the other hand, more and more muons are stopped and localized in the regions where the bias energy exceeds T. Even a simple minded estimate shows that, at 10 ppm doping, the regions of radius R_T overlap below 0.1 K. Both effects will be seen in the current interpretation of the data as an effective decrease in the hop rate. The data on doped samples are obviously too incomplete to make a more definite conclusion.

2. Aluminum

In sharp contrast to Cu, all the results on μ^+ diffusion in Al have been obtained in doped samples. The very first μ^+SR experiments in Al revealed no relaxation in pure samples (about 99.9995% Al) down to 1 K (Hartmann *et al.*, 1977) and up to the melting temperature (Gauster *et al.*, 1977), in spite of the fact that ^{27}Al has a larger magnetic moment than both ^{63}Cu and ^{65}Cu (see also Heffner *et al.*, 1978; Hartmann *et al.*, 1980). The obvious explanation of this behavior is that the muon bandwidth in Al is much higher than in Cu. It was found that alloying Al with Cu (up to 0.42 at. %) and quenching to produce a dislocation density of about 10^9–10^{10} cm^2 (Kossler *et al.*, 1978), as well as irradiating it with neutrons (Dorenburg *et al.*, 1978), caused substantial relaxation of the muon polarization with peaks between 2.6 and 297 K.

Early experiments (see also Brown *et al.* 1979; Nakai *et al.*, 1981) were unable to extract even general trends of the μ^+ dynamics at low temperatures. However, it was realized that the hop rate could be deduced from trapping studies, where μ^+ diffuses to impurities that have been deliberately introduced into a pure Al sample. Once μ^+ is trapped due to the change in impurity concentration or increase in the hop rate, its polarization is inevitably lost due to static relaxation. At high temperatures, μ^+ can experience trapping and subsequent detrapping due to thermal activation. In this case the relaxation rate can be increased or decreased depending on how fast μ^+ is trapped and for how long it is trapped. The hop rate is deduced from the time required for the muon to reach the trap. Following this picture one should be aware that the hop rate extracted from trapping studies may differ from that in the pure system. Moreover, in trapping studies τ_c^{-1} is always obtained by employing some theoretical model. Strong dissipation in the normal state, however, allows one to consider muon diffusion in Al as essentially homogeneous before it is trapped. As we shall see, the damping rate $\Omega(T) \sim T$ and the bias energy in the denominator of Eq. (89) have no noticeable effect on the muon diffusion.

Measurements of the T dependence of the muon relaxation rate in pure Al and crystals doped with Mn (500 ppm and 1300 ppm) showed that muons are essentially

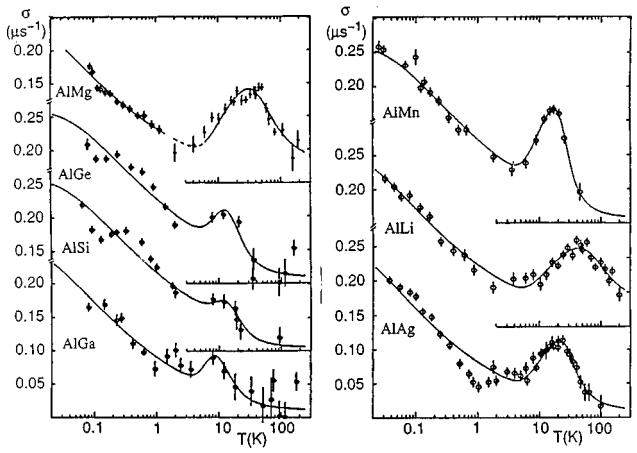

FIG. 11. Temperature dependences of Gaussian relaxation rate of the μ^+ polarization in aluminum samples doped with different impurities (Hartmann *et al.*, 1988).

localized at temperatures below 15 K in the latter, while they exhibit delocalization down to 2 K in the former (Hartmann *et al.*, 1978). The extension of these measurements to lower temperatures down to 100 mK and to lower Mn concentrations (42 ppm and 57 ppm) indicated that muons are increasingly trapped below 1 K with increasing Mn content (Hartmann *et al.*, 1980). The μ^+ localization site was found to be temperature dependent and identified as tetrahedral at $T=15$ K. A comprehensive trapping study of muon diffusion in Al doped with different impurities (Mn, Li, Ag, Mg, Ga, Si, Ge) in a wide range of impurity concentration (from 5 ppm to 1300 ppm) and temperatures within the range 50 mK–200 K was presented by Kehr *et al.* (1982) and Hartmann *et al.* (1988; see also Hartmann *et al.*, 1986). The relaxation function was approximated as either exponential or Gaussian. The temperature dependences of the Gaussian relaxation rate, T_2^{-1} (for historical reasons the notation σ for the relaxation rate is also widely used in the literature), in different samples are summarized in Fig. 11.

The interpretation of these results is based on diffusion-limited trapping (Waite, 1957). The increase of the relaxation rate $\sigma(T)$ at the lowest temperatures is common for all doped samples, and the slope of $\sigma(T)$ in this region is almost independent of impurity type, which indicates that it is characteristic of the host metal. The concentration dependence studied for AlMn (Hartmann *et al.*, 1980; Kehr *et al.* 1982) is a little slower than linear, $\sigma \sim n_{im}^{0.7}$, but, as we argue, this might be the first "signature" of large trapping radius, which results in noticeable multidefect corrections. The peak in $\sigma(T)$ at higher temperatures is also due to trapping, apparently to some other trapping sites. The explanation commonly used to account for this behavior is that the muon hop rate goes through a minimum at around 3 K and increases again so that muons reach deep traps with increasing probability. Above 15 K muons escape traps due to thermal activation and diffuse so fast that "dynamically narrowed" σ is close to zero. The procedure of extracting the absolute values of τ_c^{-1} was carried out

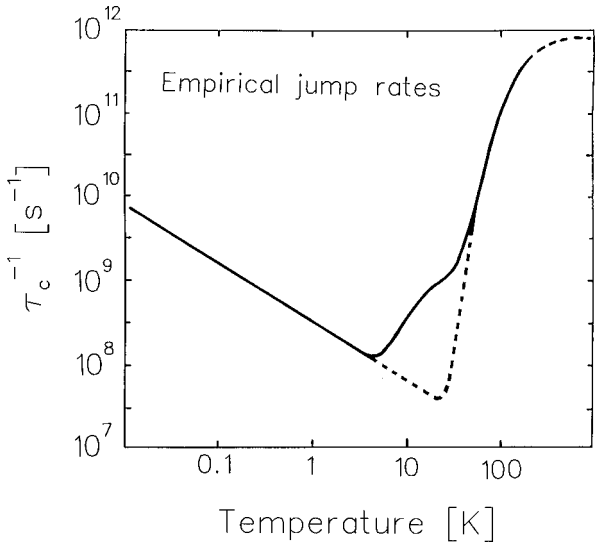

FIG. 12. Temperature dependence of the muon hop rate in Al derived from various trapping experiments on impurities below 50 K and from vacancies above 50 K. The dashed curve is the extrapolation of the low- and high-temperature dependences (Hartmann *et al.*, 1988).

in the framework of the two-state trapping model (Borghini *et al.*, 1978; Kehr *et al.*, 1978; Richter and Springer, 1978; Richter, 1986): one state was assumed to be the free muon, which experiences relaxation in the homogeneous lattice, and the other state was suggested to be the trapped muon, which undergoes static Gaussian relaxation. Solving a set of integral equations dealing with repeated "capture and release" transitions, one obtains $P(t)$ as a function of the trapping rate [which is then related to the diffusion rate; see Eq. (65)] and the trapping energy. Solid lines in Figs. 11 and 12 present the results of such a fit, which were summarized by the authors in the empirical expression

$$\tau_c^{-1}=aT^{-0.7}+be^{-20/T}+cT^{-1/2}e^{-370/T}. \tag{103}$$

It should be noted that the absolute values of τ_c^{-1} were derived under certain assumptions about the values of the trapping radii. These typically were estimated to be on the atomic scale [the absolute values for different impurities range between 2 Å and 12 Å (Hartmann *et al.*, 1988)] and their dependence on T in the fitting was neglected.

Our present understanding of the above results is, however, quite different (Kagan and Prokof'ev, 1987, 1991; Prokof'ev, 1995). We start from the low-temperature data (below 1 K) where $\Lambda_{tr}\propto T^{-\alpha}$ with $\alpha=0.7$. As noted already in Eq. (25), the potential originating from the electron-density oscillations around impurities is as large as $U_o\sim 300$ K in Al (Mahajan and Prakash, 1983). Thus at low T we are dealing with the temperature-dependent trapping radius [Eq. (66)]. Substituting Eq. (90) into the expression for the trapping rate (65) we find

$$\alpha=1-2K+1/3. \tag{104}$$

The data at low temperatures, however, were analyzed as $\tau_c^{-1}=T^{-\alpha}$, with $\alpha=1-2$ K, thus resulting in an underestimated value of the muon-electron coupling parameter, $K=0.15$. Theoretical calculations in Al predicted $K_{theor}=0.27$ (Hartmann *et al.*, 1988). From Eq. (104) one obtains $K=0.32$, which is in better agreement with the theory. We may also roughly estimate the coherent tunneling amplitude from these data using the above given value of U_o and $\omega_o\approx 0.1$ eV. First we derive the effective tunneling amplitude $\Delta_o(T)$ from the trapping rate, say at $T=0.5$ K, and then use Eqs. (53) and (54) to get

$$\Delta_{coh}\sim 3\times 10^{-3}\ \text{K}. \tag{105}$$

This estimate cannot be considered to be very accurate, because the numerical coefficient in the formula for the trapping rate in the oscillating potential is not yet known. Still, we believe that coherence is suppressed in the normal state down to the lowest measured temperatures.

According to the theory of quantum diffusion in metals, at temperatures as low as $2-20$ K (compared with $\Theta=428$ K) one-phonon processes play no role, and τ^{-1} decreases, according to the Kondo-Yamada law, with increasing temperature. No minimum in the hop rate is possible in this temperature range unless the theory of quantum diffusion is really wrong. However, the only experimental fact at our disposal is that the trapping rate increases above 5 K. This paradox may be resolved as follows. The high-T peak is due to the traps nearest to the defect sites, which are surrounded by potential barriers from all sides. Such a configuration is not at all surprising because of the radial oscillations in the electron density around the defect, Eq. (25). In order to get to the deepest traps μ^+ has to overcome the potential barrier; thus at the trapping radius we have to use Eq. (91) with negative bias and $|\xi|>T$. This picture naturally explains the data without going into the contradiction with the current theory and makes it clear that the activation energy 20 K in Eq. (103) results from the potential barrier height which separates the trap from the bulk. Thus all the data between 3 K and 50 K need to be reanalyzed.

Adopting this explanation, there must be many peaks at low temperature, because potential wells and barriers are reproduced again at larger distances. We note, however, that far from impurities the difference between the minima and maxima in $V_{inh}(r)$ is so small that traps become ineffective (closed by barriers) at the same moment as they start accumulating particles due to the Gibbs factor. Furthermore, at $r>a$ there are many more paths allowing the particle to penetrate the traps by avoiding large barriers, provided $2k_Fa>\pi$ (which is the case in Al). It is thus more probable that peaks at lower T are smoothed out and the collective effect of many different traps is actually seen below 1 K. However, the most surprising experimental fact (usually not discussed at all) is that there *are* small peaks and irregularities around 5 K and lower temperature, e.g., in Ge- and Si-doped samples (Kehr *et al.*, 1982).

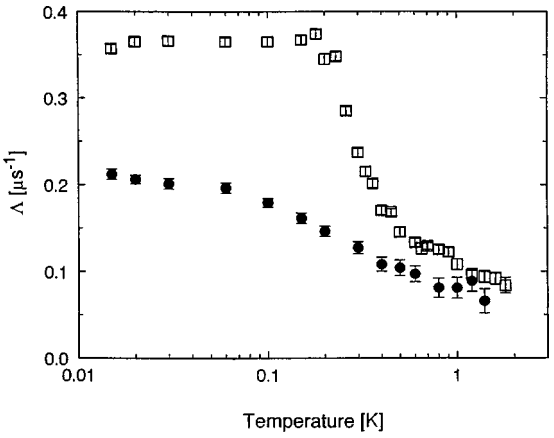

FIG. 13. The μ^+ depolarization rate *vs* temperature in Al doped with 75 ppm Li: filled symbols, in the normal state; open symbols, in the superconducting state (Karlsson *et al.*, 1995).

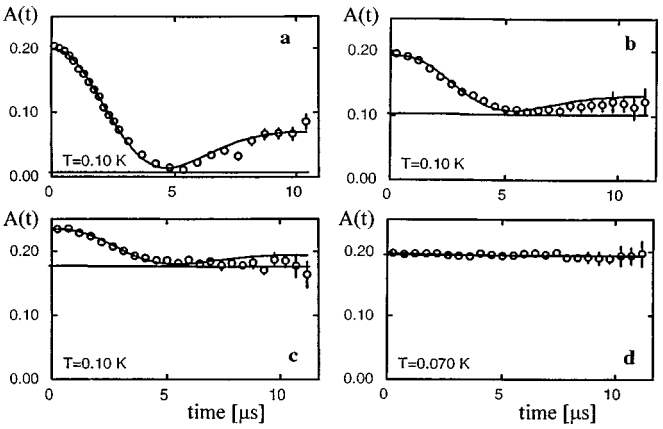

FIG. 14. Time dependences of the muon polarization in Al in zero field at 0.1 K for different Li doping: (a) 75 ppm, (b) 20 ppm, (c) 10 ppm, and (d) high-purity (6N) Al (Karlsson *et al.*, 1995). Note the decomposition of muon polarization into relaxing and nonrelaxing fractions.

The experiments on muon quantum diffusion in Cu and Al unambiguously confirm the role of particle-electron coupling effects at low temperatures. This was demonstrated most prominently in μ^+ quantum diffusion experiments in superconducting Al with impurities. The first experiments (Hartmann *et al.*, 1989; Kadono, Kiefl, Kreitzmann, *et al.*, 1990) observed a marked difference in the depolarization rates between the normal and superconducting states. The most detailed data are presented by Karlsson *et al.* (1995), who studied a high-purity (6N) polycrystalline aluminum and three samples doped with nominally 10 at. ppm, 20 at. ppm, and 75 at. ppm Li, later analyzed to be 8.3 at. ppm, 17.5 at. ppm, and 76(4) at. ppm, respectively. The μ^+SR spectra in the normal state were taken in an external transverse magnetic field of 130 Oe (10 and 20 ppm) and 200 Oe (75 ppm), which was sufficient to quench superconductivity (the critical field at $T=0$ is $B_c=100$ Oe). Measurements in the superconducting state were carried out in zero field. Figure 13 presents the temperature dependences of the muon depolarization rate in a sample Al +75 ppm Li in both the normal (filled symbols) and the superconducting (open symbols) states.

These data cannot be explained by the theory of quantum diffusion in a perfect crystal. With $D(T)$ instead of $D(T,R_T)$ in Eq. (65), the trapping rate must increase with infinite derivative right below $T_c=1.2$ K, while it demonstrates almost no effect at T_c (see Fig. 13) or even develops a tiny peak near T_c in the low-doped samples. An exponential increase in the depolarization rate is observed only below ~ 0.5 K, which saturates at 0.2 K. The activation energy deduced from the steep increase below 0.5 is less than the superconducting gap Δ_c by a factor of 2.

For Li concentrations of 20 and 10 ppm at low temperature the signal is clearly composed of two concentration-dependent contributions $P(t)=P_1(t)+P_2(t)$, one a constant and the other closely resembling a Kubo-Toyabe function (see Fig. 14). This feature gives us the most evident clue to the physics of what is happening below T_c. As discussed in Sec. III.B [Eq. (27)], such behavior is characteristic of depolarization in a doped sample when inelastic processes are ineffective. In the oscillating potential we do not expect a substantial fraction, f_d, of finite-size delocalized states; thus the signal consists of contributions coming from coherently moving muons and those stopped inside the localization region $r<R_{loc}$ [see Eq. (21)]. The fraction of the static component should be proportional to the Li concentration and eventually becomes 100% when impurity regions of radius R_{loc} overlap. This picture agrees completely with the data (Karlsson *et al.*, 1995). All muons are localized at $n_{im}=75$ ppm as it should be for the potential strength $U(a)\sim 30$ meV and the bandwidth $\Delta \approx 2z\Delta_{coh}^{(s)}\sim 50$ μeV [obtained from Eqs. (105) and (55)].

The counterintuitive behavior at T_c is explained by noting that the trapping rate is defined by the local diffusion rate at R_T, where the bias is relatively large, $\xi \sim T$. In the normal state, $D(R_T,T)$, increases as the temperature is lowered according to Eq. (90). Slightly below T_c there might be an initial even steeper rise in $D(R_T,T)$ because of the reduced damping rate, which is, however, immediately followed by an exponential decrease of the trapping rate according to Eq. (95). At lower temperatures the depolarization rate (*not* the trapping rate) increases again, this time due to the muon localization and depolarization inside the radius R_*, Eq. (72), until this process is completed at 0.2 K, when regions $V(R_*)$ overlap. The boundary between the moving and static particles, R_*, increases with temperature as $e^{\Delta_c/5T}$ [see Eqs. (70) and (71)]; thus $\Lambda_*\sim e^{2\Delta_c/5T}$ and the fraction of static particles $f_{loc}\sim e^{3\Delta/5T}$, which explains the reduced value of the activation energy in the intermediate temperature range.

The most direct comparison between theory and experiment is obtained through Monte-Carlo-type simulations (Prokof'ev, 1994). In these simulations the theory has only two constant fitting parameters, Δ_{coh} and U_o, from which all the curves $P(t)$ for different Li concen-

trations and temperatures are supposed to be reproduced. The obtained fitting is quite good (Karlsson *et al.*, 1995).

By formally fitting the data for the moving fraction of muons to the standard trapping model, Karlsson *et al.* (1995) found that $P(t)$ is reproduced if the number of muons trapped at time t is given by the stretched exponential $P_{moving}(t) \sim \exp\{-(\nu t)^{\beta}\}$. The fraction of moving particles as a function of n_{im} and T, as well as the dependences $\nu(n_{im},T)$ and $\beta(n_{im},T)$, were treated as fitting functions. At first sight this approach has no physical background; still we gain from this analogy, because it tells us that long-range trapping in the oscillating potential created by randomly distributed defects may resemble the situation with a wide distribution of trapping energies and trapping rates.

We should also mention here another experimental system in which quantum diffusion has been observed and studied in detail. The neutron-scattering experiments in $Nb(OH)_x$ ($x=0.002$ and 0.011), where the proton shows tunneling dynamics in a double-well potential (Steinbinder *et al.*, 1988), also found that the proton hop rate obeys the power law $\tau_c^{-1} \propto T^{-(1-2K)}$ with $K=0.05$ in the temperature range from 10 K to 50 K. Both the effective tunneling amplitude and the phase-correlation damping Ω in normal and superconducting phases show temperature dependences in complete agreement with the theory (Grabert *et al.*, 1986; Grabert, 1987; Wipf *et al.*, 1987).

3. Other metals (V, Nb, Bi)

In this section we discuss experimental results on the μ^+ diffusion in vanadium, niobium, and bismuth, which, although studied in less detail than Cu and Al, clearly show quantum diffusion effects in muon dynamics. Experimental data in some other metals show distinct peculiarities that may be interpreted as quantum diffusion, but the experimental situation there is far from being clear. Therefore we direct the interested reader to the Proceedings of the μ^+SR conferences edited by Gygax *et al.* (1979), Brewer and Percival (1981), Yamazaki and Nagamine (1984), Hartmann, Karlsson, Lindgren, and Wäppling (1986), Cox *et al.* (1990), Brewer *et al.* (1994), and Nagamine *et al.* (1997), where these experiments are described.

a. Vanadium

The first transverse-field measurements (37 Oe, 58 Oe, and 1786 Oe) in V crystal indicated very early an increase of σ when the temperature was lowered from 300 K down to 5.5 K, with a small peak around 80 K (Fiory *et al.*, 1978). The sample used in this experiment was a polycrystalline V containing 0.4 at. % impurities, mostly Al (1300 ppm), O (1300 ppm), and Fe (600 ppm). [Later measurements (Grebinnik *et al.*, 1978; Hartmann *et al.*, 1978; Heffner *et al.*, 1978), although showing variations of the relaxation rate, revealed qualitatively the same temperature dependence.] The observed field dependence of the μ^+ relaxation rate was attributed to the interplay between muon Zeeman and muon nuclear quadrupole interactions (Hartmann, 1977). The μ^+ hop rates were extracted using Abragam's expression (99), where δ was considered as a fitting parameter. Thus the obtained linear in T dependence of the muon τ_c^{-1} at temperatures below about 50 K was interpreted as an indication of a one-phonon-assisted tunneling mechanism. The maximum at 80 K was attributed to trapping-detrapping processes, with the final conclusion that τ^{-1} monotonically decreases over the entire temperature range.

The first systematic study of impurity effects was carried out by Heffner *et al.* (1979). For the highest-purity V (a special, rather complicated procedure of purification was applied to obtain a sample with less than 50 at. ppm of metallic impurities and an RRR of about 1000; none of the later experiments was done in that pure material) the temperature behavior was found to differ considerably from the earlier results. The temperature dependences of the relaxation rate in samples with different oxygen concentration, along with earlier measurements (Heffner *et al.*, 1978), are presented in Fig. 15. In the pure sample σ is significantly lower than in the sample with 500 ppm oxygen impurities, which indicates that muon relaxation is dynamically narrowed in a perfect crystal. This directly contradicts the previous interpretation of $\tau(T)$ in terms of one-phonon-assisted tunneling, which is slower in a pure system.

A qualitative explanation of the μ^+ dynamics in V could be suggested as follows (Kagan and Prokof'ev, 1987, 1992). The well-defined peak at 80 K is not due to trapping, but rather indicates a change of the diffusion regime. The steep decrease of $\sigma(T)$ above 100 K is characteristic of the small polaron diffusion. At 80 K, in close analogy with quantum diffusion in copper, the diffusion rate goes through a minimum and then *increases* as $T \to 0$. The linear dependence, $\sigma \sim T$ between 80 K and 30 K, is then nothing but a standard metallic behavior $\tau^{-1} \sim T^{2K-1}$ with $K \ll 1$ in the motional narrowing regime where $\sigma \sim \tau$. This also explains in passing why the position of the peak is impurity-type independent and the peak maximum is not affected by impurities at low concentrations (Heffner *et al.*, 1979). Below the minimum the μ^+ hop rate becomes high enough to reach impurity traps, and dynamic narrowing gives way to trapping. Now, in complete analogy with Al, relaxation is defined by $\Lambda_{tr} \sim R_T D(T) \sim T^{-4/3+2K}$, and experimental data at low temperature qualitatively agree with this law. In the 500-ppm sample the trapping process dominates at $T<80$ K. A quantitative analysis of the μ^+SR data (Heffner *et al.*, 1979) is required, however, to see whether the picture just described is consistent over the entire temperature range.

Summarizing results on quantum diffusion measurements in vanadium, we conclude that muon dynamics in this metal are determined by quantum effects (Heffner *et al.*, 1979). Although the data are incomplete (the dimensionless parameter K is not known, although $K \ll 1$ seems to be the case here), we may try to derive the

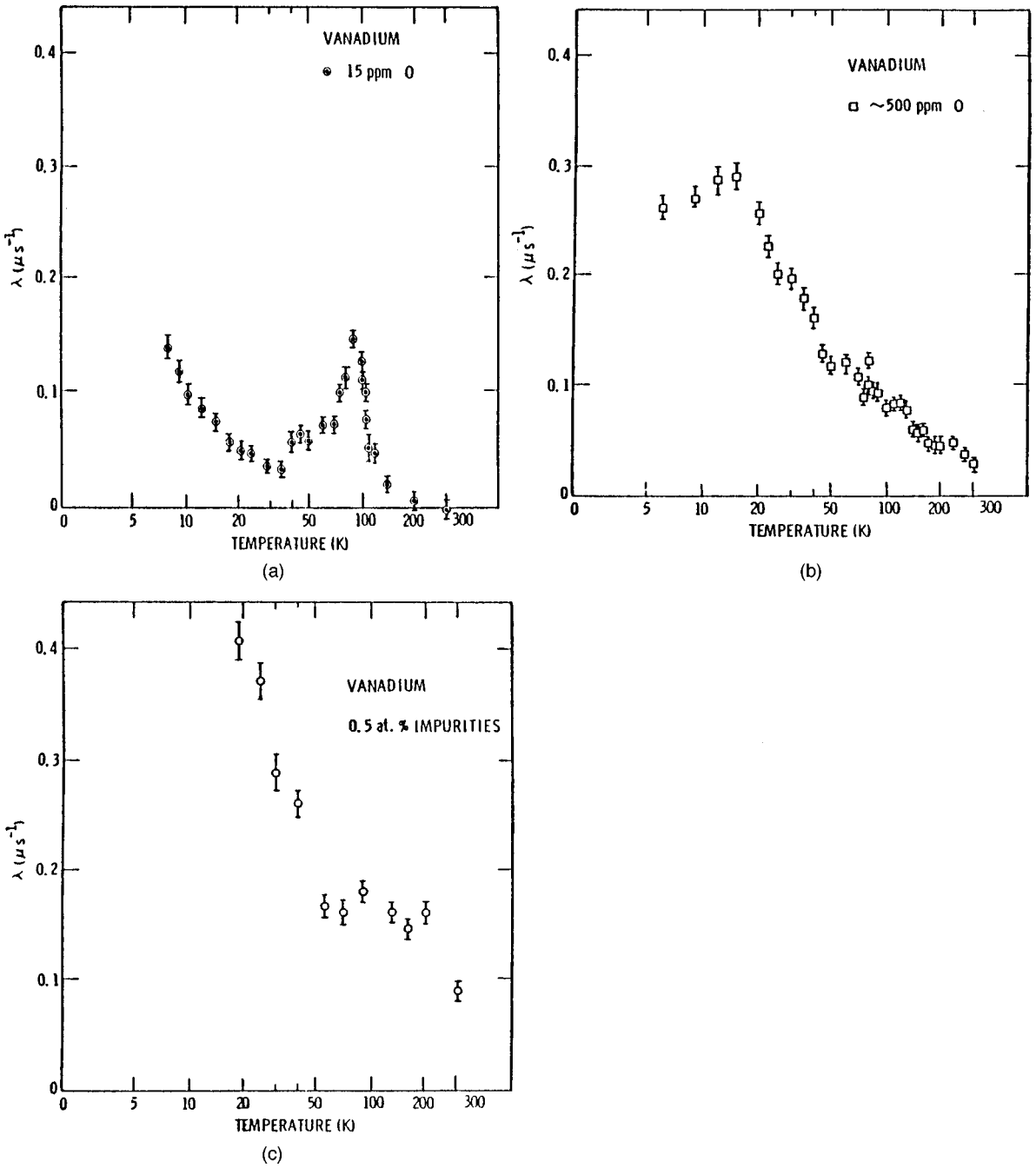

FIG. 15. Temperature dependence of the μ^+ exponential relaxation rate for three vanadium samples with different impurity content (Heffner *et al.*, 1979).

effective tunneling amplitude in V from the τ_c^{-1} values between 30 and 80 K using Eq. (90). We find it to be

$$\Delta_o(50\ \mathrm{K}) \sim 5\sqrt{K}\times 10^{-2}\ \mathrm{K}, \tag{106}$$

that is, intermediate between the Cu and Al cases. It follows immediately from this analogy that effects similar to those in Al are expected in V below the superconducting phase transition.

b. Niobium

Quantum diffusion of μ^+ in Nb was expected from the very beginning of experimental studies, as the first low-temperature measurements of hydrogen diffusion in this metal showed significant deviation from the classical Arrhenius law (Schaumann *et al.*, 1970; Sellers *et al.*, 1974; Wipf and Alefeld, 1974; Wipf and Neumaier, 1984).

Initially, just a leveling off of the transverse-field Gaussian relaxation, interpreted as "freezing" of the muon dynamics, was observed below 60 K (Hartmann *et al.*, 1977). However, the measured σ (sometimes the relaxation rate is denoted as Λ in the literature; we use the notation σ everywhere) was noticeably less than the Van Vleck value for the interstitial positions ($0.285 \pm 0.015\ \mu\mathrm{s}^{-1}$ and 0.35–$0.37\ \mu\mathrm{s}^{-1}$, respectively). A non-

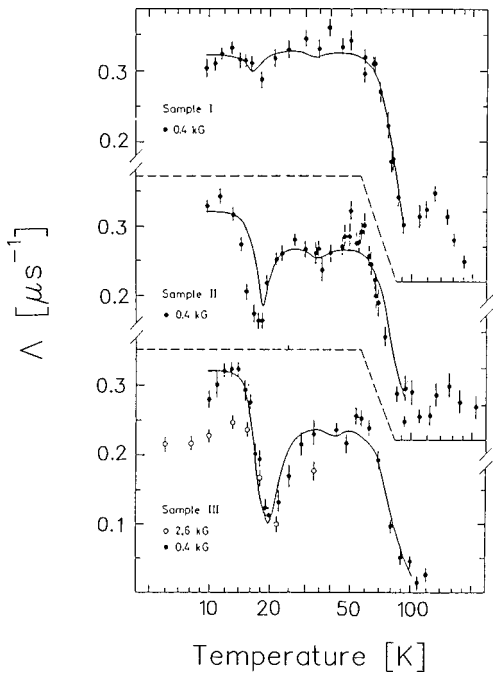

FIG. 16. Temperature dependences of the muon relaxation rate in three Nb samples with different impurity content (Borghini *et al.*, 1978).

monotonic temperature dependence of σ was first observed by Birnbaum *et al.* (1978) and Borghini *et al.* (1978). It was then suggested by Borghini *et al.* (1978) that the presence of N, O, and C impurities would dominate the μ^+ relaxation process in Nb. The relaxation rate, determined as the inverse time for the polarization decay to $1/e$ of its initial value, was found to depend strongly on impurity type, as is evident from the data for three samples with 10–20 ppm, 60 ppm, and 3700 ppm impurities, shown in Fig. 16. A characteristic "double-humped" behavior with the minimum around 20 K (most pronounced for purest sample, III) was also seen in two single crystals of Nb by Birnbaum *et al.* (1978). Above 100 K muon polarization is almost nonrelaxed in all samples. Tantalum impurities were thought originally to have no influence on μ^+ dynamics, as they are not effective traps for hydrogen (Matsumoto *et al.*, 1975). However, later experiments (Brown *et al.*, 1979; Hartmann *et al.*, 1983) unambiguously showed that Ta impurities do influence the μ^+ dynamics in Nb at low temperature.

The interpretation of the results in both papers was carried out in the framework of the diffusion-limited trapping model. It was suggested that the muon was trapped by nitrogen impurities (Borghini *et al.*, 1978) between 30 K and 50 K. The sharp drop in σ above 60 K was ascribed to the beginning of the release processes from the traps and subsequent motional narrowing. On the other side of the peak, the decrease of σ was explained by ineffective trapping because of the slowing down of the small polaron (self-trapped) state. According to this picture muons become immobile below 10 K, and one observed static Gaussian relaxation. Within this interpretation, however, it was hard to explain several peculiarities. First, the value of σ on the plateau 30–60 K is consistently lower for lower impurity content (see Fig. 16). Trapping sites are expected to have little effect on the μ^+ relaxation rate, as both natural ^{16}O and ^{12}C have zero nuclear moments, and the nuclear moment of ^{14}N is small. The static value $\sigma=\delta$ is therefore expected to be given by μ^+ interaction with the host ^{93}Nb nuclei only. Second, σ is not, in fact, constant for sample III in this temperature region. Third, the value of σ below 10 K is too small to be explained by self-trapped state localization.

Subsequent experiments figured out the role of different impurities. First, Brown *et al.* (1979) have found that oxygen had little effect on σ even at the level of 560 ppm, probably due to clusterization. Second, the decrease of the Ta content from 200 ppm down to 3 ppm led to the strong suppression of the two humps around the 20-K dip. Essentially the same picture was observed by Metz *et al.* (1979) in a Nb crystal with fewer than 2 ppm of N impurities and about 5 ppm of Ta impurities (RRR 5000). These experiments proved that the increase of the μ^+ relaxation rate below 20 K observed by Borghini *et al.* (1978) and Birnbaum *et al.* (1978) was not due to self-trapping. Finally, σ was measured to be as low as 0.1 μs^{-1} at low temperatures in the ultrapure Nb sample, with fewer than 2 ppm interstitial impurities and about 3 ppm of Ta as a substitutional impurity (Niinikoski *et al.*, 1979). Structured temperature dependence of σ was barely identified in this sample around 40 K, thus indicating that a small fraction of muons may end up in traps. Doping with 500 ppm of V, however, led to the reproduction of the "two-humped" shape with a dip shifted to 25 K.

All of the above-mentioned experiments showed that different impurities could affect μ^+ diffusion in Nb even when present in only tiny amounts. The high- and low-temperature plateaus in σ were associated with interstitial (mostly N) and substitutional (V, Ta) impurities, respectively. This was also demonstrated by Hartmann *et al.* (1983, 1984) in transverse-field measurements in Nb with nitrogen and Ta impurities. These measurements present results for the purest Nb samples (RRR 7500 and 11600) to date. The μ^+ diffusion was found to be so fast that the difference between samples containing interstitial impurities of N, C, and O on the level of 1 ppm was measurable by the standard μ^+SR transverse-field technique. All the experimental spectra were fitted to a Gaussian relaxation function independently of the temperature range and impurity content. The results are presented in Fig. 17. The purest Nb sample shows a low but nonzero and almost constant relaxation rate from 70 K down to about 0.1 K. It is about four times lower than the expected δ for static muons in Nb, but about an order of magnitude higher than the lowest measurable value.

The conventional diffusion-limited trapping model fails to explain these results. It was suggested by Hartmann *et al.* (1983, 1984) that the muon ensemble consisted of two fractions with different dynamic behavior.

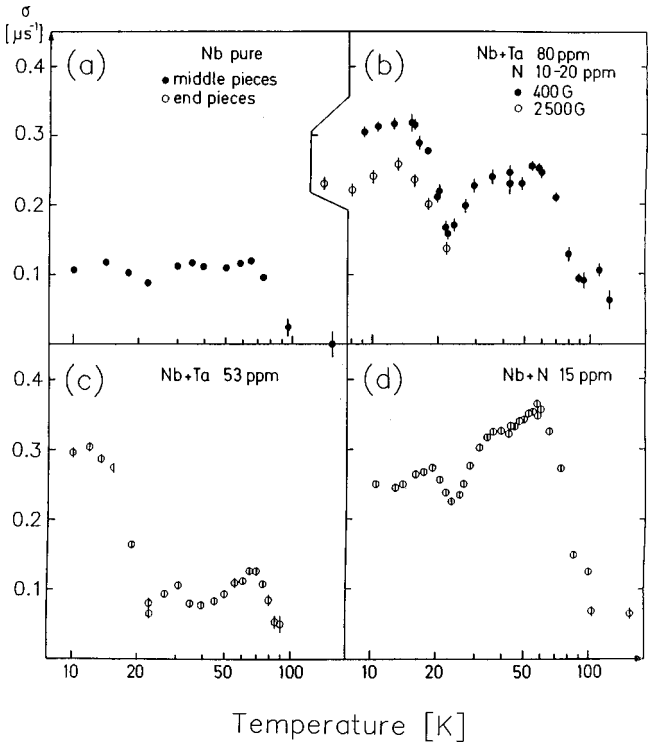

FIG. 17. Temperature dependences of the μ^+ Gaussian relaxation rate in different Nb samples. The "middle pieces" sample in (a) is the purest measured; the effect of doping with Ta and N impurities can be seen in (b)–(d) (Hartmann *et al.*, 1983).

The model was based on the assumption that muons do not always end up in a small polaron state immediately after thermalization (Emin, 1973, 1981; Emin and Holstein, 1976); self-trapping was assumed to be induced by static strains close to impurities (Browne and Stoneham, 1982). It was also suggested that the trapping rate was independent of temperature, in analogy with positron trapping, in order to explain the constant muon relaxation rate for the pure sample. With these assumptions it is virtually impossible to explain the consistently strong temperature dependence of σ in doped Nb, e.g., near the dip. Thus the whole picture looks rather confusing, since none of the measurements confirms it directly.

In any event, these experiments suggest a rather high value for the tunneling amplitude in Nb (bare or renormalized). For local tunneling of protons in niobium the tunneling splitting $2\Delta_{coh}$ was found to be 0.22 meV (Wipf *et al.*, 1987). It seems probable that Δ_{coh} for muons may be even larger, which will then naturally explain the anomalous sensitivity of the muon experiments to crystal defects. High-mobility muons easily find traps even at the level of 1 ppm. Existing data do not allow us to estimate accurately the actual tunneling amplitude, since all of them are controlled by impurities.

c. Bismuth

In bismuth the number of conduction electrons is more than five orders of magnitude smaller than that in Cu. It is expected, therefore, that the muon-electron

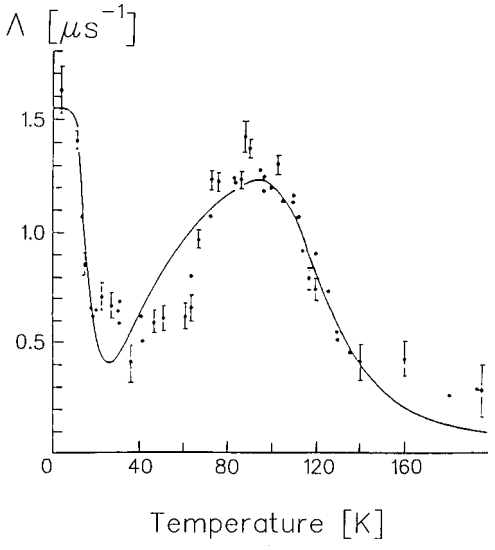

FIG. 18. Temperature dependence of the μ^+ Gaussian relaxation rate in an ultrapure Bi sample (Barsov *et al.*, 1983). The solid curve presents a fit to quantum diffusion theory in an imperfect crystal.

coupling in Bi is reduced considerably. Early transverse-field measurements were explained in terms of the two-phonon mechanism for diffusion (Grebinnik *et al.*, 1977). Later experiments led the authors to consider the influence of disorder as well, although the sample measured was ultrapure Bi with RRR 900 and impurity content below 6 ppm (Barsov *et al.*, 1983; see also Barsov *et al.*, 1984). The temperature dependence of the Gaussian relaxation rate in this sample is shown in Fig. 18. Note that there was a very small, although measurable difference between the ultrapure Bi and the sample with 100 ppm impurities used by Grebinnik *et al.* (1977). The solid curve in Fig. 18 presents the fit of the experimental results to the quantum diffusion expression for the hopping rate in a bias (Kagan and Maksimov, 1980), in an attempt to model disorder effects using a single parameter ξ [see Eq. (108) below]. The best fit was obtained for $\xi \approx 0.3$ K and $\Delta \sim 10^{-3}$ K. In the high-T regime the data were well described by the Arrhenius law with rather large activation energy $E = 1470$ K and preexponential factor $\nu_\mu \approx 10^{11}$ s^{-1}, thus indicating classical over-barrier diffusion.

There is a significant discrepancy with the experimental results around the flat minimum in $\sigma(T)$ between 20 K and 60 K, which was suggested (Barsov *et al.*, 1983) to originate from the spatial distribution of energy levels in the sample (neglected in the theoretical fit). This point is precisely confirmed by the result (71), which predicts $\sigma = \Lambda_* \sim \Omega^{-2/7}$; a much weaker temperature dependence than that for the biased homogeneous result with sharp minimum $\sigma \sim (\xi^2 + \Omega^2)/\Omega$ used in the original fit (the new fit has never been done for reasons given below).

Another explanation (Ivanter, 1984) suggests a turnover from long-range diffusion at low temperatures to local motion within an extended trap region at intermediate temperatures. At higher temperature detrapping and long-range diffusion were assumed to come into

play again. This approach involves three different states for μ^+ in Bi: two different sites at low and high temperatures for the static muon and an extended (delocalized) state. However, the nature of the muon states and diffusion mechanisms was not discussed by Ivanter (1984), thus making the entire explanation a bare fit.

An identification of the muon states (static and delocalized) in high-purity Bi with about 10 ppm impurities has been carried out by Gygax *et al.* (1988; see also Baumann *et al.*, 1986a) using a single crystal and studying the angular dependence of δ. These results have convincingly proved that μ^+ is well localized below 10 K (τ_c^{-1} values were determined to be less than 0.1 μs^{-1}) and between 90 K and 100 K in different interstitial sites in these two temperature regions, in remarkable correlation with different angular dependences of the μ^+ Knight shifts below 10 K and in the range 90–100 K (Gygax *et al.*, 1986; see also Baumann *et al.*, 1986b). This fact alone rules out the validity of the previous interpretation in terms of quantum diffusion proceeding via only one type of interstitial positions (Barsov *et al.*, 1983).

Although the overall temperature dependence of $\sigma(T)$ in these experiments was rather close to that previously observed, the absolute values were different, and the major difference was in the *temperature-independent* relaxation rate in the minimum (almost a straight plateau). Above 10 K a reduction of σ was interpreted as the result of dynamic narrowing, and the data were analyzed using the dynamic Kubo-Toyabe function. This conclusion was made on the basis of nearly constant anisotropy of the relaxation rate between 10 K and 15 K, despite its reduction [a procedure that was objected to by Kadono *et al.* (1988) on the basis of mainly longitudinal-field measurements; however, the longitudinal fields of 10 Oe used in this experiment seem to be too high to make a definite conclusion]. On the plateau between 20 and 60 K, however, this picture completely breaks down, since no anisotropy in the second moment was detected at these temperatures, and a T-independent σ can hardly be explained in terms of any diffusion theory. Gygax *et al.* (1988) proposed that a fast, locally restricted motion over few positions was responsible for the observed relaxation. Local motion was thought to be a tunneling or hopping along the chains of alternating positions, which are stable sites for μ^+ at low temperatures and in the 90–100 K range. The result of such a limited motion would be a reduced effective second moment $\sim \delta_\mu^2/N_d$ (see Sec. III.B). The spatial extension of the local motion was suggested to be limited by lattice impurities and imperfections and estimated to include few lattice spacings (depending on the sample quality). The local delocalization of μ^+ in the temperature range 20–60 K was also suggested by Kadono *et al.* (1988). In this paper an alternative fitting of the experimental spectra was done under the assumption that the μ^+ polarization consisted of two contributions: from muons in the stable and in the metastable states. The origin of the metastable state, however, was not clearly specified.

To sum up, concerning μ^+ diffusion in Bi, one could argue that experiments do not even prove unambiguously that it is of quantum nature below 90 K. The question still remains open whether the temperature independence of the μ^+ relaxation rate between 20 K and 60 K is due to spatial distribution of the energy-level shifts in the regime of static destruction of the band (Barsov *et al.*, 1983) or due to local tunneling (Gygax *et al.*, 1988; Kadono *et al.*, 1988), analogous to that found for hydrogen in $Nb(OH)_x$ (Wipf *et al.*, 1987; Steinbinder *et al.*, 1988). The first explanation is much less probable, because it predicts a weak, but not constant $\sigma(T)$. In our opinion the most reasonable physical model should employ both ingredients, e.g., the Kagan-Maksimov picture with an even deeper minimum, which is, however, cut in the region of the fastest diffusion by the finite-size delocalized states. In this connection we should also like to mention recent results on muon depolarization in Sc at low temperature, which have been interpreted in terms of muon delocalization between the two adjacent sites (Gygax *et al.*, 1994, 1995).

VI. QUANTUM DIFFUSION OF MUONIUM ATOMS IN INSULATORS

The formation of a muonium atom in matter usually takes place at times much shorter than the characteristic time of Mu dynamics (Schenck, 1985; Cox, 1987; Brewer, 1994), even in the case of delayed muonium formation (at least for a certain fraction of muons) (Storchak, Brewer, and Morris, 1994a, 1995a, 1995b, 1996a, 1997; Storchak, Brewer, and Cox, 1997; Storchak, Brewer and Eschenko, 1997). The huge ionization energy of Mu ensures that the captured electron follows the μ^+ adiabatically.

The quantum diffusion of Mu in insulators, like that of μ^+ in metals, shows both homogeneous and inhomogeneous regimes. However, much weaker coupling to the crystal defects and the superb quality of insulating crystals has hampered the observation of the inhomogeneity in Mu quantum diffusion. The phonon broadening of Mu energy levels Ω and large bandwidth Δ in many cases overcome crystal disorder. At low temperature, the phonon coupling is suppressed, and quantum diffusion may be dominated by impurities. This results in drastic changes both in the temperature dependence of the muonium hop rate and the time decay of the polarization function. In this section we shall describe Mu quantum diffusion in insulating crystals of alkali halides and van der Waals cryocrystals, as well as in compound semiconductors GaAs and CuCl. Both the one-phonon regime at high temperatures and the two-phonon regime at low temperatures will be discussed in detail along with the band motion regime. Inhomogeneous quantum diffusion and trapping phenomena in insulators will be considered in comparison to those for μ^+ diffusion in metals.

It is worth mentioning that Mu quantum diffusion shares many common features with another notable system: ^{3}He solid solution in a ^{4}He crystal (Mikheev *et al.*,

1977; Allen and Richards, 1978); many of the ideas are equally well applicable to both systems.

A. Transition probabilities, trapping, and diffusion rates in insulators

We discussed in Sec. V.A the high-temperature limit for incoherent tunneling in metals and found that it is governed by one-phonon processes. Thus all the results presented there are valid for insulators as well, except that in Eq. (49) one has to set $K=0$.

At low temperatures and in a perfect crystal the one-phonon processes are forbidden by conservation laws. The special role of the two-phonon interaction was clear in our discussion of coherence in Sec. III.D. Formally, the theory is identical to that considered for metals if one assumes a temperature-dependent coupling constant $K=\Omega_{2ph}/\pi T \ll 1$. Thus we find for the incoherent regime (for simplicity in the rest of this section we shall use $\Omega \equiv \Omega_{2ph}$, so as not to confuse it with Ω_{el})

$$D(T)=\frac{Za^2}{3}\frac{\Delta_o^2(T)}{\Omega}. \tag{107}$$

This result was first obtained by Kagan and Maksimov (1973). It should be emphasized that the asymptotic law $\Omega \sim T^{7+(2)}$ [again, the factor 2 in parentheses is present for translationally invariant coupling (Fujii, 1979)] works only at sufficiently low temperatures $T<\Theta/10-\Theta/20$ in real crystals (Kagan and Prokof'ev, 1991). At higher temperatures (but still $T \ll \Theta$) it depends crucially on the details of the phonon spectrum and approaches $\Omega \sim T^2$ at $T \lesssim \Theta$ [see Eq. (51)].

Let us now analyze the role of one-phonon processes at low T. To this end we consider the time-dependent terms in $\Psi(t)$ in Eq. (39) as a weak perturbation and expand the exponent up to the second term. We obtain the correction to the first-order result (107) in the form $W^{(1)}=2\pi\Delta_o^2(T)T[f_{1ph}(\omega)/\omega^2]_{\omega\to 0}$. This gives nonzero $W^{(1)}$ only if $f_{1ph}\sim\lambda_1\omega^2$ at low frequencies, that is, for tunneling between the sites that may not be obtained by translational invariance. One then finds (Kagan and Maksimov, 1980; Teichler and Seeger, 1981)

$$W^{(1)}=2\pi\lambda_1\frac{\Delta_o^2(T)T}{\Theta^2}. \tag{108}$$

Obviously, the correction is negligibly small at low temperatures. The correction is nonzero because, having more than one particle site in the unit cell, we have few bands in the momentum representation. In this case one-phonon scattering between the tunneling bands is not prohibited by the conservation laws.

Consider now the biased case. If the bias energy ξ is small enough (see below), then only two-phonon processes are important, and (Kagan and Maksimov, 1980, 1983)

$$W=\frac{2\Delta_o^2(T)\Omega}{\xi^2+\Omega^2}\xrightarrow[\xi\gg\Omega]{}\frac{2\Delta_o^2(T)\Omega}{\xi^2}. \tag{109}$$

We see that just as in superconductors there is a strong tendency toward localization at low temperatures. However, the law $W\sim\Omega/\xi^2$ may not hold for long as $T\to 0$, because one-phonon processes will take over (momentum conservation is not an issue in the disordered crystal). With the one-phonon processes included we have the transition probability

$$W=\frac{2\Delta_o^2(T)}{\xi^2+\Omega^2}(\Omega+\pi T[f_1(\xi)+h(\xi)])\frac{\xi/T}{1-e^{-\xi/T}}. \tag{110}$$

The crossover temperature T_ξ is evidently defined from $\Omega(T_\xi)/\pi T_\xi=f_1(\xi)+h(\xi)$. Since $h(\omega)\sim h_1\omega^4$ at low frequencies, barrier fluctuation effects are important in the particle dynamics only for translationally invariant coupling, when $f(\omega)\sim\lambda_1\omega^4$ also. At $T<T_\xi$ the transition probability has a linear temperature dependence

$$W\approx 2\pi\lambda_1\frac{\Delta_o^2(T)T}{\Theta^2}\left(\frac{\xi}{\Theta}\right)^{(2)}\frac{\xi/T}{1-e^{-\xi/T}}. \tag{111}$$

We see that not only the temperature dependence, but also the bias dependence, changes below the crossover. Now the particle dynamics are either completely independent of the disorder (unless it is trapped, $\xi>T$) or $W(\xi)\sim\xi^2$ and the disorder promotes tunneling. The result seems trivial to those who used to study phonon-assisted transitions in, say, NMR, but it is certainly not in the mainstream of the intuition developed while starting from the coherent delocalized states in a perfect crystal. Note that at the trapping radius (66) we always have $\xi>\Omega$, and the local diffusion rate goes to zero as $T\to 0$, no matter how far R_T is from the defects.

As before, the crossover temperature T_{min} between the low-temperature (110) and high-temperature (97) asymptotic expressions is obtained very accurately by matching the two results. It depends, of course, on one-phonon coupling (shifting T_{min} downwards for large $\overline{C}_\alpha$) and two-phonon couplings (shifting T_{min} upwards for small $\overline{C}_{\alpha\beta}$).

B. Experimental results on muonium quantum diffusion in ionic insulators, compound semiconductors, and cryocrystals

1. Two-phonon muonium diffusion

The theory of quantum diffusion in insulators predicts the existence of an ubiquitous minimum in the temperature dependence of the diffusion coefficient $D(T)$ (Andreev and Lifshitz, 1969; Kagan and Maksimov, 1973), and divergent $D(T)\propto T^{-\alpha}$ dependence with $\alpha=7$ or 9 in the low-temperature limit. Surprisingly, the experimental results on Mu diffusion in ionic insulators (Kiefl *et al.*, 1989; Kadono, 1990; Kadono *et al.*, 1990) and compound semiconductors (Kadono, Kiefl, Brewer, *et al.*, 1990; Schneider *et al.*, 1992a; 1992b) indicate that α is generally close to 3; this "universal" power-law behavior even led Stamp and Zhang (1991) to suspect that muonium diffusion is governed by *one*-phonon scattering, but the numbers obtained for τ_c^{-1} were too high to ex-

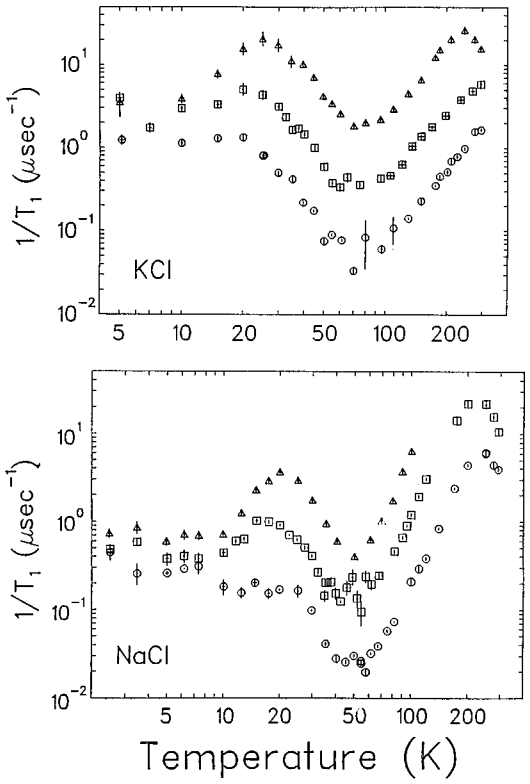

FIG. 19. Temperature dependences of the average muon-spin relaxation rate in KCl and NaCl in longitudinal magnetic fields: circles, 200 Oe; squares, 500 Oe; triangles, 1500 Oe (Kadono, 1990).

plain the data (as was later recognized by the authors). As explained above, $2<\alpha<7$ is not at all in contradiction with the two-phonon scattering processes. The first direct observation of the T^{-7} temperature dependence for the Mu hop rate was reported in a van der Waals insulating crystal of solid nitrogen (s-N_2) (Storchak *et al.*, 1994a) whose phonon spectrum is much closer to the Debye model (see also Storchak, Brewer, and Morris, 1996b).

a. Ionic insulators

Measurements of the muonium diffusion in KCl (Kiefl *et al.*, 1989; Kadono, 1990), NaCl (Kadono, 1990; Kadono *et al.*, 1990) and KBr (Kadono, 1990) were carried out using the longitudinal-field technique (see Sec. IV.B). We were unable to find the temperature dependence of the muonium hop rate in KBr in the published literature, although the slow-relaxing component shows $T_1^{-1}(T)$ relaxation with a characteristic minimum very similar to that in KCl and NaCl. Therefore we shall concentrate on analysis of the experimental results in KCl and NaCl only.

Muonium diffusion measurements in KCl and NaCl were performed in pure single crystals. The temperature dependences of T_1^{-1} for both crystals are shown in Fig. 19. Although the data in KCl and NaCl look pretty much the same, in NaCl the relaxation rates are considerably different at the two maxima. The spin Hamiltonian for Mu in the tetrahedral interstitial site in alkali halides is similar to Eq. (83) (one should also take into account the anisotropy of the nuclear hyperfine interaction; Spaeth, 1969). ESR and electron-nuclear double-resonance results on the hydrogen center (Spaeth, 1969) have shown that the dominant nuclear hyperfine interaction is with the four nearest-neighbor spins of the Cl nuclei. Below 200 K the observed Mu relaxation is attributed entirely to the motion of interstitial muonium, since it is consistent with the results of transverse-field measurements (Kiefl *et al.*, 1984). This is compatible neither with charge-exchange reactions seen at higher temperatures (Nishiyama *et al.*, 1985; Morozumi *et al.*, 1986) nor with spin-exchange reactions on paramagnetic impurities (Kiefl *et al.*, 1989). In KCl δ_{Mu} is independent of temperature, yielding on average the same value as derived from the high-transverse-field data at room temperature (Baumeler *et al.*, 1986) and the corresponding value for the hydrogen atom from ESR and electron-nuclear double-resonance data (Spaeth, 1969). As for δ_{Mu} in NaCl, analysis (Kadono *et al.*, 1990) revealed its significant temperature dependence. It should be mentioned that in KCl a small nonrelaxing component of muon polarization was observed at temperatures above about 200 K (Kadono, 1990), which may reflect the conversion of Mu into a diamagnetic state (Nishiyama *et al.*, 1985; Morozumi *et al.*, 1986). In NaCl the same effect was seen above 200 K and below 20 K (we shall comment more on this below).

The Mu hop rate τ_c^{-1} and nuclear hyperfine interaction parameter δ_{Mu} were determined within the framework of the effective-field approximation by simultaneous fitting of the μ^+SR time spectra taken at two or three external magnetic fields using the general expression for muon spin relaxation derived from the Redfield equations (see Sec. IV.B). The maxima in $T_1^{-1}(T)$ for both crystals are clearly seen at about 20 K and 200 K and reflect the T_1-minimum effect. The temperature dependences of Mu τ_c^{-1} and δ_{Mu} for both crystals are shown in Fig. 20. First, we notice the spectacular increase of τ_c^{-1} by 2.5–3 orders of magnitude with decreasing temperature below T_{min}. This is a direct manifestation of Mu quantum diffusion. Below about 10 K τ_c^{-1} levels off, indicating the onset of coherent propagation. Second, above T_{min} the hop rate increases by almost two orders of magnitude, which also undoubtedly reflects the sub-barrier motion of muonium, as the pre-exponential terms in the corresponding activation dependences lack about three orders of magnitude to be explained by classical diffusion. In the entire temperature range Mu shows remarkable dynamic properties with at least 200 hops during its lifetime.

The nature of the Mu diffusion between 10 K and the corresponding minimum, which was approximated by a power law as $T^{-\alpha}$ with $\alpha\approx 3$, has caused some confusion (Kadono *et al.*, 1990; Kadono and Kiefl, 1991; Stamp and Zhang, 1991; Kadono, 1992). Although it was initially recognized that large α clearly reflects the difference between metals and insulators in light interstitial diffusion, the nature of Mu diffusion in KCl and NaCl in this tem-

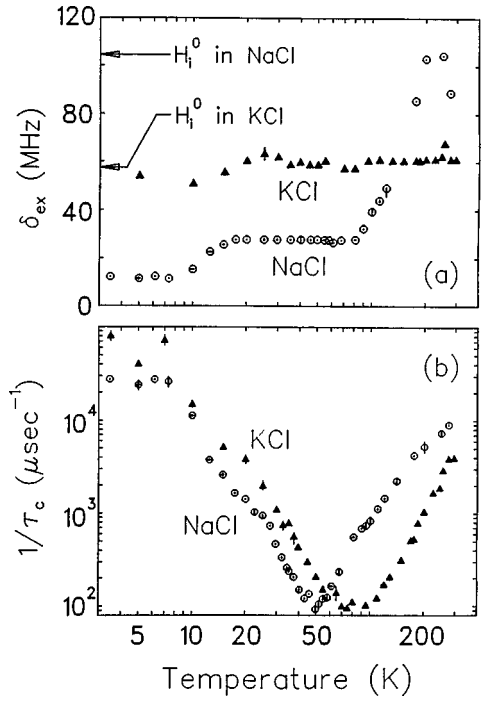

FIG. 20. Temperature dependences of (a) the nuclear hyperfine frequency parameter δ_{Mu} and (b) the Mu hop rate in KCl and NaCl (Kadono *et al.*, 1990). Arrows in (a) indicate the values estimated for a hydrogen atom in each material.

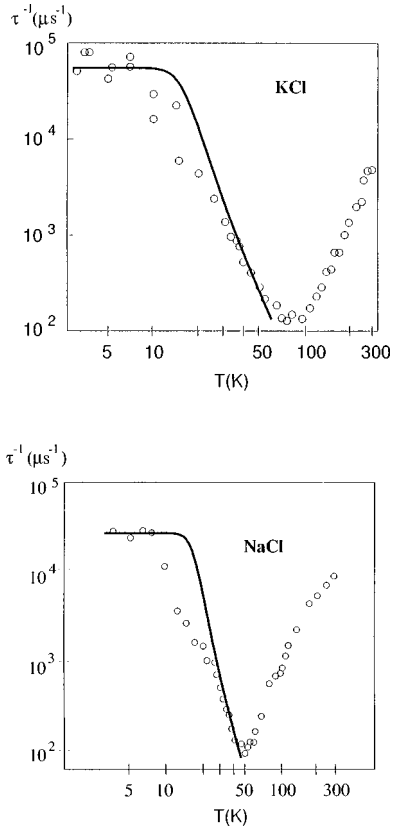

FIG. 21. Low-temperature behavior of the Mu hop rate in (a) KCl (Kiefl *et al.*, 1989) and (b) NaCl (Kadono *et al.*, 1990). The parameters of theoretical curves (Kagan and Prokof'ev, 1990a) are described in the text.

perature range was first interpreted as coherent hopping (Kiefl *et al.*, 1989; Kadono *et al.*, 1990). However, *any* observed temperature dependence inevitably involves particle interaction with the phonon bath. The low value of α (smaller than 7) cannot be explained by the one-phonon interaction assuming a wide coherent band $\Delta \sim \Theta$ for Mu in KCl (Stamp and Zhang, 1991), for two reasons: (i) The experimental correlation time (between 10^7 and 3×10^{10} s^{-1}) is incompatible with that estimated from $\Delta\sim\Theta$; (ii) the diffusion rate in the coherent regime has nothing to do with the measured τ_c^{-1}, because only correlations local in space are measured in the μSR experiment, and τ_c^{-1} does not depend on the large mean free path $l_{mfp}\gg a$, as explained in Sec. III.

It was shown by Kagan and Prokof'ev (1990a) that the temperature dependence of τ_c^{-1} in KCl and NaCl below T_{min} is not at all in contradiction with the two-phonon scattering theory, provided the real structure of the phonon spectrum of these crystals [measured in inelastic neutron-scattering experiments (Bilz and Kress, 1979)] is accounted for. In crystals with many atoms in the unit cell, this structure deviates from the Debye law well below Θ. For the experimental data of Kiefl *et al.*, (1989) and Kadono *et al.* (1990), intermediate phonon frequencies are essential, and $\Omega_{2ph}\sim T^7$ cannot be applied. The results of these theoretical calculations, including smooth interpolation between coherent and incoherent tunneling in the form $\tau_c^{-1}=\tau_0^{-1}/(1+\Omega\tau_0)$, are presented in Fig. 21. Only one fitting parameter for the two-phonon constant λ_{2ph} was used in this analysis, that is, the unknown function $\overline{C}_{\alpha\beta}$ was approximated as $|\overline{C}_{\alpha\beta}|^2=\lambda_{2ph}\omega_\alpha\omega_\beta$ to account for the correct low-frequency properties of $\overline{C}_{\alpha\beta}$ in this crystal. This approximation is very simple indeed. Still, without rigorous calculations of the coupling constants from first principles, one can use λ_{2ph} for rough estimates. This parameter controls the scale but not the shape of the $\tau_c^{-1}(T)$. The agreement between experimental and theoretical results is nevertheless reasonably good. The results of the numerical calculation lead to $\alpha=3.5$ for KCl, while in Kiefl *et al.* (1989) it was 3.3(1). For NaCl the calculation gave $\alpha=4.3$.

It should be noted that the irregular character of the experimental data in NaCl around 20 K seems to be related not to the behavior of τ^{-1}, but rather to the drastic variation of the hyperfine interaction. While in the earlier work (Kiefl *et al.*, 1989), where τ^{-1} was extracted with the fixed value of δ_{Mu}, experimental points show a smooth dependence of $\tau^{-1}(T)$, in later publications (Kadono *et al.*, 1990; Kadono, 1990, 1992) we see distinct correlations between the irregular behavior of τ_c^{-1} and variations of δ_{Mu}. This might be the result of the instability of the χ^2 fit of the experimental time spectra.

b. Compound semiconductors

When implanted into semiconductors positive muons often form Mu, as happens in insulators (Patterson,

1988). The application of the longitudinal-field technique for Mu diffusion measurements developed by Kiefl *et al.* (1989) to GaAs has revealed that τ_c^{-1} varies by more than two orders of magnitude. Although two types of Mu have been observed in GaAs [an isotropic atom with a formation probability of about 60% (Kiefl *et al.*, 1985), which exhibits remarkable dynamic properties, and a highly anisotropic center (Kiefl *et al.*, 1987)], the isotropic atom is readily distinguished from the anisotropic center, because its hyperfine coupling constant A is more than an order of magnitude larger. From now on we shall discuss the study of the former while the latter just causes a nonrelaxing part of the muon polarization, as its frequencies are completely decoupled in the high longitudinal fields used in the experiments.

The first measurements of Mu diffusion in GaAs, carried out in the temperature range 3–300 K, revealed $\tau_c^{-1}(T)$ with a characteristic minimum around 90 K, leveling off below 10 K (Kadono, Kiefl, Brewer, *et al.*, 1990). The experiment was performed using a single-crystal GaAs wafer of high resistivity (8×10^7 Ohm$\times$cm). The observation of the T_1 minimum at high temperatures (around 240 K) allowed Kadono *et al.* to determine $\delta_{\mathrm{Mu}}=236(3)$ MHz (see Sec. IV.B). This value was fixed throughout the analysis in order to extract $\tau_c^{-1}(T)$, which was done by following the same procedure as for KCl (Kiefl *et al.*, 1989). Note that the sensitivity of the longitudinal-field measurements was insufficient to prove that δ_{Mu} is T independent over the entire temperature range. The extension of the Mu diffusion measurements in GaAs down to 20 mK in the same sample and measurements of two other undoped samples of comparable resistivity (Schneider *et al.*, 1992a) revealed essentially the same $\tau_c^{-1}(T)$. Figure 22 shows the temperature dependence of the average relaxation rate at three different applied longitudinal fields obtained by fitting the individual spectra separately with a single exponential (a), and the muonium τ_c^{-1} resulting from the simultaneous fit of the three spectra per temperature point (b). Below 90 K the hop rate increases by almost two orders of magnitude with decreasing temperature, according to $T^{-\alpha}$ with $\alpha=3.0(1)$, pretty much resembling $\tau_c^{-1}(T)$ in ionic insulators.

A rather anomalous picture of Mu dynamics was observed in CuCl (Schneider *et al.*, 1992a; Schneider *et al.*, 1992b). High-transverse-field μ^+SR experiments (Kiefl *et al.*, 1986) have shown that in CuCl there are two distinct muonium centers, Mu^I and Mu^{II}, with small but comparable isotropic hyperfine coupling parameters. Although the two centers coexist at low temperatures, one of them, Mu^I, is metastable and eventually converts into the stable form, Mu^{II}, above about 100 K. Subsequent muon level-crossing resonance experiments (Schneider *et al.*, 1990) established unambiguously that both Mu^I and Mu^{II} are centered at a tetrahedral interstice and their nuclear hyperfine interaction parameters differ very little. This puzzle was resolved by Schneider *et al.* (1992a), who found that Mu^I undergoes fast but local tunneling between the four off-center positions, while

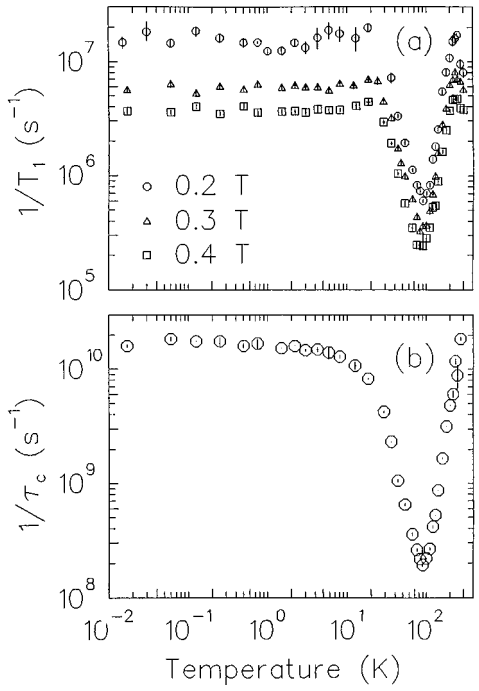

FIG. 22. Temperature dependences of (a) the average longitudinal muon relaxation rate at three different magnetic fields and (b) the muonium hop rate τ_c^{-1} in GaAs (Schneider *et al.*, 1992).

Mu^{II} is localized. Therefore the dependence $\tau^{-1}(T)$ in CuCl shown in Fig. 23 corresponds to local tunneling of Mu^I. It obeys a power law $T^{-\alpha}$ with $\alpha=2.7(1)$ below 30

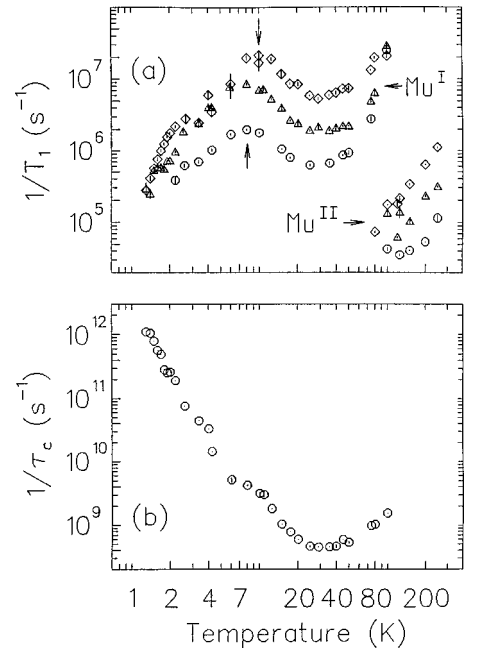

FIG. 23. Temperature dependences of (a) the average T_1^{-1} relaxation rate and (b) the corresponding muonium τ_c^{-1} in CuCl (Schneider *et al.*, 1992a). Diamonds, triangles, and circles in (a) correspond to magnetic fields of 1000 Oe, 2000 Oe, and 4000 Oe, respectively. The unmarked arrows indicate T_1 minima.

K, in remarkable similarity to ionic insulators. Although we are reluctant to change our opinion that this behavior is due to two-phonon scattering, we cannot ignore the importance of one-phonon processes at very low temperatures, because the momentum conservation law does not apply for local tunneling.

The overall temperature dependence of $\tau_c^{-1}(T)$ resembles that in GaAs, having a characteristic minimum at 30 K, but at low temperatures $\tau_c^{-1}(T)$ does not level off. At the lowest measured temperature (about 1 K), the hop rate is higher than in GaAs by about two orders of magnitude and even exceeds T. In Sec. VI.B.1.c we demonstrate that what was interpreted as τ_c^{-1} in CuCl is in fact a "nonphysical" parameter.

c. Solid nitrogen

The "universality" of the power law $\tau_c^{-1} \sim T^{-\alpha}$ with $\alpha \approx 3$ below the minimum was upset by the experiments in solid nitrogen (Storchak *et al.*, 1993; 1994a; see also Storchak, Brewer, and Morris, 1994b, 1996b; Storchak, Brewer, Hardy, *et al.*, 1994a), which reported that below T_{min} the temperature dependence of the Mu hop rate obeyed the same power law but now with α close to 7. Measurements were done in perfect, absolutely transparent crystals of ultrahigh-purity nitrogen ($^{14}N_2$ with $\sim 10^{-5}$ impurity content). Muonium formation was first detected in a weak transverse field by observing the triplet Mu precession. Typical weak-transverse-field-μ^+SR spectra in s-N_2 are shown in Fig. 2. Time spectra taken at 28 K in transverse fields of up to 170 Oe were analyzed using Eq. (85) to obtain the hyperfine coupling constant $A = 4494(5)$ MHz, significantly higher than the vacuum value 4463 MHz. This suggests that the Mu atom is slightly compressed by interactions with the crystal lattice.

Measurements in transverse fields revealed a strong nonmonotonic temperature dependence of T_2^{-1}. Below about 10 K there is a typical leveling off of T_2^{-1}, expected for very slow diffusion ($\tau_c^{-1} \lesssim \delta$), which gives the value of the nuclear hyperfine interaction parameter $\delta_{Mu} = T_2^{-1}$. Subsequent T_1^{-1} measurements were carried out to study slow Mu dynamics (see Sec. IV.B); one can see the μSR time spectra in longitudinal fields in Fig. 3. The observed relaxation is attributed entirely to the muonium fraction, as the relaxation rate of the diamagnetic complex $N_2\mu^+$, which is known to be static (Storchak *et al.*, 1992), is about 0.1×10^6 s^{-1}, i.e., far slower than that evident in Fig. 4. Moreover, the amplitude of the relaxing component in a longitudinal field is equal to the amplitude of the muonium precession signal in a transverse field. Complete quenching of the low-temperature relaxation in longitudinal fields ≈ 1 kG allows one to rule out spin-exchange reactions with possible paramagnetic impurities (e.g., O_2) as the cause of muonium spin relaxation. We are therefore confident that the relaxation presented in Fig. 4 is due entirely to Mu motion.

Figure 24 shows the temperature dependence of T_2^{-1} in a transverse field and T_1^{-1} for several values of longitudinal field for Mu in solid nitrogen. The T_1^{-1}-maximum effect is clearly seen around 10–11 K for all longitudinal fields. Using the standard analysis described in the Sec. IV, the value of $\delta_{Mu} = 14.9(0.8)$ MHz (which is within 7% of the value obtained from transverse-field measurements at low T) and the temperature dependence of the hop rate were extracted. These results are presented in Fig. 25. First we notice the characteristic minimum at $T = 50$ K with a steep increase of τ_c^{-1} between 50 K and 30 K as the temperature is lowered — an unambiguous manifestation of Mu quantum diffusion. In the temperature range $30 < T < 50$ K, the hop rate exhibits an empirical temperature dependence $\tau_c^{-1} \propto T^{-\alpha}$ with $\alpha = 7.3(2)$. This is a direct experimental confirmation that the dependence of $\tau_c^{-1}(T)$ is not at all "universal" below T_{min}, and higher values of α are also possible, although in this particular case we do not think that the observed dependence is entirely due to the two-phonon scattering mechanism. It is somewhat puzzling that the asymptotic low-

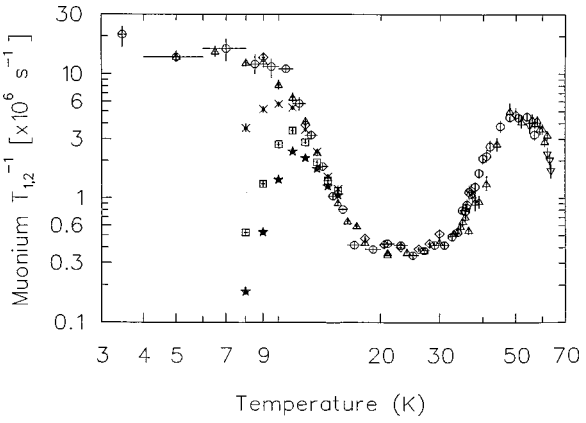

FIG. 24. Muonium relaxation rates in ultra-high-purity solid N_2 in a weak transverse field [circles, triangles, diamonds, and inverted triangles correspond to different samples] and several longitudinal fields: stars, 12 G; squares, 8 G; crosses, 4 G (Storchak *et al.*, 1994a).

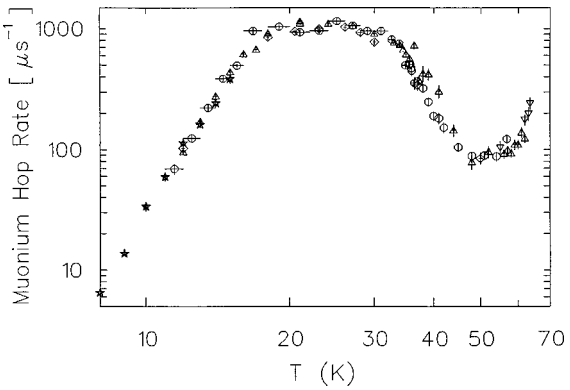

FIG. 25. Temperature dependence of the muonium hop rate in ultra-high-purity solid N_2. Stars correspond to the combined longitudinal-field measurements; circles, triangles, diamonds, and inverted triangles correspond to transverse-field measurements in different samples (Storchak *et al.*, 1994a).

temperature dependence is observed at temperatures as high as $\Theta/2$ in solid nitrogen. It may not be explained by the $\Omega(T)$ dependence, at least at temperatures between 50 and 30 K, even within the Debye model for the phonon spectrum (in solid nitrogen $\Theta=83$ K; Verkin and Prikhotko, 1983). Rather, one gets $\Omega(T)$ close to T^2 in this temperature range. An alternative explanation may be based on the relatively high value of $T_{min}>\Theta/2$. In this temperature range (as we learned from all the previous examples) one-phonon effects are very strong and may result in a strong temperature dependence of $\Delta_o(T)$. Apparently the strong temperature dependence of τ_c^{-1} near the minimum is largely due to one-phonon exponential renormalization of the tunneling amplitude. To answer this question one has to calculate the hop rate in nitrogen with all the interactions included, Eq. (39).

Below about 30 K the hop rate levels off, presumably due to Mu band motion. This regime of Mu diffusion in solid N_2 is discussed in Sec. VI.B.2 below. Surprisingly, and quite in contrast with the other materials considered above, Mu motion slows down again below about 18 K. This happens, presumably, due to the orientational ordering of N_2 molecules. Heat capacity (Bagatskii *et al.*, 1968), thermal expansion (Manzhelii *et al.*, 1966), and NMR data (DeReggi *et al.*, 1969) in solid nitrogen all show peculiarities at about 20 K which are attributed to "orientational defects" caused by an anisotropic interaction between N_2 molecules. Above about 20 K, large-angle librations of the host molecules average the Mu-N_2 interaction energy to a well-defined, site-independent value; below the ordering temperature, Mu energy levels at neighboring sites may differ by a typical static shift ξ, which impedes Mu diffusion according to Eq. (109). However, independent experimental data confirming this assumption are not available. For H atoms in solid nitrogen these energy shifts are $\xi\sim 1$ K (Sieghban and Lui, 1978); the value of the Mu-libron interaction is most probably of comparable magnitude. Since $\tau_c^{-1}(T)$ below 18 K is unaffected by doping with up to 0.01% impurities (Storchak *et al.*, 1993), this slowing down of Mu diffusion at low temperature is believed to be an intrinsic property of solid nitrogen. For $T<18$ K and down to ~ 8 K, the data in Fig. 25 obey $\tau_c^{-1}=\tau_0^{-1}(T/\Theta)^{\alpha}$ with $\tau_0^{-1}=3.6(8)\times 10^{13}$ s^{-1} and $\alpha=6.7(1)$. The change in the temperature dependence of the Mu hop rate to a T^7 law reflects the crossover from Eq. (107) to Eq. (109). In this temperature range we hardly expect that the one-phonon dependence of $\Delta_o(T)$ plays any role, and the observed law has to be due to two-phonon dissipation (Kagan and Maksimov, 1983, 1984).

We note here that the two-phonon scattering mechanism was also found to determine quantum diffusion of ^{3}He atoms in solid ^{4}He (Mikheev *et al.*, 1977; Allen and Richards, 1978; Allen *et al.*, 1982), where the diffusion rate diverges in the dilute limit as $D(T)\sim T^{-\alpha}$ with $\alpha=9\pm 2$.

2. Muonium band tunneling

Muonium band motion occurs if disorder is weak, $\xi\ll\Delta$, and coherence is preserved, $\Omega\ll\Delta$ (see Sec. III). In this case Mu τ_c^{-1} is temperature independent and defined by Eq. (14). This section is devoted to the band motion regime observed in ionic insulators, compound semiconductors, neon, and nitrogen.

a. Ionic insulators, GaAs and CuCl

The band motion of Mu in KCl (Kiefl *et al.*, 1989), NaCl (Kadono *et al.*, 1990), GaAs (Kadono, Kiefl, Brewer, *et al.*, 1990; Schneider *et al.*, 1992b), and in CuCl (Schneider *et al.*, 1992a) is seen as $\tau_c(T)$ levels off at low temperature. Initially it was attributed to Mu interaction with crystal imperfections. The fact that impurities cannot result in the T-independent τ_c is evident from Eq. (109), which is relevant because disorder may influence particle dynamics on an atomic scale only if $\Delta<\xi$ (see Sec. III). Thus one expects an inevitable decrease in τ_c^{-1} as the temperature is lowered in this case, in contradiction with the experimental data. Moreover, at low enough temperatures Mu relaxation in disordered insulators should show a multicomponent time dependence, also not observed in these experiments (Sec. III.B). The formal averaging procedure proposed by Kondo (1986) and Sugimoto (1986) is obviously ill defined for $(\Omega,\xi)<\Delta$ (apart from other weak points mentioned in Sec. III), because it uses an *incoherent* expression for the correlation time in a regime where the particle is already propagating coherently in the band. A special set of measurements was carried out (Schneider *et al.*, 1992b) in the temperature range 3–40 K in three different crystals of GaAs (expected to have noticeably different purity due to different sources of the samples), with the net result that weak disorder had no effect on τ_c^{-1} in GaAs.

Muonium band motion presents an obvious explanation of the temperature-independent τ_c^{-1} at low T, Eq. (14). From the plateau value of τ_c^{-1} one can derive the coherent tunneling amplitude Kagan and Prokof'ev (1990a) found it to equal $\Delta_{coh}\approx 0.13$ K in KCl [in a later experiment (Macfarlane *et al.*, 1994) this was corrected to 0.157(5) K], $\Delta_{coh}\approx 0.07$ K in NaCl, and $\Delta_{coh}\approx 0.03$ K in GaAs.

As for the possibility of Mu delocalization (band motion) at temperatures just below 200 K in NaCl (Kadono *et al.*, 1990; Kadono, 1990, 1993), we doubt that it can be physically justified. This idea was introduced on the basis of a steplike reduction in δ_{Mu} below 200 K (see Fig. 20). The indication of a further reduction in δ_{Mu} was also found below 20 K, although the fit of the experimental time spectra in this temperature range was not always satisfactory (Kadono *et al.*, 1990). The reduction of δ_{Mu} was explained as an averaging of the magnetic interaction between muonium and nuclear spins over all nuclei in the region of coherence, $\delta_{\mathrm{Mu}}\rightarrow\delta_{\mathrm{Mu}}/\sqrt{N_d}$, where N_d is the number of Mu sites inside the region of coherence (Stoneham, 1983). To explain the data one needs N_d to be as large as 100. The origin of the delocalized state below 200 K was attributed to delay in the formation of

a small polaron (Browne and Stoneham, 1982), while above 200 K such a delay is absent. The authors thus arrived at a picture in which Mu participated both in the delocalized coherent motion, described by reduced δ_{Mu}, and in incoherent hopping diffusion, described by τ_c^{-1}. In the absence of any microscopic calculations explaining how this might work consistently (including "coherent on top of coherent" motion at low temperature) we shall not comment further on it.

It was suggested by Kagan and Prokof'ev (1990a) that Mu may be an off-center interstitial in NaCl. In comparison with the cubic lattice of Mu sites in KCl, each position in NaCl is further split into four equivalent wells, having the same host atoms around them. If this is the case, then Mu will undergo two types of motion simultaneously—one corresponding to local four-level tunneling with τ_{c1}^{-1} and very small δ_1, and another corresponding to Mu transitions between the different unit cells of a simple cubic lattice with τ_{c2}^{-1} and large δ_2 (as in KCl). This interpretation is only qualitative and requires more elaborate calculations along with a more flexible fitting of the raw experimental data, which have to allow at least two sets of δ and τ_c^{-1}. It should be pointed out that peculiarities in δ_{Mu} in NaCl are accompanied by irregularities in muonium τ_c^{-1}. This may imply the existence of several minima in a χ^2 fit of the experimental spectra and ambiguity in the determination of δ_{Mu} and τ_c^{-1} at each temperature.

A careful search for direct evidence of muonium coherent motion has been carried out in KCl at very low temperatures (Macfarlane *et al.*, 1994) in an attempt to see coherence, which is expected at $T,\omega_{\mathrm{Mu}} \ll \Delta$, through the spectral analysis of the signal to confirm the square-root laws, $T_1^{-1} \sim T^{1/2}$ and $T_1^{-1} \sim \omega_{\mathrm{Mu}}^{1/2}$ [see Eq. (18)]. For incoherent muonium diffusion, τ_c^{-1} is extracted from the relaxation functions by invoking the effective-field approximation model (see Sec. IV). The local magnetic field is assumed to be uncorrelated in space (for unpolarized nuclei) and the field autocorrelator is expressed by Eq. (80), yielding the Lorentzian spectral density for the field fluctuations $J(\omega)=\tau_c/(1+\omega^2\tau_c^2)$. This expression does not apply for coherently moving Mu, for which the correct spectral function is given by $C(\omega)$ (see Sec. III.A). The experiment was performed in an ultrahigh-purity single crystal of KCl. The muon polarization time spectra were measured in a longtidinal field up to 0.4 T in the temperature range from 20 mK to 2 K. Single exponential fits to the polarization time spectra below 2 K showed no significant temperature dependence of the muonium T_1^{-1}, though the field dependence of the initial asymmetry was found to be qualitatively different from that at high temperatures. This peculiarity was attributed to the existence of an unobservably fast-relaxing Mu precursor. It was found that the muonium τ_c^{-1} is constant in the entire measured temperature range. The use of the spectral density function for the delocalized particle did not improve the fits significantly, which was not too surprising since both spectral densities have very similar shapes, and the sum of the two relevant contributions at frequencies ω_{12} and ω_{14} is almost insensitive to the actual line shape. Thus the data did not allow an unambiguous discrimination between the two mechanisms.

No evidence for a decrease in T_1^{-1} was found, even for temperatures $T \ll \Delta_{coh}$. This quite surprising circumstance suggests that the Mu atom does not reach thermal equilibrium with the environment during its lifetime (Macfarlane *et al.*, 1994). This explanation seems to be plausible, since the phonon scattering of Mu is greatly suppressed at such a low temperature. Indeed, from the onset of coherent delocalization at $T=15$ K we know the value of $\Omega(15\ \mathrm{K})$ to be of order $2\sqrt{2}\Delta_{coh} \sim 0.5$ K. At low temperatures we expect $\Omega \sim T^7$, which gives extremely long thermal relaxation times, $\Omega^{-1}(0.5\ \mathrm{K}) \sim 1\ s$. Even the empirical law $\Omega \sim T^{3.3}$ is sufficient to claim that at $T \sim \Delta_{coh}$ muonium is not in thermal equilibrium with the lattice. The unfortunate delay in Mu thermalization is thus the most probable reason for the T-independent correlation time down to 20 mK in all insulating materials.

It was mentioned in Sec. VI.B.2.a that the case of CuCl is singular, because in this material Mu undergoes local tunneling between four equivalent positions. This case requires a more detailed explanation of why there is no leveling off in the temperature dependence of T_1^{-1} for local tunneling and how one may resolve the unphysical result $\tau_c^{-1} \gg T$ at the lowest temperature. The solution is found in the fine structure of the spectral function for the nuclear field fluctuations. Consider first the simplest case of local tunneling between two equivalent states, well studied in the literature (Kagan and Maksimov, 1980; Weiss and Wollensak, 1989; Kagan and Prokof'ev, 1990b). The two-level system autocorrelation function at $T > \Delta_{coh}$ has the form

$$J_{(2)}(\omega) = \frac{\Delta_{coh}^2 \Omega}{(\omega^2 - \Delta_{coh}^2)^2 + \omega^2 \Omega^2}. \tag{112}$$

When $\Omega \gg \Delta_{coh}$ it is well approximated by the simple Lorentzian $J_{(2)}(\omega) \approx \tau_c/(1+\omega^2\tau_c^2)$ with $\tau_c = \Omega/\Delta_{coh}^2$. This limit corresponds to the incoherent regime of motion and agrees completely with the Celio model (Celio, 1987; Yen, 1988). The crossover to coherent dynamics at $\Omega < \Delta_{coh}$ is seen as a transformation of the single Lorentzian centered at $\omega=0$ into two Lorentzian peaks centered around $\omega = \pm\Delta_{coh}$, which are well separated when $\Omega \ll \Delta_{coh}$. However, the low-frequency response is as before, $J_2(0) \equiv \Omega/\Delta_{coh}^2$ or $J_2(0)=\tau_c$ if we use the same formal definition for τ_c (clearly, now τ_c has nothing to do with the hop rate between the wells, nor has it any physical meaning of, say, relaxation time, when $\Omega \ll \Delta_{coh}$). By measuring $T_1^{-1} = \delta^2 J(0) \equiv \delta^2 \tau_c$ at low frequencies we miss the crossover and observe an "as if" diverging correlation time. This problem does not arise in the band continuum, where $J(\omega)$ acquires a limiting form at low temperature.

The same considerations apply to the four-level case, although the spectral function is more complicated now. It is thought (Schneider *et al.*, 1992a) that in CuCl the

four-level Hamiltonian has the form $H_{nn'}=(1/4)\Delta_{coh}[1-\delta_{nn'}]$, with the energy spectrum $E_{1,2,3}=-\Delta_{coh}/4$, $E_4=3\Delta_{coh}/4$. Introducing the damping rate for the phase correlations between the wells Ω, we write the density matrix equation as

$$[i\omega-\Omega(1-\delta_{nn'})]\rho_{nn'}-i[H_o,\rho]_{nn'}=0. \tag{113}$$

The rest is just the standard procedure of solving for the eigenvectors $|\chi\rangle$ and eigenvalues E_χ of these 15 linear equations ($Tr\rho=1$) and then calculating the on-site correlation function $C(\omega)$. Omitting rather standard details we write here only the final answer,

$$J_{(4)}(\omega)=\frac{\Delta_{coh}^2\Omega}{2}\times\frac{\omega^2+\Omega^2+\Delta_{coh}^2/2}{\omega^2(\omega^2-\Delta_{coh}^2-\Omega^2)^2+\Omega^2(2\omega^2-\Delta_{coh}^2/2)^2}. \tag{114}$$

As before, when $\Omega\gg\Delta_{coh}$, we are back to the Lorentzian line around $\omega\approx0$ with the linewidth defined by $\tau_c=2\Omega/\Delta_{coh}^2$. In the opposite limit three peaks are developed in the spectral function, centered at $\omega=0$ and $\omega=\pm\Delta_{coh}$. The peak at the zero frequency is due to the ground-state degeneracy of the original problem. We note that in very weak fields the temperature dependence, $T_1^{-1}=\delta^2(\tau_c+1/\Omega)$, is nonmonotonic and will be interpreted in the standard Celio model as particle localization as $T\to0$. On the other hand, at some intermediate frequency, say $\Delta_{coh}/2$, the dependence of T_1^{-1} on temperature is monotonic after the T_1-minimum effect and will be misinterpreted at low T as a diverging τ_c^{-1}, in exact analogy with the two-level case. At present we do not see any other way to explain the observed data in CuCl. An interesting test of the theory would be the level-crossing resonance at low temperature when $\omega\approx\Delta_{coh}$.

b. Solid neon and solid nitrogen

Solid Ne is one of the rare-gas solids, which are characterized by very weak van der Waals interatomic interactions about several tens of K (Verkin and Prikhotko, 1983), whereas in "regular" solids this value can be as high as 10^4 K. One may expect the potential barriers to be rather low for Mu diffusion in such solids. Muonium spin relaxation, while it diffuses in natural s-Ne, differs from that observed in other materials because of the low concentration of the nuclear magnetic moments (only one isotope of neon—^{21}Ne with natural abundance $x_\gamma=0.27\%$—possesses nonzero spin). Usually the local field at muonium changes at each hop. In a solid with low abundance, x_γ, only long-range muonium diffusion can be determined from the transverse-field spin-relaxation measurements (short-range diffusion might be hidden).

In a recent experiment (Storchak *et al.*, 1994b) Mu diffusion was studied in ultrahigh-purity natural Ne (impurity content $x_{im}\sim10^{-5}$). Muonium formation and the hyperfine interaction energy A were detected using a conventional scheme (see Sec. IV.B). The electronic structure of Mu was found to be almost unaffected by the lattice since the hyperfine frequency was found to be very close to vacuum value of A. Figure 26 shows the temperature dependences of the muonium relaxation rate T_2^{-1} in pure and doped (with H_2 and CO) samples. In the "dirty" samples, T_2^{-1} is evidently independent of the kind and amount of impurity, which rules out the trapping, or chemical reaction, mechanism of relaxation on impurities. This fact strongly suggests that T_2^{-1}(dirty) = 0.2 MHz is an intrinsic Ne property, which can be considered to be the result of dipole interaction with the dilute Ne magnetic moments. The corresponding estimate gives a $T_2^{-1}=\delta(x_\gamma)=\gamma_{\rm Ne}\gamma_{\rm Mu}4\pi n_\gamma/3$ very close to the experimental result. It seems that the effect of impurities is mainly to generate long-range crystal disorder, which establishes a spatial distribution of energy-level shifts $\xi(r)$ among otherwise equivalent Mu sites, disrupting the free diffusion of Mu and producing a characteristic "static" relaxation rate T_2^{-1}. Mu atoms are seen as static if the energy shifts between the defects localize Mu on a length scale given by the natural abundance of ^{21}Ne, $x_\gamma=2.7\times10^{-3}$. Assuming that $\xi(r)$ is due to the elastic strain fields [see Eq. (19)], we find the corresponding criterion as

$$4\pi\frac{U_o x_{im}^{4/3}}{x_\gamma^{1/3}}>\Delta, \tag{115}$$

which is satisfied in doped samples.

The above condition does not necessarily mean that Mu is static, even on the time scale of T_2^{-1}; what is required is that it does not move as far as the distance between the ^{21}Ne nuclei in a time T_2. Thus dynamic effects of incoherent hopping are hidden if $\tau_c^{-1}\leqslant\gamma_{\rm Ne}\gamma_{\rm Mu}/a^3\approx10$ MHz, which makes transverse-field measurements rather ineffective in magnetically dilute substances. Only when τ_c^{-1} is sufficiently high can it influence spin relaxation through the motional narrowing

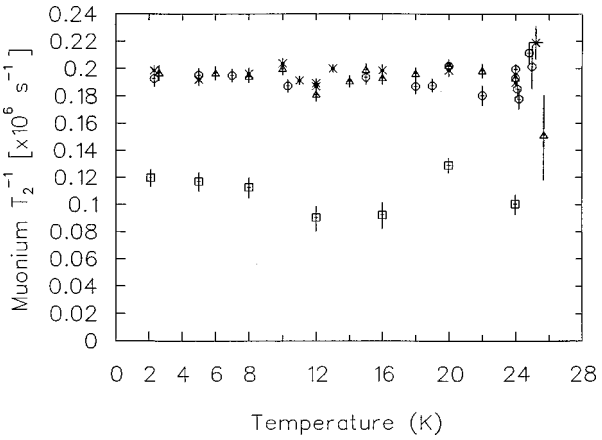

FIG. 26. Temperature dependences of the Mu T_2^{-1} relaxation rate in ultra-high-purity samples: squares, Ne; crosses, Ne+1.5×10^{-4} CO; circles, Ne+1.7×10^{-3} H_2; triangles, Ne+3.4×10^{-4} H_2 (Storchak *et al.*, 1994b).

effect. Generally (Abragam, 1961)

$$T_2^{-1} \simeq \begin{cases} \delta(x_\gamma) & \text{for } \tau_c^{-1} < \gamma_{\mathrm{Ne}}\gamma_{\mathrm{Mu}}/a^3, \\ \delta^2(x_\gamma) 3\tau_c/(4\pi x_\gamma) & \text{for } \tau_c^{-1} > \gamma_{\mathrm{Ne}}\gamma_{\mathrm{Mu}}/a^3. \end{cases} \tag{116}$$

In pure Ne, muonium apparently diffuses rapidly enough that dynamic narrowing takes place, and the lower part of Eq. (116) applies, giving $\tau_c^{-1} \approx 3.5 \times 10^7$ s^{-1}. The absence of any dramatic temperature dependence of τ_c^{-1} accompanied by unmistakable dynamic narrowing prompted Storchak *et al.* (1994b) to suggest bandlike motion of Mu in pure Ne. Rough estimates do not exclude this possibility at low T. If we calculate the static level shifts due to the strain fields (19) caused by residual impurities, using $x_{im} \sim 10^{-5}$ and $U_o \sim 10$ K, then Eq. (115) gives $\Delta > 5 \times 10^{-4}$ K, in line with the value deduced from τ_c^{-1} using Eq. (14), namely, $\Delta \approx (Z/\sqrt{2})\tau_c^{-1} \sim 10^{-3}$ K. This interpretation, however, has some difficulty explaining why the two-phonon scattering is so small that $\Omega < \Delta$ up to 25 K.

There are some other problems not answered by the experiments in solid Ne. It is known that dipole fields due to dilute magnetic moments have Lorentzian field distribution (Abragam, 1961). However, in the experiment of Storchak *et al.* (1994b) the relaxation function was rather Gaussian in dirty samples. In pure Ne, the relaxation function is slightly closer to exponential, as would be expected for a dynamically narrowed regime, but it is still inconsistent with a Lorentzian field distribution. The reason for this discrepancy is not understood and actually leads us to think that the explanation of the experimental data proposed here is only the most straightforward one; it may radically change when more experimental data become available.

This discrepancy is obviously absent in solid nitrogen (all nitrogen nuclei have nonzero magnetic moments), where the temperature-independent τ_c^{-1} between 20 K and 30 K was attributed to Mu band motion (Storchak *et al.*, 1994a; Storchak, Brewer, and Morris, 1996b). The renormalized bandwidth was estimated to be $\Delta_{coh} \sim 10^{-2}$ K, in agreement with the value deduced from the high-temperature data (see Sec. V1.B.3 below). In fact, the temperature dependence of muonium τ_c^{-1} in solid nitrogen above 20 K is very reminiscent of that in ionic insulators and GaAs.

3. One-phonon muonium quantum diffusion

The main issues we shall address in this subsection are (a) whether Mu diffusion at $T > T_{min}$ is quantum in nature and (b) what is the relative role of different one-phonon couplings in this regime, i.e., the polaron effect versus fluctuational preparation of the barrier. This kind of study is impossible to conduct at low temperature because one-phonon interactions are then reduced to constant renormalization $\Delta_o \to \Delta_o \exp\{B_o - \Phi + G\}$, and different terms in the exponent may not be discriminated. The high-T dynamics of the small-polaron expression [Eq. (97)], allows for the separation of the polaron effect from fluctuational preparation of the barrier through their temperature dependences—the polaron effect disappears as $\sim 1/T$, due to increased lattice vibrations, and for exactly the same reason the barrier fluctuation effect increases as $\sim T$.

The conditions under which one can experimentally separate the effects of fluctuational preparation of the barrier from the polaron effect (Storchak, Brewer, Morris, *et al.*, 1994; Storchak *et al.*, 1996) are rather specific: the best choice would be to study the temperature range $T > \Theta$, but still $T < T_* = \nu_o$, to ensure that classical diffusion may be disregarded. To separate the energy scales Θ and ν_o, one should study tunneling of a very light particle (to increase T_*; Mu perfectly satisfies this condition) in a crystal with low Debye temperature. Small Θ may result both from the heavy mass of the host atoms and from "soft" interatomic forces; the last idea leads to van der Waals crystals of Xe and Kr.

In this subsection we shall discuss high-T quantum diffusion in KCl, NaCl, and GaAs, which are already familiar to the reader, along with N_2 and the rare-gas solids of Kr and Xe.

a. Ionic insulators and GaAs

In KCl the high-T data were initially interpreted as a classical Arrhenius-type diffusion (Kiefl *et al.*, 1989). However, the low value of the preexponential factor $\nu_\mu = 8.2(8) \times 10^9$ s^{-1} along with the low value of the activation energy $E = 388(12)$ K, which is more than five times smaller than the corresponding value for hydrogen diffusion in KCl, $E_H = 2300$ K (Ikeya *et al.*, 1978), clearly indicated that Mu diffusion above T_{min} was quantum in nature. It was argued by Kagan and Prokof'ev (1990a) that an analysis in terms of the polaron effect alone (Kadono, 1990) was inconsistent with the low-temperature data and barrier fluctuations must be involved as well. Below we shall follow the analysis given in this work.

Both the polaron effect and the barrier fluctuation effect lead to the increase of τ_c^{-1} with temperature. The idea of separating the two contributions is to impose restrictions on the tunneling amplitude renormalization exponent $\Phi - G$, which can be done by invoking precise knowledge of Δ_{coh} at low T (see Sec. VI.B.2 above). In the rest of this section we shall often assume the simplest form of the Mu-phonon coupling,

$$|C_\alpha|^2 = \lambda_1 \omega \Theta, \quad |B_\alpha|^2 = \lambda_B \omega/\Theta. \tag{117}$$

Suppose that $\lambda_B = 0$. The preexponential factor, polaron energy, and Δ_{coh} then constitute three equations that are to be satisfied simultaneously by fitting $\Delta_o e^{B_o}$ and λ_1. In addition [since the two-phonon scattering is fixed by known $\tau_c(T)$ behavior below T_{min}] one may require the position of the minimum and $\tau_c^{-1}(T_{min})$ to be reproduced. This rather stringent test shows [the numerical calculation was done using the actual phonon spectrum of KCl and NaCl (Bilz and Kress, 1979)] that with $\lambda_B = 0$ a consistent description of the data is not possible, missing the data by orders of magnitude. On the other hand, the overall fitting is very good assuming $\lambda_1 = 0$ and a nonzero value of λ_B. The curve in Fig. 27 was ob-

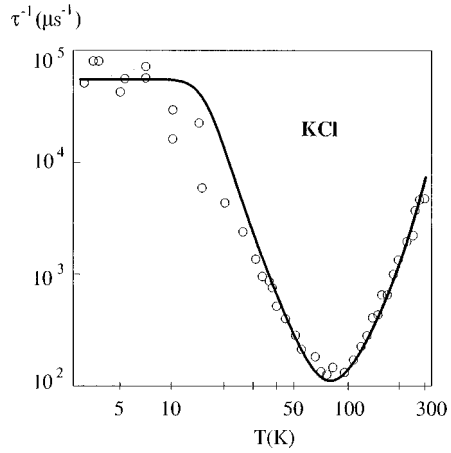

FIG. 27. The result of the numerical calculations of the Mu quantum diffusion in KCl (solid line) (Kagan and Prokof'ev, 1990a). The parameters of the calculations are presented in the text.

tained using two independent parameters λ_{2ph} and λ_B for the two-phonon and one-phonon regimes, respectively. The parameters obtained [$\lambda_B=0.25$, or $G(0)\approx 0.4$, $E_B\approx 50$ K and $\gamma\approx 40$ K; see Eq. (97)] reflect only a small renormalization of Δ_0 at low temperatures, while the barrier fluctuation effect turns out to be quite important at high temperatures.

The striking contrast between the two limiting cases in KCl left little doubt that the barrier fluctuation effect governs Mu quantum diffusion at high temperature. This is probably related to the structure of the ionic crystals in which the Mu-ion interaction strongly depends on their proximity. This interaction has its maximum value when the tunneling particle goes through the atomic plane between neighboring wells and it is relatively weak for Mu in the potential well.

We note that the strict correlation between high- and low-temperature parameters disappears immediately if one tries to describe the experimental data assuming a separate set of τ_c^{-1} and δ_{Mu} at each temperature [as was done in NaCl by Kadono *et al.* (1990)]. The difference between the results of the same theoretical analysis in KCl and NaCl can be taken as additional evidence of the need for a thorough analysis of the experimental time spectra in NaCl.

In contrast to the case of KCl, all the data in GaAs (Kadono, Kiefl, Brewer, *et al.*, 1990; Schneider *et al.*, 1992b) seem to be in good agreement with the standard fit, which takes into account only the polaron effect.

b. Solid nitrogen

The same analysis relating low- and high-temperature data was done for N_2 by Storchak *et al.*, (1993, 1994a). In the original treatment the authors tried to utilize the low-temperature results for the plateau below 8 K. Later on, precise measurements revealed that the T_2^{-1} of muonium is temperature independent in s-N_2 between 20 K and 30 K, which strongly supports the hypothesis of particle band motion in this temperature range and makes $\Delta_{coh}\approx 10^{-2}$ K available directly from experiment. Three possibilities were considered separately for the high-temperature behavior: the polaron effect, fluctuational preparation of the barrier, and classical diffusion. The results of fitting were then tested for self-consistency within the Debye model for the phonon spectrum, when $\Phi(0)=3E/\Theta$ and $G(0)=3\Theta/32E_B$, and for the Einstein model, when $\Phi(0)=2E/\Theta$ and $G(0)=\Theta/8E_B$. Unfortunately, in nitrogen the high-T regime is restricted from above by a rather low melting temperature ($T_m=63.1$ K); thus only large discrepancies were taken into account.

By considering the polaron effect alone one gets $E\approx 300$ K and $\nu_{\mathrm{Mu}}\approx 10^{10}$ s^{-1} (or $\Delta_o\approx 2$ K), which, after the recalculations described above, gives Δ_{coh} between 10^{-3} and 10^{-4} K (depending on the model). This is one or two orders of magnitude smaller than the experimental value. Fitting the data to the barrier fluctuation expression alone gives a much better description: $E_B\approx 10$ K, $G(0)\approx 0.8$, and the corresponding tunneling amplitudes $\Delta_o e^{B_o}\approx 10^{-2}$ K, $\Delta_{coh}\approx 2\times 10^{-2}$ K. Classical diffusion [which, in fact, is very close in fitting to the small-polaron expression (98)] was ruled out because of the smallness of the preexponential factor $\nu_{\mathrm{Mu}}\approx 10^{10}$ s^{-1}. The conclusion made in this study was that the high-temperature Mu dynamics in solid N_2 are due to tunneling, with dominant one-phonon coupling originating from potential barrier fluctuations.

c. Solid xenon and solid krypton

Despite the strength of the arguments in favor of the barrier fluctuation effect in KCl and nitrogen, it is only through the theoretical estimates that one can judge whether they are valid or not. The high-temperature data are not sufficient on their own for separating the linear term from the polaron term in the exponent in Eq. (97) in these substances. Hydrogen diffusion in metals is usually explained in terms of the polaron effect alone (see, for example, Steinbinder *et al.*, 1988). Still, some of the data (Völkl and Alefeld, 1978), were found to be in disagreement with the simple activation-type dependence, and theoretical attempts were made to explain this discrepancy by the fluctuational preparation of the barrier (Teichler and Klamt, 1985; Klamt and Teichler, 1986). Comparatively small variations of τ_c^{-1} at high temperature in all previous experiments precluded *any* firm conclusion about the nature of particle tunneling in this regime. At temperatures above 200 K one also has to worry about a possible change of the interstitial site visited by the diffusing particle and crossover to over-barrier classical diffusion. The idea of studying Mu diffusion in a material with the heaviest possible lattice atoms, in order to expand the temperature range where the full expression (97) is expected to be valid, was realized in solid xenon (Storchak, Brewer, Morris, *et al.*, 1994) ($\Theta=64.0$ K) and solid krypton (Storchak *et al.*, 1996) ($\Theta=71.7$ K). For the first time the data on quantum hopping became available on a scale (muo-

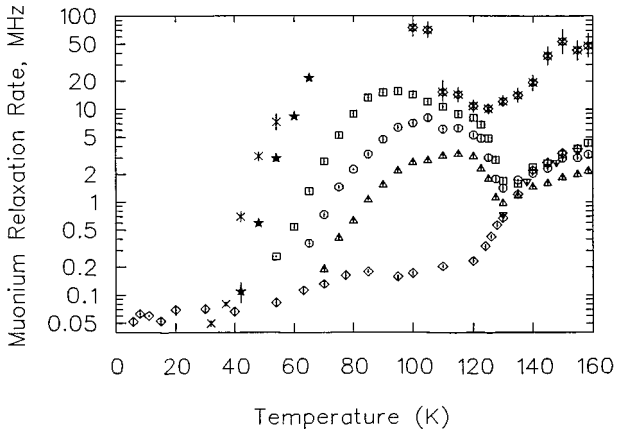

FIG. 28. Temperature dependences of the muonium T_2^{-1} (crossed diamonds) and T_1^{-1}: crosses, 21 G; stars, 72 G; squares, 363 G; circles, 725 G; triangles, 1451 G in natural s-Xe; T_2^{-1} (diamonds) and T_1^{-1} (inverted triangles, 363 G) in ^{136}Xe (Storchak, Brewer, Morris, Arseneau, and Senba, 1994).

nium τ_c^{-1} has been measured to vary by about four orders of magnitude) that allowed a direct test of the theory.

Experiments in solid Xe were carried out both in research grade (99.999% purity) natural Xe (^{129}Xe–26.2%, ^{131}Xe–21.2%; other isotopes have zero spin) and in pure (99.996%) ^{136}Xe. By standard methods, the hyperfine parameter A_{Mu} was measured in isotopically pure ^{136}Xe (to exclude fast nuclear hyperfine interaction relaxation) with the result $A_{\mathrm{Mu}}=4325(8)$ MHz; this value is believed to be the same in natural s-Xe, suggesting that the Mu atom is slightly expanded in the Xe lattice. The nuclear hyperfine interaction parameter δ_{Mu} for Mu in s-Xe is not known but can be inferred from the value for atomic hydrogen ($\delta_H \approx 35$ MHz; Foner *et al.*, 1960), which should be only slightly different due to zero-point vibrations. The high-longitudinal-field technique was then applied in order to extract values for both δ_{Mu} and τ_c^{-1} in natural s-Xe by simultaneous fitting of the μ^+SR time spectra taken at three or four external magnetic fields using an expression for the muon spin relaxation in the framework of the effective-field approximation (see Sec. IV). The observed relaxation was attributed entirely to the Mu fraction, since the small diamagnetic fraction is believed to be due to the molecular ion $\mathrm{Xe}\mu^+$ (Storchak, Kirillov, *et al.*, 1992), in analogy with the directly observed $\mathrm{N}_2\mu^+$ ion (Storchak *et al.*, 1992), which should be nonrelaxing in high longitudinal fields. Moreover, weak-transverse-field measurements in ^{136}Xe, where long-lived Mu precession was observed, yielded the same value for the muonium amplitude as that measured in longitudinal fields; one has no reason to expect the probability of Mu formation to be different for natural Xe and ^{136}Xe.

Figure 28 presents the temperature dependence of the average muonium relaxation rates T_1^{-1} (taken at various values of longitudinal field) and T_2^{-1} (in a weak transverse field of 5.2 G) in natural Xe. The same figure shows T_1^{-1} for a longitudinal field of 362 G and T_2^{-1} for

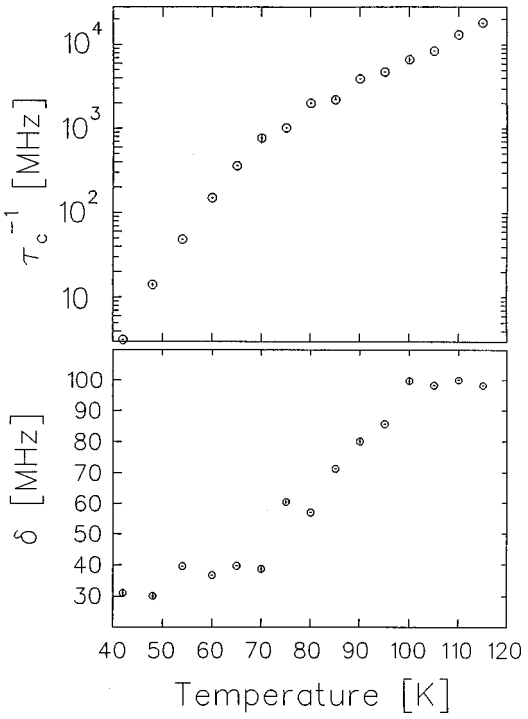

FIG. 29. Temperature dependence of the Mu hop rate τ_c^{-1} and the nuclear hyperfine frequency coupling constant δ in natural s-Xe (Storchak, Brewer, Morris, Arseneau, and Senba, 1994).

a weak transverse field of 5.2 G in ^{136}Xe. Below about 125 K the magnetic-field dependence of T_1^{-1} in natural s-Xe was found to be consistent with the Celio model. Above this temperature muonium spin relaxation was claimed to be no longer primarily due to the nuclear hyperfine interaction, as illustrated by the fast relaxation in ^{136}Xe; instead, above 125 K, Mu spin-exchange processes were suggested to be dominant. Therefore the analysis of Mu diffusion was restricted to temperatures below 125 K, where clear T_1^{-1} maxima were seen around 100 K at three magnetic fields. For lower longitudinal fields the T_1 minimum was shifted to lower temperatures, indicating that Mu slows down with decreasing temperature. Both the Mu hop rate τ_c^{-1} and nuclear hyperfine interaction frequency δ_{Mu} (shown in Fig. 29) were calibrated at the T_1 minima conditions.

An approximation of the experimental data by expressions taking into account the polaron effect or fluctuational barrier effects separately gave poor fits in both cases. Therefore the two effects were considered simultaneously according to Eq. (97). The bandwidth in the Debye approximation was estimated to be $\Delta_{coh} \approx 10^{-9}$ K. In the Einstein approximation it was considerably larger: $\Delta_{coh} \approx 10^{-6}$ K. Preference was given to none of these models, but these calculations showed that they both imply very strong one-phonon interactions. Fitting indicates that the polaron effect plays a dominant role in the temperature region from 40 K to about 70 K, while the barrier fluctuation effect prevails at higher temperatures.

The hyperfine interaction parameter δ_{Mu} displays a dramatic temperature dependence (Fig. 29) with a step-

like increase above about 70 K, similar to that observed in NaCl (Kadono *et al.*, 1990). However, Storchak, Brewer, Morris, *et al.*, (1994) and Storchak, Brewer and Morris (1994b), have given another interpretation of such an increase in δ_{Mu} based on a classical evaluation of the spin dynamics for a rapidly diffusing particle. The Mu atom produces a large magnetic field $B_{\mathrm{eff}} \sim \delta_{\mathrm{Mu}}/\gamma_N$ at the lattice nuclei. For slowly diffusing Mu ($2\pi\delta_{\mathrm{Mu}}\tau_c \gg 1$), fast Larmor precession of the surrounding nuclear spins leads to averaging of the nonsecular part of the interaction. When the Mu hop rate becomes higher than δ_{Mu}, it leaves the unit cell *before* the nearest nuclei undergo noticeable rotation in its magnetic field. Therefore, for rapidly diffusing Mu, one has to consider the full nuclear hyperfine interaction Hamiltonian, which in turn results in a higher effective δ_{Mu}. Thus the high-temperature value $\delta \approx 100$ MHz corresponds to the full magnitude of the interaction, whereas the low-temperature value, $\delta_{\mathrm{Mu}} = 30$–$40$ MHz, is consistent with that of a static hydrogen atom in s-Xe (Foner *et al.*, 1960). This classical picture is valid only in the high-magnetic-field limit, when ω_{Mu} is much higher than δ_{Mu} [the same restriction as for the effective-field approximation (Kiefl *et al.*, 1989)]. Comparison of the τ_c^{-1} and δ_{Mu} values shown in Fig. 29 reveals that the increase in δ_{Mu} takes place when $2\pi\delta_{\mathrm{Mu}}\tau_c \sim 1$, as expected. These considerations may also apply to NaCl.

Measurements of muonium diffusion in solid krypton (s-Kr) were performed in ultrahigh-purity (less than 10^{-5} impurity content) samples (Storchak *et al.*, 1996). As in the cases of N_2 and Xe, it was possible to separate and ignore the contribution of the diamagnetic fraction (due to $\mathrm{Kr}\mu^+$ ions and μ^+ stopped in the sample walls). The analysis below is restricted to the temperature range up to 55 K only, where muonium relaxation was attributed to dipole or hyperfine interactions between the Mu spin and ^{83}Kr nuclei (natural abundance 11.55%). At higher temperatures two-component relaxation was observed [also reported in the first experiment by Kiefl *et al.* (1981) at 90 K], most probably due to Mu interactions with paramagnetic species liberated in the incoming muon's ionization track (Storchak, Brewer, and Cox, 1997; Storchak, Brewer, and Morris, 1994b, 1995a, 1995b, 1996a, 1997; Storchak *et al.*, 1997). An additional fast-relaxing component was also observed at high temperatures in the Mu relaxation function for solid Xe (Storchak, Brewer, Morris, *et al.*, 1994), Ar (Storchak, Brewer, and Morris, 1996c), and ice (Cox *et al.*, 1994).

The increase in T_2^{-1} observed in s-Kr as the temperature was lowered to 40 K (Fig. 30) may be explained by the slowing down of the diffusion. It is tempting then to consider the characteristic maximum and abrupt drop in T_2^{-1} around 40 K as the onset of fast coherent motion and resulting dynamic narrowing. This drop, however, is accompanied by a drop in the amplitude of the transverse-field precession signal from 0.0671(5) to 0.0395(5), equivalent to a reduction of the Mu fraction to 58.9% of its value at higher temperatures. This behavior cannot be explained by the onset of a fast-diffusion

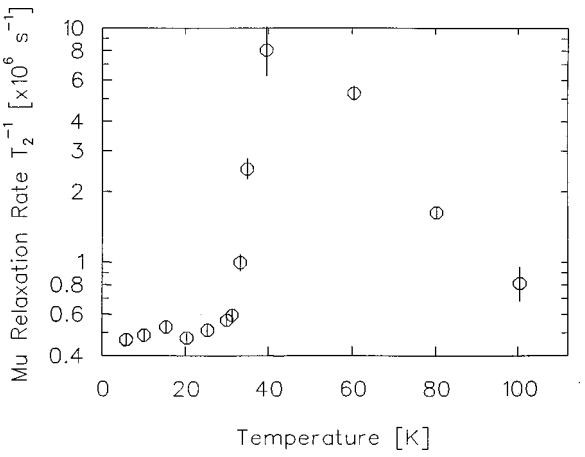

FIG. 30. Temperature dependence of the muonium relaxation rate T_2^{-1} in solid Kr in a transverse magnetic field $B = 2$ G (Storchak *et al.*, 1996).

regime. It can, on the other hand, be explained in terms of the isotopic composition of krypton and the consequent fact that not all crystallographically equivalent sites have equivalent local nuclear magnetism. Particles that localize at sites having ^{83}Kr as nearest neighbors experience strong nuclear hyperfine interactions and are rapidly and completely depolarized, whereas particles having only spinless nearest neighbors (experiencing only much smaller, and predominantly dipole, local fields from remote ^{83}Kr nuclei) exhibit a relatively slowly damped precession signal. Within this picture Mu sites in Kr were readily identified as tetrahedral. This contrasts with the H atoms deposited in Kr, which apparently take up a substitutional position (Foner *et al.*, 1960). It is not surprising, therefore, that the nuclear hyperfine interaction parameters for muonium and hydrogen in solid Kr were found to be considerably different (Storchak *et al.*, 1996). The abrupt decrease of T_2^{-1} with decreasing temperature was explained by localization (or diffusion freezing) of the Mu atoms. Above about 35 K, particles began moving faster, and all Mu atoms experienced strong nuclear hyperfine interactions with ^{83}Kr nuclei in the course of diffusion through the lattice. This was seen as a stepwise increase in $T_2^{-1}(T)$.

The hypothesis of muonium localization in s-Kr at low temperatures was unambiguously confirmed in a subsequent zero-field experiment (Storchak *et al.*, 1996) Figure 5 presents the time evolution of the muon polarization (circles) and shows that it exhibits a relaxation function of the static Kubo-Toyabe type (79). The fit of the experimental spectrum took into account both Mu sites with nearest-neighbor (NN) ^{83}Kr nuclear spins and those without. The correlation time τ_c was assumed to be the same for both types of sites, since they are electrostatically identical. Very slow muonium diffusion rates were measured both in zero field and in a very weak longitudinal field (0.2 G). Typical weak-longitudinal-field time spectra are shown in Fig. 6. Both the Mu hop rate τ_c^{-1} and the nuclear hyperfine interaction frequency δ_{nnn} (with next-nearest neighbors) were determined by simultaneous fits of zero-field and weak-

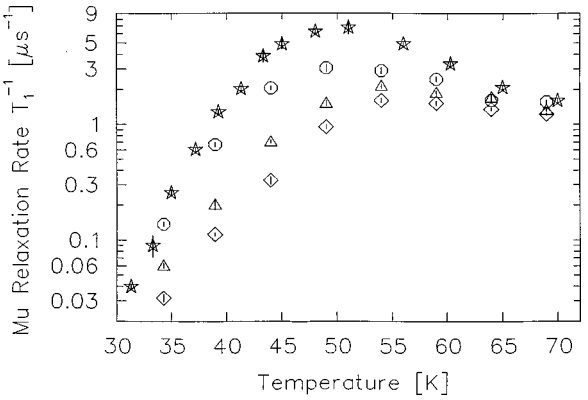

FIG. 31. Temperature dependences of the muonium relaxation rate T_1^{-1} in solid Kr in several longitudinal magnetic fields: stars, 40 G; circles, 60 G; triangles, 120 G; diamonds, 180 G. Note the T_1 minima (T_1^{-1} maxima) around 50 K (Storchak *et al.*, 1996).

longitudinal-field data to corresponding dynamic Gaussian Kubo-Toyabe relaxation functions (Brewer *et al.*, 1987; Luke *et al.*, 1991) with $\Delta \equiv \delta_{nnn}$. At temperatures above about 30 K, the high-longitudinal-field technique was applied to measure faster hop rates. The temperature dependence of T_1^{-1} for different values of applied field is shown in Fig. 31. Between about 30 K and 55 K, the longitudinal-field relaxation data were interpreted in terms of muonium diffusion, as the variation of T_1^{-1} with magnetic field is consistent with a diffusion model (Celio, 1987; Yen, 1988). Muonium nuclear hyperfine interaction parameters for nearest neighbors and next-nearest neighbors were determined to be $\delta_{nn} = 55(5)$ MHz (from longitudinal-field data) and $\delta_{nnn} = 0.67(6)$ MHz (from zero-field and weak-longitudinal-field data), respectively. That huge difference between the two values suggests that these interactions are, respectively, contact and dipole in character.

The temperature dependence of τ_c^{-1} for Mu in s-Kr is shown in Fig. 32 along with that for s-Xe. The overall range of the muonium hop rates, spanning over six orders of magnitude, is especially noteworthy. A fit of the

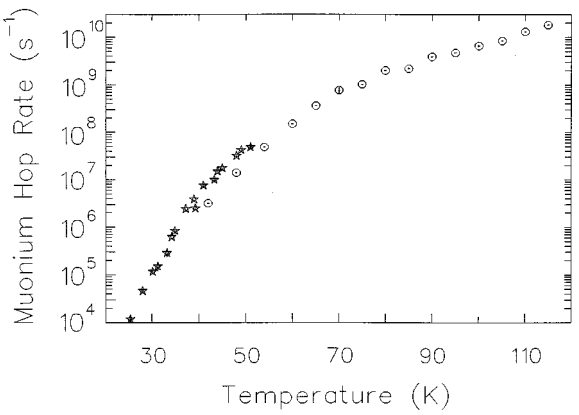

FIG. 32. Temperature dependence of the muonium hop rate in solid Kr (stars; Storchak *et al.*, 1996) and solid Xe (circles; Storchak, Brewer, Morris, Arseneau, and Senba, 1994).

experimental $\tau_c^{-1}(T)$ dependence in s-Kr for 25 K$<T<$55 K to the Arrhenius law gave the preexponential factor $\nu_\mu = 1.6(3)\times 10^{11}\ s^{-1}$ and $E = 409(2)$ K. Although the value of ν is rather large in this case, it is still at least two orders of magnitude less than ν_0, which was considered as sufficient grounds to exclude classical diffusion. Analysis showed that the polaron effect is much stronger than the barrier fluctuation effect. Fitting the data to Eq. (98) ($\lambda_B = 0$) gave a better χ^2 parameter than fitting to Eq. (97) with $\lambda_1 = 0$. The parameters obtained from the polaronic-effect fitting were $\tilde{\Delta}_o = 3.2(1)\times 10^{-5}$ K and $E = 432(2)$ K. Keeping both effects in the analysis did not produce marked improvement. Unfortunately, Mu relaxation on nuclear spins was masked in solid Kr by the onset of additional relaxation mechanisms at temperatures comparable to and above Θ. This hampered a quantitative separation of the polaron effect from the barrier fluctuation effect. Yet again, as in many previous studies, the narrowness of the temperature range was the main reason why Storchak *et al.* (1996) could not extract precise values for the parameters of both effects.

4. Muonium quantum diffusion in imperfect crystals

The influence of crystalline imperfections on quantum diffusion of neutral particles in insulating crystals is much harder to observe than that on charged particles in metals for two reasons: (i) the strain fields are so much weaker than the potential due to charge oscillations in metals (e.g., for a ^{3}He atom in a ^{4}He crystal $U_o \sim 10^{-2}$ K), and (ii) the Mu bandwidth $2Z\Delta_{coh}$ in insulators usually turns out to be several orders of magnitude higher than Δ for μ^+ in metals, partly due to specific electronic polaron effect. Still, the inequality $\Delta \ll U_o$ holds even in insulators, and disorder may cause drastic changes in Mu quantum diffusion. Inhomogeneous diffusion has direct consequences for the T_2^{-1} and T_1^{-1} spectra (see Secs. III.B, III.E.2, and III.E.3). In this section we describe experiments on inhomogeneous muonium quantum diffusion in s-N_2 and KCl with impurities. We also analyze the Mu trapping phenomena in insulators, employing the case of Mu diffusion in s-N_2 with CO impurities.

a. Inhomogeneous quantum diffusion in solid nitrogen

As we have mentioned already, at temperatures below 18 K a gradual Mu localization takes place, which reflects the suppression of band motion by static disorder (Storchak *et al.* 1993, 1994a; also see Storchak, Brewer, and Morris, 1994b, 1996b). Inhomogeneous muonium quantum diffusion in s-N_2 has been detected in weak-longitudinal-field experiments at low temperatures (Storchak, Brewer, and Morris, 1996d). Typical μSR time spectra in $B = 8$ G are shown in Fig. 33. At temperatures above about 10 K, excellent fits to the data were obtained using Eq. (88), which assumes that *all* Mu atoms diffuse at the same rate during their lifetimes. However, below 10 K it was impossible to fit experimental spectra using a single exponential relaxation function. Figure 33 clearly shows that at low temperatures the polarization function consists of at least two expo-

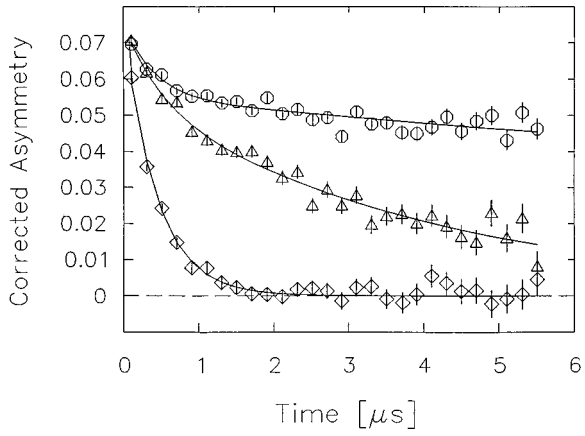

FIG. 33. Muon-spin relaxation spectra for muonium in solid nitrogen in a longitudinal field of $B=8$ Oe: diamonds, at $T=10$ K; triangles, at $T=8$ K; circles, at $T=6$ K (Storchak *et al.*, 1995; Storchak, Brewer, and Morris, 1996d). Note the presence of two components in the relaxation function at low temperatures.

nential terms. At temperatures below about 8 K, a large, almost nonrelaxing component (on the μSR time scale) was observed. It was attributed to an almost static part of the Mu ensemble. A multicomponent $P(t)$ is clear evidence for the spatial inhomogeneity of the crystal; muon diffusion experiments in superconducting Al with impurities also show a multicomponent $P(t)$ (Karlsson *et al.*, 1995).

Experimental time spectra were compared with the simplest possible two-component expression,

$$A(t)=A_F\exp(-T_{1_F}^{-1}t)+A_S\exp(-T_{1_S}^{-1}t), \qquad (118)$$

where A_F and A_S are the asymmetries (amplitudes) of the fast- and slow-relaxing components and $T_{1_F}^{-1}$ and $T_{1_S}^{-1}$ are their relaxation rates. Figure 34 shows the temperature dependences of these asymmetries (a) and relaxation rates (b). Above 10 K there is no measurable fast-relaxing component. As the temperature is reduced below 10 K, A_S decreases and the fast-relaxing component correspondingly increases, clearly indicating the onset of inhomogeneous Mu diffusion. At lower temperatures both A_S and A_F level off, accounting for about 70% and 30% of the Mu polarization, respectively. At $T=6$ K, $T_{1_F}^{-1}$ exceeds $T_{1_S}^{-1}$ by more than two orders of magnitude. Figure 34(c) displays the temperature dependences of the Mu hop rates for the fast and slow components derived from Eq. (88), with a fixed value of $\delta=14.9(0.8)$ MHz obtained from T_1^{-1}-maximum conditions. Above about 9 K, Mu exhibits quantum tunneling with a characteristic $\tau_c^{-1}\propto\Omega/\xi^2 \propto T^7$ temperature dependence. Below this temperature the slow component displays strong localization, while the fast component shows temperature-independent Mu motion with about two jumps per muon lifetime.

The reduction of the Mu diffusion rate in solid nitrogen at low temperatures has been explained (Storchak *et al.*, 1994a) in terms of orientational ordering of N_2 molecules in s-N_2. This is a peculiar intrinsic property of crystalline nitrogen, which can be considered as homogeneous at high temperature but has the properties of a translationally disordered lattice below 20 K, presumably due to frozen orientational defects, which produce "crystal disorder" for Mu diffusion. The hop rate is also decreased according to Eq. (109). This picture is consistent with the behavior of the slow-relaxing component. The nature of the fast-relaxing component and its temperature-independent hop rate remains a puzzle and requires further investigation. Some possibilities include, coherent motion with the reduced bandwidth in the orientationally ordered state, local tunneling between few near-resonance sites, etc., but existing data are too incomplete to continue this argumentation.

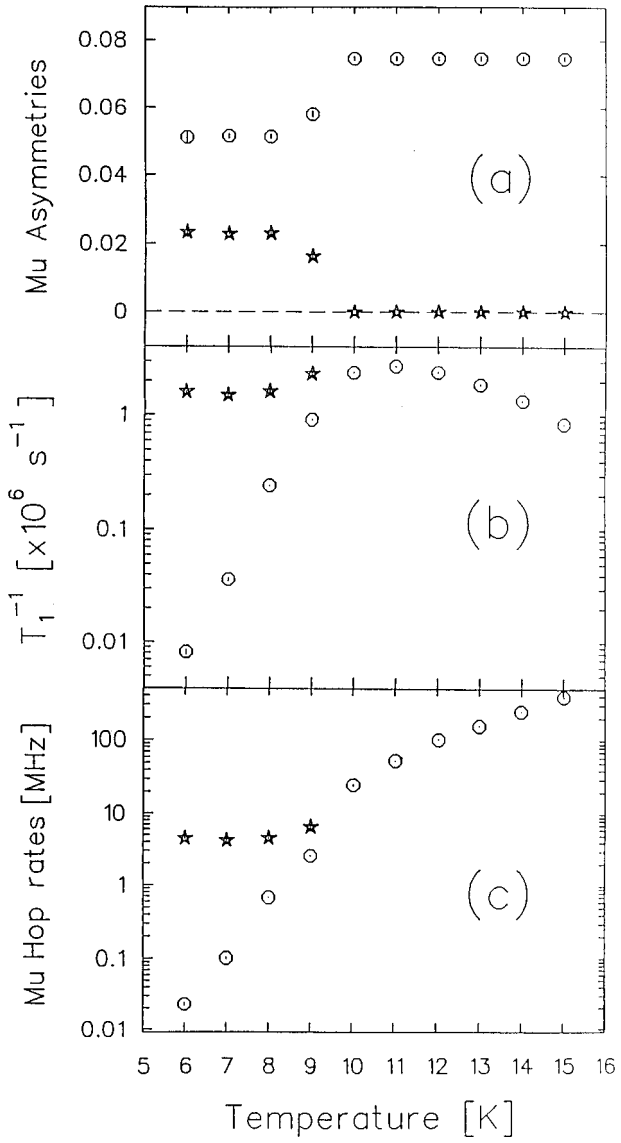

FIG. 34. Temperature dependences of muonium signals in solid nitrogen: ○, slow-relaxing; stars, fast-relaxing (Storchak *et al.*, 1995; Storchak, Brewer, and Morris, 1996d). (a) slow (A_S) and fast (A_F) muonium asymmetries (amplitudes); (b) slow ($T_{1_S}^{-1}$) and fast ($T_{1_F}^{-1}$) longitudinal relaxation rates; (c) slow ($\tau_{c_S}^{-1}$) and fast ($\tau_{c_F}^{-1}$) muonium hop rates.

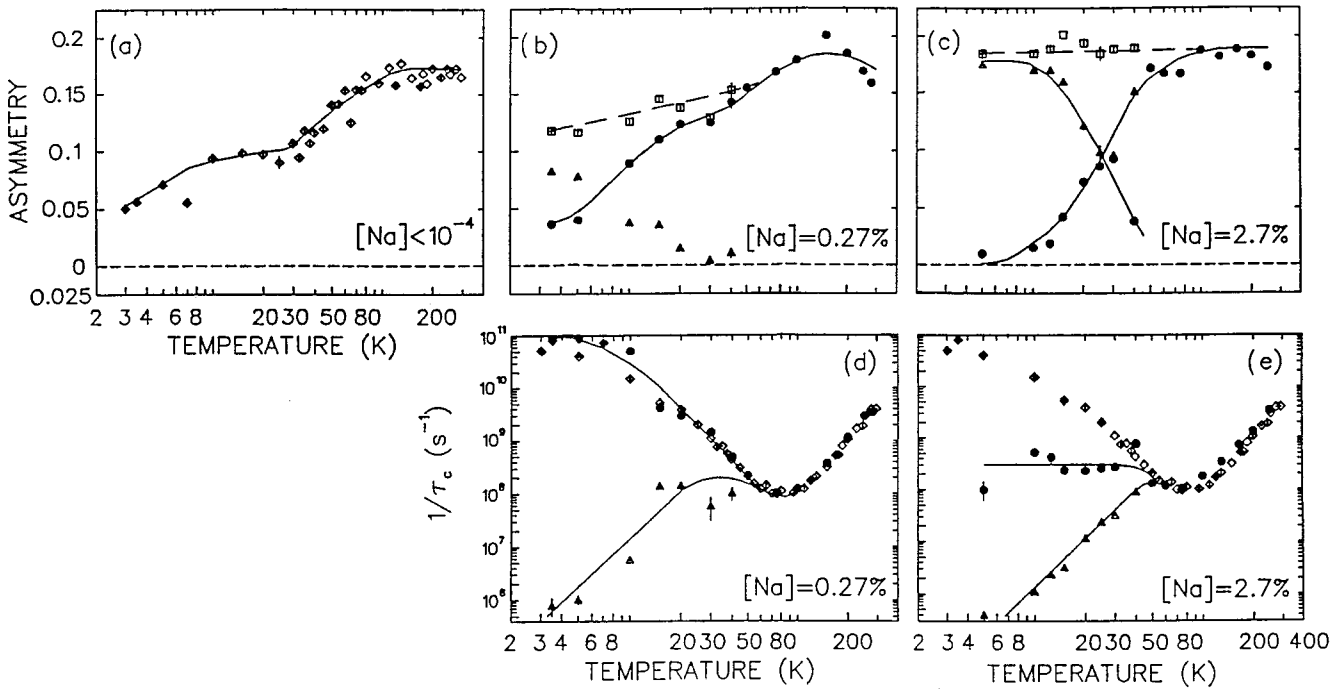

FIG. 35. Temperature dependences of the muonium hop rate and partial asymmetry in KCl ([Na] = 2.7×10^{-3} and 2.7×10^{-2}) compared with the data in pure KCl ([Na] $<10^{-4}$, shown by diamonds). Triangles are A_S and the hop rate τ_S^{-1} of the slow component, filled circles are A_F and the hop rate τ_F^{-1} of the fast component, and squares are A_S+A_F in each sample. Lines are to guide the eye (Kadono *et al.*, 1996).

b. Inhomogeneous Mu diffusion in Na-doped KCl

Experiments in pure KCl (Kiefl *et al.*, 1989; Kadono, 1990) give us a perfect example of homogeneous quantum diffusion in a regular lattice. Therefore it is an ideal starting point to study disorder effects due to deliberately inserted impurities. Measurements in single crystals of KCl with Na concentrations of $2.7(3)\times10^{-3}$ and $2.7(3)\times10^{-2}$ were carried out in a longitudinal field (Kadono *et al.*, 1996). The diffusion-limited trapping on Na centers was discarded by comparing the estimated trapping rate with the Mu relaxation rate in both crystals. This result agrees with the general conclusion on the ineffectiveness of trapping phenomena in insulators at low temperatures due to suppression of the inelastic interaction with the environment (Prokof'ev, 1994; Storchak, Brewer, and Morris, 1996d). An analysis of the Mu relaxation time spectra below about 50 K revealed the existence of at least two distinct components with different correlation times, while only a single component was observed at higher temperatures. For simplicity it was assumed that the time spectra were described by a two-component expression similar to Eq. (118). Common values were adopted for the muonium hyperfine parameter $A=2\pi\times4280$ MHz (Kiefl *et al.*, 1984) and the nuclear hyperfine interaction parameter $\delta_{\rm Mu}=2\pi\times60(2)$ MHz (Kadono *et al.*, 1990) throughout the analysis.

The temperature dependences of the muonium asymmetries and τ_c^{-1} in both samples are shown in Fig. 35, where the data of pure KCl (nominally 99.99%) are also included for comparison. It is evident from Figs. 35(d) and 35(e) that the hop rate in both samples is not affected by the presence of sodium impurities above 50 K, except for a very slight enhancement in the sample with 2.7% sodium. In the sample with 0.27% sodium, $\tau_c^{-1}(T)$ of the fast-diffusing component observed below 50 K virtually coincides with the muonium $\tau_c^{-1}(T)$ in pure KCl. Plainly, the spheres of radius R_{loc}, Eq. (21), around impurities do not overlap, and a substantial volume of the sample supports delocalized states. A slowly diffusing component emerges below 50 K and increases with decreasing temperature as inferred by $A_{\rm s}$ in Fig. 35(b). The hopping rate associated with this component shows that Mu localizes at low temperatures.

The effect of 2.7% sodium is more drastic [see Fig. 35(e)]. There is no increase of τ_c^{-1} with decreasing temperature below 50 K and no further leveling off below 10 K. Thus one may conclude that spheres of radius R_Δ overlap [note that R_Δ and R_{loc} differ in insulators, Eqs. (20) and (21)]. It is quite surprising, therefore, that the analysis (Kadono *et al.*, 1996) showed a leveling off of the $\tau_c^{-1}(T)$ for the fast-relaxing component, suggesting temperature-independent dynamics with τ_c^{-1} about two orders of magnitude less than that for Mu band motion in pure KCl. This leveling off can be explained neither by a "single-phonon scattering" nor by a "residual disorder" outside disturbed spheres (Kadono *et al.*, 1996). A one-phonon scattering mechanism would inevitably produce some temperature dependence, which is in evident contradiction with the experiment. The alternative possibility is that even at 2.7% doping there are "lakes" (in the percolation theory sense) of finite-size delocalized states with $\xi<\Delta$ (the fraction f_d described in Sec.

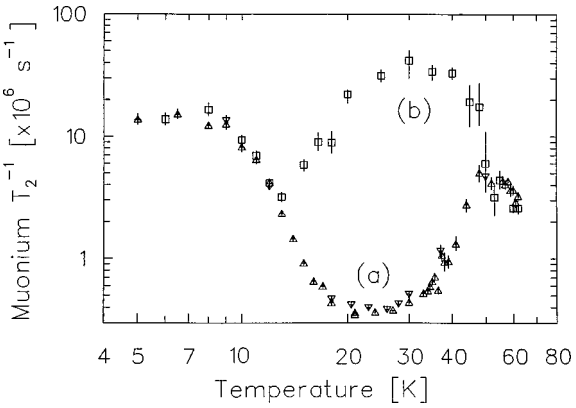

FIG. 36. Temperature dependences of the muonium transverse relaxation rate (a) in pure nitrogen crystals (triangles, two different samples) and (b) in a crystal of N_2 + 10^{-3} CO (Storchak, Brewer, and Morris, 1994b, 1996b).

III.B). These "lakes" do not overlap, but a small fraction of Mu stopped there may be responsible for the observed behavior. Note also that in the experiment this fraction is vanishingly small and the actual behavior at $T\to 0$ is not known.

The slow-relaxing component shows a power law $\tau_c^{-1}\propto T^{3.2}$. This is consistent with the reverse temperature dependence of the muonium τ_c^{-1} in pure KCl, where $\tau_c^{-1}\propto T^{-3.3}$ (Kiefl *et al.*, 1989), in accordance with Eqs. (107) and (109). The complete Mu localization in KCl with 2.7% Na impurities at low temperatures was unambiguously demonstrated by measurements of the magnetic-field dependence of the muon polarization in a longitudinal field, which was in good agreement with the theoretical prediction for static Mu in the presence of a nuclear hyperfine interaction with surrounding nuclei (Beck *et al.*, 1975).

We should also like to mention recent experiments in solid methanes (CH_4 and CD_4) (Storchak, Brewer, Eschenko, *et al.*, 1997), which also claim to observe Mu bandlike propagation disrupted by disorder, but we are running out of space to discuss it here.

c. Trapping phenomena in insulators

At low temperatures, even a weak interaction with defects may be larger than T, leading to effective traps for diffusing particles. As a result, for many years μ^+ and Mu quantum diffusion in crystals was discussed in terms of trapping effects regardless of the temperature range or the nature of the crystal (see, for example, Kadono, 1992, and references therein). Here we present strong experimental evidence that trapping effects, which are very important in metals (Hartmann *et al.*, 1988), are rather ineffective in insulators at low temperatures. This was demonstrated in experiments on Mu diffusion in s-N_2 doped with 10^{-3} CO impurities (Storchak, Brewer, and Morris, 1996d; see also Storchak, Brewer, and Morris, 1994b, 1996b).

Figure 36 shows the temperature dependence of the transverse relaxation rate T_2^{-1} of muonium in pure and doped samples. When Mu moves rapidly (causing low values of T_2^{-1} due to dynamic "narrowing"), it easily finds a CO impurity and reacts chemically [probably to form the MuCO radical (Cox, Eaton, and Magraw, 1990)], which explains why the maximum T_2^{-1} value for Mu in s-N_2+CO significantly exceeds the static relaxation rate $\delta_{\rm Mu}$. Here we are dealing with the standard diffusion-limited chemical reaction, which is described by Eq. (65) with the obvious replacement of R_T with the lattice constant a—the reaction radius in a crystal.

At high temperatures the clear maximum in T_2^{-1} in s-N_2+CO marks the crossover from fast to slow Mu diffusion near CO impurities, which in turn reflects the interplay between $\Omega(T)$ and $\xi\sim U_o$ in the denominator of Eq. (109). Note, the energy shift ξ that the particle has to overcome is much larger near the defect than far from it, making the hop rate strongly dependent on distance from the defect when $\Omega<\xi(r)$. Above the maximum, when $\Omega>U_o$, the diffusion rate at the reaction radius (and T_2^{-1}) increases towards low temperatures. When $\Omega<U_o$, Mu atoms are stuck (or "frozen") at some distance far from CO impurities, which can be seen as a reduction of the reaction rate (Mu T_2^{-1}). Note that this reduction starts at 30 K, when Mu has the fastest dynamics far from impurities, as is evidenced by the motional narrowing effect in T_2^{-1} in a pure sample. At very low temperatures, Mu atoms simply cannot approach CO impurities due to suppression of the inelastic interactions, and T_2^{-1} becomes the same in pure and doped crystals (Fig. 36).

VII. CONCLUSIONS

Looking back over the last few decades one cannot help noticing how difficult was the progress in our understanding of quantum diffusion phenomena experienced by μ^+ or Mu in crystals. From the very beginning of the extensive μ^+SR study of this problem, quantum diffusion experiments have continued to bring new puzzles. There have been a number of occasions when early conclusions derived from the experiments were misleading. We have mentioned a few examples. By no means, however, do these accidental erroneous interpretations cast a shadow upon the quality of the experiments. Rather, they underline the difficulties which hampered attempts at progress.

The advancement in our understanding of μ^+ and Mu quantum diffusion phenomena, however, has been quite substantial. This has been made possible by the real progress in experimental techniques for measurements of μ^+ and Mu dynamics by application of zero-field and longitudinal-field (especially, weak-longitudinal-field) methods. These experimental achievements have been accompanied by progress in the theory of μ^+ quantum diffusion in metals. Subsequent experimental findings of Mu quantum diffusion in alkali halides have strongly supported theoretical predictions for insulating systems. Experiments in heavy solid rare gases have opened the way for studying particle interaction with a phonon bath

TABLE I. Bandwidth Δ_{coh} in different materials.

Substance	Particle	Δ_{coh}, K
Cu	μ^+	10^{-4}
Al	μ^+	3×10^{-3}
V	μ^+	$5\sqrt{K}\times10^{-2}$
Nb	μ^+	>1
Bi	μ^+	10^{-3}
KCl	Mu	0.16
NaCl	Mu	0.07
GaAs	Mu	0.03
N_2	Mu	0.01
Ne	Mu	$>5\times10^{-4}$
Kr	Mu	3×10^{-5}
Xe	Mu	$<10^{-6}$

at high temperatures. Substantial progress in the theory and in experiment (in superconducting aluminum and nitrogen) has been connected with μ^+ and Mu quantum diffusion in inhomogeneous media. Our current understanding of μ^+ and Mu quantum diffusion allows us to estimate the key parameter of the phenomenon—the tunneling amplitude Δ_{coh}—in different substances (see Table I).

It is simply impossible to indicate all the aspects of our current knowledge of quantum diffusion. Let us, however, list some of them that we consider to be crucial to the phenomenon. We know that the screening of μ^+ by conduction electrons, which cannot follow the particle adiabatically, greatly reduces its tunneling probability. It is well established that below the superconducting transition μ^+ dynamics are considerably enhanced because of the freezing out of electron excitations. It is generally accepted that in insulators and semiconductors the two-phonon interaction governs Mu quantum diffusion at low temperatures. At high temperatures, the one-phonon interaction takes over via both the polaron effect and the effect of fluctuational preparation of the barrier in insulators, while in metals μ^+ diffusion can be explained by the polaron effect only. We now understand that in an inhomogeneous crystal both μ^+ and Mu show spatial distributions of τ_c^{-1} in their quantum diffusion. Trapping phenomena in quantum diffusion in metals and insulators are now considered separately because of essentially different damping, due to interaction with the phonons and conduction electrons.

Summarizing this substantially enhanced knowledge, one obviously faces the question of where to proceed. The field has become so large and diversified that we expect progress in many directions. There is no doubt that new metallic systems will be found to support our current understanding of muon quantum diffusion (in fact, even in "old" systems like Nb, V, and Bi, the situation with quantum diffusion is far from clear). Experiments in superconducting materials will deepen our understanding of the interaction with conduction electrons. We believe that measurements in insulating systems will shed a new light on the phenomenon of Mu quantum diffusion. But one direction, to our mind, deserves particular attention. This is quantum diffusion in inhomogeneous crystals. It seems that our understanding of the phenomenon has achieved a level at which quantum diffusion may be developed into an extremely sensitive microscopic tool for measurement of the impurity content in crystals, energy-level shifts produced by impurities, phonon constants, etc.

ACKNOWLEDGMENTS

This work was made possible by the Kurchatov Institute (Moscow, Russia), the Yukawa Institute for Theoretical Physics (Kyoto, Japan), the Engineering and Physical Sciences Research Council of the United Kingdom, the Natural Sciences and Engineering Research Council and (through TRIUMF) the National Research Council of Canada, the International Science Foundation (through Grants No. N9D000 and N9D300) and the Russian Foundation for Basic Research (through Grants No. 95-02-06191-a and 96-02-16080-a). One of us (V.G.S.) was also supported by the INTAS Foundation (through Grant No. 94-3394), the Royal Society of the United Kingdom (through the Royal Society fellowship), NATO (through Grant No. HTECH.LG 960534), and the Russian Foundation for Studying Condensed Matter with Neutrons. Constant encouragement and support by S. T. Belyaev, J. H. Brewer, and Yu. M. Kagan are most gratefully acknowledged by both authors. V.G.S. also wishes to express his gratitude to J. H. Brewer and S. F. J. Cox for their hospitality during his stay at TRIUMF and Rutherford Appleton Laboratory.

REFERENCES

Abragam, A., 1961, *The Principles of Nuclear Magnetism* (Clarendon, Oxford).
Allen, A. R., and M. G. Richards, 1978, Phys. Lett. A **65**, 36.
Allen, A. R., M. G. Richards, and J. Schratter, 1982, J. Low Temp. Phys. **47**, 289.
Anderson, P. W., 1967, Phys. Rev. Lett. **18**, 1047.
Anderson, P. W., Phys. Rev. **164**, 342.
Andreev, A. F., 1976, Usp. Fiz. Nauk **118**, 251 [Sov. Phys. Usp. **19**, 137].
Andreev, A. F., and I. M. Lifshitz, 1969, Zh. Éksp. Teor. Fiz. **56**, 2057 [Sov. Phys. JETP **29**, 1107 (1969)].
Bagatskii, M. I., V. A. Kucheryavy, V. G. Manzhelii, and V. A. Popov, 1968, Phys. Status Solidi **26**, 453.
Barsov, S. G., *et al.*, 1983, Zh. Éksp. Teor. Fiz. **85**, 341 [Sov. Phys. JETP **58**, 198].
Barsov, S. G., *et al.*, 1984, Hyperfine Interact. **17-19**, 145.
Baumann, D., F. N. Gygax, E. Lippelt, A. Schenck, R. Schmid, and S. Barth, 1986a, Hyperfine Interact. **31**, 53.
Baumann, D., F. N. Gygax, E. Lippelt, A. Schenck, R. Schmid, and S. Barth, 1986b, Hyperfine Interact. **31**, 455.
Baumeler, H. P., *et al.*, 1986, Hyperfine Interact. **32**, 659.
Beck, R., P. F. Meier, and A. Schenck, 1975, Z. Phys. B **22**, 109.
Bilz, H., and W. Kress, 1979, *Phonon Dispersion Relations in Insulators* (Springer, Berlin).

Birnbaum, H. K., M. Camani, A. T. Fiory, F. N. Gygax, W. J. Kossler, W. Rüegg, A. Schenck, and H. Schilling, 1978, Phys. Rev. B **17**, 4143.
Black, J. L., and P. Fulde, 1979, Phys. Rev. Lett. **43**, 453.
Borghini, M., T. O. Niinikoski, J. C. Soulie, O. Hartmann, E. Karlsson, L. O. Norlin, K. Pernestal, K. W. Kehr, D. Richter, and E. Walker, 1978, Phys. Rev. Lett. **40**, 1723.
Brewer, J. H., 1994, "Muon Spin Rotation/Relaxation/Resonance," in *Encyclopedia of Applied Physics* **11** (*Mößbauer Effect* to *Nuclear Structure*), p. 23.
Brewer, J. H., *et al.*, 1986, Hyperfine Interact. **31**, 191.
Brewer, J. H., R. F. Kiefl, and P. W. Percival, 1994, Eds., *Proceedings of the 6th International Conference on Muon Spin Rotation/Relaxation/Resonance (μSR)*, Maui, Hawaii, 1993, Hyperfine Interact. **85-87**, 3-122.
Brewer, J. H., S. R. Kreitzman, K. M. Crowe, C. W. Clawson, and C. Y. Huang, 1987, Phys. Lett. A **120**, 199.
Brewer, J. H., and P. W. Percival, 1981, Eds., *Proceedings of the Second International Topic Meeting on Muon Spin Rotation*, Vancouver, Canada, 1980, Hyperfine Interact. **8**, 307.
Brown, J. A., *et al.*, 1979, Hyperfine Interact. **6**, 233.
Brown, J. A., R. H. Heffner, M. Leon, M. E. Schillaci, D. W. Cooke, and W. B. Gauster, 1979, Phys. Rev. Lett. **43**, 1513.
Browne, A., and A. M. Stoneham, 1982, J. Phys. C **15**, 2709.
Caldeira, A. O., and A. J. Leggett, 1983, Ann. Phys. (N.Y.) **149**, 374.
Camani, M., F. N. Gygax, W. Rüegg, A. Schenck, and H. Schilling, 1977, Phys. Rev. Lett. **39**, 836.
Celio, M., 1986a, Phys. Rev. Lett. **56**, 2720.
Celio, M., 1986b, Hyperfine Interact. **31**, 153.
Celio, M., 1987, Helv. Phys. Acta **60**, 600.
Celio, M., and P. F. Meier, 1983, Phys. Rev. B **27**, 1908.
Chappert, J., A. Yaouanc, O. Hartmann, E. Karlsson, L.-O. Norlin, and T. O. Ninikoski, 1982, Solid State Commun. **44**, 13.
Clawson, C. W., K. M. Crowe, S. E. Kohn, S. S. Rosenblum, C. Y. Huang, J. L. Smith, and J. H. Brewer, 1982, Physica (Amsterdam) **109**, 2164.
Clawson, C. W., K. M. Crowe, S. S. Rosenblum, S. E. Kohn, C. Y. Huang, J. L. Smith, and J. H. Brewer, 1983, Phys. Rev. Lett. **51**, 114.
Cox, S. F. J., 1987, J. Phys. C **20**, 3187.
Cox, S. F. J., 1995, private communication.
Cox, S. F. J., G. H. Eaton, D. Herlach, and V. P. Koptev, 1990, Eds., *Proceedings of the 5th International Conference on Muon Spin Rotation, Relaxation, and Resonance*, Oxford, UK, Hyperfine Interact. **64**, 613–749.
Cox, S. F. J., G. H. Eaton, and J. E. Magraw, 1990, Hyperfine Interact. **65**, 773.
Cox, S. F. J., R. M. Macrae, D. S. Sivia, N. Ayres de Campos, P. J. Mendes, and J. M. Gil, 1994, Hyperfine Interact. **85**, 67.
Dorenburg, K., M. Gladisch, D. Herlach, W. Mansel, H. Metz, H. Orth, G. zu Putlitz, A. Seeger, W. Wahl, and M. Wigand, 1978, Z. Phys. B **31**, 165.
DeReggi, A. S., P. C. Canepa, and T. A. Scott, 1969, J. Magn. Reson. **1**, 144.
Echt, O., H. Holzschuh, E. Recknagel, A. Weidinger, and Th. Wichert, 1978, Phys. Lett. A **67**, 427.
Emin, D., 1973, Adv. Phys. **22**, 57.
Emin, D., 1981, Hyperfine Interact. **8**, 515.
Emin, D., and T. Holstein, 1976, Phys. Rev. Lett. **36**, 323.
Fiory, A. T., K. G. Lynn, D. M. Parkin, W. J. Kossler, W. F. Lankford, and C. E. Stronach, 1978, Phys. Rev. Lett. **40**, 968.
Fisher, M. P. A., and A. T. Dorsey, 1985, Phys. Rev. Lett. **54**, 1609.
Flynn, C. P., and A. M. Stoneham, 1970, Phys. Rev. B **1**, 3966.
Foner, S. N., E. L. Cochran, V. A. Bowers, and C. K. Jen, 1960, J. Chem. Phys. **32**, 963.
Fujii, S., 1979, J. Phys. Soc. Jpn. **46**, 1833 (Part I); **46**, 1843 (Part II).
Gauster, W. B., R. H. Heffner, C. Y. Huang, R. L. Hutson, M. Leon, D. M. Parkin, M. E. Schillaci, W. Triftahäuser, and W. R. Wampler, 1977, Solid State Commun. **24**, 619.
Grabert, H., 1987, in *Quantum Aspects of Molecular Motions in Solids*, Springer Proceedings in Physics, No. 17, edited by A. Heidemann *et al.* (Springer, Berlin), p. 130.
Grabert, H., S. Linkwitz, S. Dattagupta, and U. Weiss, 1986, Europhys. Lett. **2**, 631.
Grabert, H., and U. Weiss, 1985, Phys. Rev. Lett. **54**, 1605.
Grebinnik, V. G., *et al.*, 1977, Pis'ma Zh. Éksp. Teor. Fiz. **25**, 322 [JETP Lett. **25**, 298 (1977)].
Grebinnik, V. G., *et al.*, 1978, Pis'ma Zh. Éksp. Teor. Fiz. **75**, 1989 [Sov. Phys. JETP **48**, 1002 (1978)].
Grebinnik, V. G., I. I. Gurevich, V. A. Zhukov, A. P. Manych, E. A. Muratova, B. A. Nikolskii, V. I. Selivanov, and V. A. Seutin, 1975, Zh. Éksp. Teor. Fiz. **68**, 1548 [Sov. Phys. JETP **41**, 777 (1976)].
Gurevich, I. I., E. A. Meleshko, E. A. Muratova, B. A. Nikolskii, V. S. Roganov, V. I. Selivanov, and B. V. Sokolov, 1972, Phys. Lett. **40**, 143.
Guyer, R. A., and L. I. Zane, 1969, Phys. Rev. **188**, 445.
Gygax, F. N., A. Amato, R. Feyerherm, A. Schenck, I. S. Anderson, T. J. Udovic, and G. Solt, 1995, J. Alloys Compd. **231**, 248.
Gygax, F. N., A. Amato, A. Schenck, I. S. Anderson, J. J. Rush, and G. Solt, 1994, Hyperfine Interact. **85**, 73.
Gygax, F. N., B. Hitti, E. Lippelt, A. Schenck, and S. Barth, 1988, Z. Phys. B **71**, 473.
Gygax, F. N., W. Kundig, and P. F. Meier, 1979, Eds., *Proceedings of the First International Topical Meeting on Muon Spin Rotation*, Rorschach, Switzerland, 1978, Hyperfine Interact. **6**, 1-450.
Gygax, F. N., A. Schenck, and A. J. van der Wal, 1986, Phys. Rev. Lett. **26**, 2842.
Hartmann, O., 1977, Phys. Rev. Lett. **39**, 832.
Hartmann, O., E. Karlsson, S. Harris, R. Wäppling, and T. O. Niinikoski, 1989, Phys. Lett. A **142**, 504.
Hartmann, O., E. Karlsson, B. Lindgren, and R. Wäppling, 1986, Eds., *Proceedings of the 4th International Conference on Muon Spin Rotation, Relaxation and Resonance*, Uppsala, Sweden, 1986, Hyperfine Interact. **31-32**, 3-948.
Hartmann, O., E. Karlsson, L. O. Norlin, T. O. Niinikoski, K. W. Kehr, D. Richter, J.-M. Welter, A. Yaouanc, and J. Le Hericy, 1980, Phys. Rev. Lett. **44**, 337.
Hartmann, O., E. Karlsson, L. O. Norlin, D. Richter, and T. O. Niinikoski, 1978, Phys. Rev. Lett. **41**, 1055.
Hartmann, O., E. Karlsson, K. Pernestal, M. Borghini, T. O. Niinikoski, and L. O. Norlin, 1977, Phys. Lett. A **61**, 141.
Hartmann, O., E. Karlsson, E. Wäckelgard, R. Wäppling, D. Richter, R. Hempelmann, and T. O. Niinikoski, 1986, Hyperfine Interact. **31**, 223.
Hartmann, O., E. Karlsson, E. Wäckelgard, R. Wäppling, D. Richter, R. Hempelmann, and T. O. Niinikoski, 1988, Phys. Rev. B **37**, 4425.

Hartmann, O., E. Karlsson, R. Wäppling, D. Richter, R. Hempelmann, K. Schulze, B. Patterson, E. Holzschuh, W. Kündig, and S. F. J. Cox, 1983, Phys. Rev. B **27**, 1943.

Hartmann, O., E. Karlsson, R. Wäppling, D. Richter, R. Hempelmann, K. Schulze, B. Patterson, E. Holzschuh, W. Kündig, and S. F. J. Cox, 1984, Hyperfine Interact. **17**, 183.

Hayano, R. S., Y. J. Uemura, J. Imazato, N. Nishida, T. Yamazaki, and R. Kubo, 1979, Phys. Rev. B **20**, 850.

Heffner, R. H., J. A. Brown, R. L. Hutson, M. Leon, D. M. Parkin, M. E. Schillaci, W. B. Gauster, O. N. Carlson, D. K. Rehbein, and A. T. Fiory, 1979, Hyperfine Interact. **6**, 237.

Heffner, R. H., W. B. Gauster, D. M. Parker, C. Y. Huang, R. L. Hutson, M. Leon, M. E. Schillaci, M. L. Simmons, and W. Triftshauser, 1978, Hyperfine Interact. **4**, 838.

Holstein, T., 1959, Ann. Phys. (N.Y.) **8**, 343.

Holzschuh, E., and P. F. Meier, 1984, Phys. Rev. B **29**, 1129.

Ikeya, M., L. O. Schwan, and T. Miki, 1978, Solid State Commun. **27**, 891.

Ivanter, I. G., 1984, Fiz. Tverd. Tela (Leningrad) **26**, 3658 [Sov. Phys. Solid State **26**, 2200 (1984)].

Jäckle, J., and K. W. Kehr, 1983, J. Phys. F **13**, 753.

Kadono, R., 1990, Hyperfine Interact. **64**, 615.

Kadono, R., 1992, in *Perspectives in Meson Science*, edited by T. Yamazaki, K. Nakai, and K. Nagamine (North-Holland, Amsterdam), p. 113.

Kadono, R., 1993, Z. Phys. Chem. (Munich) **181**, 195.

Kadono, R., J. Imazato, T. Matsuzaki, K. Nishiyama, K. Nagamine, T. Yamazaki, D. Richter, and J.-M. Welter, 1989, Phys. Rev. B **39**, 23.

Kadono, R., J. Imazato, K. Nishiyama, K. Nagamine, T. Yamazaki, D. Richter, and J.-M. Welter, 1984, Hyperfine Interact. **17-19**, 109.

Kadono, R., J. Imazato, K. Nishiyama, K. Nagamine, T. Yamazaki, D. Richter, and J.-M. Welter, 1985, Phys. Lett. **109A**, 61.

Kadono, R., and R. F. Kiefl, 1991, Phys. Rev. Lett. **66**, 2414.

Kadono, R., and R. F. Kiefl, 1993, Defect Diffus. Forum **95-98**, 279.

Kadono, R., R. F. Kiefl, E. J. Ansaldo, J. H. Brewer, M. Celio, S. R. Kreitzman, and G. M. Luke, 1990, Phys. Rev. Lett. **64**, 665.

Kadono, R., R. F. Kiefl, J. H. Brewer, G. M. Luke, T. Pfiz, T. M. Riseman, and B. J. Sternlieb, 1990, Hyperfine Interact. **64**, 635.

Kadono, R., R. F. Kiefl, S. R. Kreitzman, Q. Li, T. Pfiz, T. M. Riseman, H. Zhou, R. Wäppling, S. W. Harris, O. Hartmann, E. Karlsson, R. Hempelmann, D. Richter, T. O. Niinikoski, L. P. Lee, G. M. Luke, B. Steinlieb, and E. J. Ansaldo, 1990, Hyperfine Interact. **64**, 737.

Kadono, R., R. F. Kiefl, W. A. MacFarlane, and S. R. Dunsiger, 1996, Phys. Rev. B **53**, 3177.

Kadono, R., T. Matsuzaki, K. Nagamine, T. Yamazaki, D. Richter, and J.-M. Welter, 1986, Hyperfine Interact. **31**, 205.

Kadono, R., K. Nishiyama, K. Nagamine, and T. Matsuzaki, 1988, Phys. Lett. A **132**, 195.

Kagan, Yu., and M. I. Klinger, 1974, Z. Phys. C **7**, 2791.

Kagan, Yu., and M. I. Klinger, 1976, Zh. Éksp. Teor. Fiz. **70**, 255 [Sov. Phys. JETP **43**, 132 (1976)].

Kagan, Yu., and L. A. Maksimov, 1973, Zh. Éksp. Teor. Fiz. **65**, 662 [Sov. Phys. JETP **38**, 307 (1974)].

Kagan, Yu., and L. A. Maksimov, 1980, Zh. Éksp. Teor. Fiz. **79**, 1363 [Sov. Phys. JETP **52**, 688 (1980)].

Kagan, Yu., and L. A. Maksimov, 1983, Zh. Éksp. Teor. Fiz. **84**, 792 [Sov. Phys. JETP **57**, 459 (1983)].

Kagan, Yu., and L. A. Maksimov, 1984, Zh. Éksp. Teor. Fiz. **87**, 348 [Sov. Phys. JETP **60**, 201 (1984)].

Kagan, Yu., and N. V. Prokof'ev, 1986, Zh. Éksp. Teor. Fiz. **90**, 2176 [Sov. Phys. JETP **63**, 1276 (1986)].

Kagan, Yu., and N. V. Prokof'ev, 1987, "Quantum diffusion and depolarization of μ^+-mesons in metals," I. V. Kurchatov Atomic Energy Institute Report No. IAE-4461/9.

Kagan, Yu., and N. V. Prokof'ev, 1989a, Zh. Éksp. Teor. Fiz. **96**, 1473 [Sov. Phys. JETP **69**, 836 (1989)].

Kagan, Yu., and N. V. Prokof'ev, 1989b, Zh. Éksp. Teor. Fiz. **96**, 2209 [Sov. Phys. JETP **69**, 1350 (1989)].

Kagan, Yu., and N. V. Prokof'ev, 1990a, Phys. Lett. A **150**, 320.

Kagan, Yu., and N. V. Prokof'ev, 1990b, Zh. Éksp. Teor. Fiz. **97**, 1698 [Sov. Phys. JETP **70**, 990 (1990)].

Kagan, Yu., and N. V. Prokof'ev, 1991, Phys. Lett. A **159**, 289.

Kagan, Yu., and N. V. Prokof'ev, 1992, in *Quantum Tunneling in Condensed Media*, edited by A. J. Leggett and Yu. M. Kagan (North-Holland, Amsterdam), p. 37.

Karlsson, E., R. Wäppling, S. W. Lidström, O. Hartmann, R. Kadono, R. F. Kiefl, R. Hempelmann, and D. Richter, 1995, Phys. Rev. B **52**, 6417.

Katz, L., M. Guinan, and R. I. Borg, 1971, Phys. Rev. B **4**, 330.

Kehr, K. W., G. Honig, and D. Richter, 1978, Z. Phys. B **32**, 49.

Kehr, K. W., D. Richter, J.-M. Welter, O. Hartmann, E. Karlsson, L.O. Norlin, T. O. Niinikoski, and A. Yaouanc, 1982, Phys. Rev. B **26**, 567.

Kiefl, R. F., M. Celio, T. L. Estle, G. M. Luke, S. R. Kreitzman, J. H. Brewer, D. R. Noakes, E. J. Ansaldo, and K. Nishiyama, 1987, Phys. Rev. Lett. **58**, 1780.

Kiefl, R. F., E. Holzschuh, H. Keller, W. Kündig, P. F. Meier, B. D. Patterson, J. W. Schneider, K. W. Blazey, S. L. Rudaz, and A. B. Denison, 1984, Phys. Rev. Lett. **53**, 90.

Kiefl, R. F., R. Kadono, J. H. Brewer, G. M. Luke, H. K. Yen, M. Celio, and E. J. Ansaldo, 1989, Phys. Rev. Lett. **62**, 792.

Kiefl, R. F., W. Odermatt, Hp. Baumeler, J. Felber, H. Keller, W. Kündig, P. F. Meier, B. D. Patterson, J. W. Schneider, K. W. Blazey, T. L. Estle, and C. Schwab, 1986, Phys. Rev. B **34**, 1474.

Kiefl, R. F., J. W. Schneider, H. Keller, W. Kündig, W. Odermatt, B. D. Patterson, K. W. Blazey, T. L. Estle, and S. L. Rudaz, 1985, Phys. Rev. B **32**, 530.

Kiefl, R. F., J. B. Warren, G. M. Marshall, and C. J. Oram, 1981, J. Chem. Phys. **74**, 308.

Klamt, A., and H. Teichler, 1986, Phys. Status Solidi B **134**, 103.

Kondo, J., 1976, Physica B **84**, 207.

Kondo, J., 1984, Physica B & C **126**, 377.

Kondo, J., 1986, Hyperfine Interact. **31**, 117.

Kondo, J., 1992, in *Perspectives in Meson Science*, edited by T. Yamazaki, K. Nakai, and K. Nagamine (North-Holland, Amsterdam), p. 137.

Kossler, W. J., A. T. Fiory, W. F. Lankford, J. Lindemuth, K. G. Lynn, S. Mahajan, R. P. Minnich, K. G. Petzinger, and C. E. Stronach, 1978, Phys. Rev. Lett. **41**, 1558.

Kubo, R., and T. Toyabe, 1967, in *Magnetic Resonance and Relaxation*, edited by R. Blink (North Holland, Amsterdam), p. 810.

Landau, L. D., and E. M. Lifshitz, 1974, *Quantum Mechanics. Non Relativistic Theory* (Nauka, Moscow).

Leggett, A. J., S. Chakravarty, A. T. Dorsey, M. P. A. Fisher, A. Garg, and W. Zwerger, 1987, Rev. Mod. Phys. **59**, 1.

Lifshitz, I. M., and Yu. M. Kagan, 1972, Zh. Éksp. Teor. Fiz. **62**, 385 [Sov. Phys. JETP **35**, 206 (1972)].
Luke, G. M., J. H. Brewer, S. R. Kreitzman, D. R. Noakes, M. Celio, R. Kadono, and E. J. Ansaldo, 1990, Hyperfine Interact. **64**, 721.
Luke, G. M., J. H. Brewer, S. R. Kreitzman, D. R. Noakes, M. Celio, R. Kadono, and E. J. Ansalso, 1991, Phys. Rev. B **43**, 3284.
MacFarlane, W. A., R. F. Kiefl, J. W. Schneider, K. H. Chow, G. D. Morris, T. L. Estle, and B. Hitti, 1994, Hyperfine Interact. **85**, 23.
Mahajan, S., and S. Prakash, 1983, Phys. Status Solidi B **119**, 381.
Manzhelli, V. G., A. M. Tolkachev, and E. I. Boitovich, 1966, Phys. Status Solidi **13**, 351.
Matsumoto, T., Y. Sasaki, and M. Hihara, 1975, J. Phys. Chem. Solids **36**, 215.
McMullen, T., and E. Zaremba, 1978, Phys. Rev. B **18**, 3026.
Metz, H., *et al.*, 1979, Hyperfine Interact. **6**, 271.
Mikheev, V. A., B. N. Eselson, V. N. Grigor'ev, and N. P. Mikhin, 1977, Fiz. Nizk. Temp. **3**, 386 [Sov. J. Low Temp. Phys. **3**, 186 (1977)].
Mikheev, V. A., V. A. Maydanov, and N. P. Mikhin, 1983, Solid State Commun. **48**, 361.
Morosov, A. I., 1979, Zh. Éksp. Teor. Fiz. **77**, 147 [Sov. Phys. JETP **50**, 738 (1979)].
Morozumi, Y., K. Nishiyama, and K. Nagamine, 1986, Phys. Lett. A **118**, 93.
Nagamine, K., R. M. MacRae, R. Kadono, and K. Nishiyama, 1997, Eds., *Proceedings of the 7th International Conference on Muon Spin Rotation/Relaxation/Resonance (μSR'96)*, Nikko, Japan, 1996, Hyperfine Interact. **105**, 189-284.
Nakai, R., M. Doyama, R. Yamamoto, Y. J. Uemura, T. Yamazaki, and J. H. Brewer, 1981, Hyperfine Interact. **8**, 717.
Niinikoski, T. O., O. Hartmann, E. Karlsson, L.-O. Norlin, K. Pernestal, K. W. Kehr, D. Richter, E. Walker, and K. Schulze, 1979, Hyperfine Interact. **6**, 229.
Nishiyama, K., Y. Morozumi, T. Suzuki, and K. Nagamine, 1985, Phys. Lett. A **111**, 369.
Patterson, B. D., 1988, Rev. Mod. Phys. **60**, 69.
Petzinger, K. G., 1980, Phys. Lett. A **75**, 225.
Petzinger, K. G., 1981, Hyperfine Interact. **8**, 639.
Petzinger, K. G., 1982, Phys. Rev. B **26**, 6530.
Poole, Ch. P., 1967, *Electron Spin Resonance: A Comprehensive Treatise on Experimental Technique* (Interscience, New York).
Prokof'ev, N. V., 1994, Hyperfine Interact. **85**, 3.
Prokof'ev, N. V., 1995, Phys. Rev. Lett. **74**, 2748.
Puska, M. J., and R. M. Nieminen, 1983, Phys. Rev. B **27**, 6121.
Regelmann, T., L. Schimmele, and A. Seeger, 1995, Philos. Mag. B **72**, 209.
Richter, D., 1986, Hyperfine Interact. **31**, 169.
Richter, D., and T. Springer, 1978, Phys. Rev. B **18**, 126.
Schaumann, G., J. Völkl, and G. Alefeld, 1970, Phys. Status Solidi **42**, 401.
Schenck, A., 1985, *Muon Spin Rotation: Principles and Applications in Solid State Physics* (Adam Hilger, Bristol/London).
Schilling, H., M. Camani, F. N. Gygax, W. Rüegg, and A. Schenck, 1982, J. Phys. F **12**, 875.
Schmid, A., 1983, Phys. Rev. Lett. **51**, 1506.
Schneider, J. W., *et al.*, 1990, Phys. Rev. B **41**, 7254.
Schneider, J. W., *et al.*, 1992a, Phys. Rev. Lett. **68**, 3196.
Schneider, J. W., *et al.*, 1992b, Mater. Sci. Forum **83-87**, 569.
Sellers, G. J., A. C. Anderson, and H. K. Birnbaum, 1974, Phys. Rev. B **10**, 2771.
Sieghban, P., and B. Lui, 1978, J. Chem. Phys. **68**, 2457.
Slichter, C. P., 1980, *Principles of Magnetic Resonance* (Springer, Berlin).
Spaeth, J. M., 1969, Phys. Status Solidi **34**, 171.
Stamp, P. C. E., and Chao Zhang, 1991, Phys. Rev. Lett. **66**, 1902.
Steinbinder, D., H. Wipf, A. Magerl, D. Richter, A.-J. Dianoux, and K. Neumaier, 1988, Europhys. Lett. **6**, 535.
Stoneham, A. M., 1983, Phys. Lett. A **94**, 353.
Storchak, V., J. H. Brewer, and S. F. J. Cox, 1997, Hyperfine Interact. **105**, 189.
Storchak, V. G., J. H. Brewer, and D. G. Eschenko, 1997, Appl. Magn. Reson. **13**, 15.
Storchak, V., J. H. Brewer, D. G. Eschenko, S. F. J. Cox, and S. P. Cottrell, 1997, unpublished.
Storchak, V., J. H. Brewer, W. N. Hardy, S. Johnston, S. R. Kreitzman, and G. D. Morris, 1994a, Hyperfine Interact. **85**, 103.
Storchak, V., J. H. Brewer, W. N. Hardy, S. R. Kreitzman, and G. D. Morris, 1994b, Phys. Rev. Lett. **72**, 3056.
Storchak, V., J. H. Brewer, W. N. Hardy, S. R. Kreitzman, and G. D. Morris, 1994c, Hyperfine Interact. **85**, 109.
Storchak, V., J. H. Brewer, W. N. Hardy, S. R. Kreitzman, and G. D. Morris, 1995, Philos. Mag. B **72**, 233.
Storchak, V., J. H. Brewer, W. N. Hardy, G. D. Morris, T. M. Riseman, and C. Niedermayer, 1993, Phys. Lett. A **182**, 449.
Storchak, V., J. H. Brewer, and G. D. Morris, 1994a, Phys. Lett. A **193**, 199.
Storchak, V., J. H. Brewer, and G. D. Morris, 1994b, Hyperfine Interact. **85**, 31.
Storchak, V., J. H. Brewer, and G. D. Morris, 1995a, Phys. Rev. Lett. **75**, 2384.
Storchak, V., J. H. Brewer, and G. D. Morris, 1995b, Philos. Mag. B **72**, 241.
Storchak, V., J. H. Brewer, and G. D. Morris, 1996a, Phys. Rev. Lett. **76**, 2969.
Storchak, V., J. H. Brewer, and G. D. Morris, 1996b, Hyperfine Interact. **97/98**, 323.
Storchak, V., J. H. Brewer, and G. D. Morris, 1996c, unpublished.
Storchak, V., J. H. Brewer, and G. D. Morris, 1996d, Phys. Rev. B **53**, 11 300.
Storchak, V., J. H. Brewer, and G. D. Morris, 1997, Phys. Rev. B **56**, 55.
Storchak, V., J. H. Brewer, G. D. Morris, D. J. Arseneau, and M. Senba, 1994, Hyperfine Interact. **85**, 117.
Storchak, V., F. J. Cox, S. P. Cottrell, J. H. Brewer, G. D. Morris, D. J. Arseneau, and B. Hitti, 1997, Phys. Rev. Lett. **78**, 2835.
Storchak, V., F. J. Cox, S. P. Cottrell, J. H. Brewer, G. D. Morris, and N. V. Prokof'ev, 1996, Phys. Rev. B **53**, 662.
Storchak, V., B. F. Kirillov, A. V. Pirogov, V. N. Duginov, V. G. Grebinnik, T. N. Mamedov, V. G. Ol'shevsky, V. A. Zhukov, J. H. Brewer, and G. D. Morris, 1992, Phys. Lett. A **32**, 77.
Storchak, V., G. D. Morris, K. Chow, W. N. Hardy, J. H. Brewer, S. R. Kreitzman, M. Senba, J. W. Schneider, and P. Mendels, 1992, Chem. Phys. Lett. **200**, 546.
Sugimoto, H. J., 1986, J. Phys. Soc. Jpn. **55**, 1687.
Teichler, H., 1977, Phys. Lett. A **64**, 78.
Teichler, H., and A. Seeger, 1981, Phys. Lett. A **82**, 91.

Teichler, H., and A. Klamt, 1985, Phys. Lett. A **108**, 281.
Van Vleck, J. H., 1948, Phys. Rev. **74**, 1168.
Verkin, B. I., and A. F. Prikhotko, 1983, Eds., *Cryocrystals* (Naukova Dumka, Kiev).
Vladar, K., and A. Zawadowski, 1983, Phys. Rev. B **28**, 1564.
Völkl, J., and G. Alefeld, 1978, in *Hydrogen in Metals*, edited by G. Alefeld and J. Völkl (Springer, Berlin), Vol. 1, p. 321.
Waite, T. R., 1957, Phys. Rev. **107**, 463.
Weiss, U., and M. Wollensak, 1989, Phys. Rev. Lett. **62**, 1663.
Weiss, U., 1993, *Quantum Dissipative Systems*, Series in Modern Condensed Matter Physics, Vol. 2 (World Scientific, Singapore).
Welter, J.-M., D. Richter, R. Helpenman, O. Hartmann, E. Karlsson, L. O. Norlin, T. O. Niinikoski, and D. Lenz, 1983, Z. Phys. B **52**, 303.
Welter, J.-M., D. Richter, R. Helpenman, O. Hartmann, E. Karlsson, L. O. Norlin, and T. O. Niinikoski, 1984, Hyperfine Interact. **17-19**, 117.
Wipf, H., and G. Alefeld, 1974, Phys. Status Solidi A **23**, 175.
Wipf, H., and K. Neumaier, 1984, Phys. Rev. Lett. **52**, 1308.
Wipf, H., D. Steinbinder, K. Neumaier, P. Gutsmiedl, A. Magerl, and A.-J. Dianoux, 1987, Europhys. Lett. **4**, 1379.
Yamada, K., 1984, Prog. Theor. Phys. **72**, 195.
Yamada, K., A. Sakurai, S. Miyazima, and H. S. Hwang, 1986, Prog. Theor. Phys. **75**, 1030.
Yamazaki, T., and K. Nagamine, 1984, Eds., *Proceedings of the Yamada Conference VII on Muon Spin Rotation and Associated Problems*, Shimoda, Japan, 1983, Hyperfine Interact. **17-19**, 1-1034.
Yen, H. K., M.Sc. thesis, 1988, University of British Columbia.